The significance of microbiota-immune system interactions for the induction of inflammation

vorgelegt von
M. Sc.
Justus Hubert Bernd Ninnemann

an der Fakultät III- Prozesswissenschaften
der Technischen Universität Berlin
zur Erlangungen des akademischen Grades

Doctor rerum naturalium
-Dr. rer. nat.-

genehmigte Dissertation

Promotionsausschuss:

Vorsitzender: Prof. Dr. Peter Neubauer
Gutachterin: Prof. Dr. Chiara Romagnani
Gutachter: Prof. Dr. Andreas Radbruch
Gutachter: Prof. Dr. Hyun-Dong Chang

Tag der wissenschaftlichen Aussprache: 30. Mai 2022

Berlin 2022

Acknowledgements

This work is finally my dissertation but I would never be able to finalize it without the help, support and trust of the many wonderful people around me.

First of all I want to thank Andrey Kruglov who gave me the opportunity to do my PhD in his lab. I did not only learn a lot about science and immunology from you but also about the precious gift of a supportive and positive surrounding for successful work. Thank you Andrey.

Lisa thank you for walking part of this journey with me together. You always motivated me and reminded me why it is awesome to be a scientist in the first place. Thank you for all the joy you brought into my professional and personal life and your strength which had to carry sometimes the both of us. I have no idea where I would be now without you.

Thanks to Hyun-Dong Chang for enabling me to do my PhD and all the helpful conversations but also for being around, whenever I did not know where to go to. I did not take it for granted, thank you!
Thanks also to the whole Chang group and the wonderful lunch breaks and festivities. Special thanks to Ute, without you a lot of my organizational work would have been less successful.

Thanks to Andreas Radbruch who always had important contributions and was always eager to help me make the most out of the projects.

Thanks to Prof. Dr. Denis Poddubnyy and Dr. Valeria Rios-Rodriguez for the AS cooperation.

Thanks to the group of Mir-Farzin Mashreghi with all the help concerning sequencing and the COVID cooperation.

Thanks to my lab fellows Marina and Iaroslav. You always helped me with big experiments and having you around in the lab made everything easier. Seems like I need a new running partner now for Marishka and a new music enthusiast for Iarik.
Thanks to Selin and Aigul who contributed to several experiments.
Thank you Katharina for being a short but bright sunshine in the lab, even though you are maybe not aware of it, you had a great impact on me.

Thanks to Quirin and Josefine whom I use as an orientation in this academic world. Quirin you already helped me in my masters and luckily never stopped. I know we will keep in touch no matter where we are in this world and I am thankful for having you two as friends.

Thanks to Padde, Francesco and Markus, you were my first friends in this institute and gave me the confidence that my sense of humor is not totally isolated.

Thanks to Nils, Dani, Marion, Christo, Alex and Marina. You were my second lab family.
Thanks to Tina and Timo. You each should get your own paragraph and it would be beyond the scope of this work to mention all the great moments we have shared and all the deep discussion we had about everything from life to work. Thank you for being a part of my life!

Thanks to the laboratory of flow cytometry and cell sorting, Kerstin, Daniel Alex and especially Jenny Kirsch and Toralf Kaiser. I will never forget how I started and what I know now. Whenever the analyzers or sorters were causing trouble you saved my day. Frequently passing by in your lab without any flow cytometry problem was also always a great joy, at least for me.

Thanks to Virginie who saved me whenever I ran out of anything and to Angela, Regina and Ronaldo from the media kitchen. I still do not fully understand all the rules but I know you will always explain them again and again to me.

Thanks to the central lab management, Katrin, Manuela and Christin. Whether it was the fragment analyzer or antibody isolation or just me wondering where reagents are, you always helped and never judged me, at least in my presence.

Es gab allerdings schon Personen in meinem Leben, die vor der Dissertation eine wichtige Rolle gespielt haben.

Danke Mama und Papa für eure grenzenlose Unterstützung egal in welcher Hinsicht und welcher Phase meines Lebens. Danke auch an dich mein Schwesterherz. Du bist immer für mich da und hast mir im Frühjahr 2013 diese FU Email mit der freien Stelle der studentischen Hilfskraft am DRFZ geschickt.

Danke auch an dich Höffi. Wir kennen uns seit wir geboren sind und haben alle Lebensphasen gemeinsam durchlaufen. Ohne dich wäre das Studium nicht so gewesen und der Rest des Lebens auch nicht.

Danke an Sarah und Feli, meine Wegbegleiterinnen und Freundinnen aus Potsdam.

Danke auch an meine Freunde Florian, Patrick, Marius, Gerrit, Robert, Finn, Chenming, Lars, Kevin, Ilkan, Biff und Niklas. Ihr seid mein engster Kreis und dafür bin ich dankbar.

Zusammenfassung

Die Mikrobiota umfasst alle lebenden Mikroorganismen, die die äußeren und inneren Oberflächen des menschlichen Körpers, wie die Mundhöhle und den Darmtrakt, besiedeln, wobei die meisten zum Reich der Bakterien gehören. Die Darmmikrobiota spielt nicht nur eine wichtige Rolle bei verschiedenen Aspekten der menschlichen Gesundheit wie der Bereitstellung von Stoffwechselprodukten durch den Abbau unverdaulicher Fasern, der Verhinderung des Wachstums von Krankheitserregern und der Unterstützung der Entwicklung des Immunsystems, sondern wird auch mit entzündlichen Erkrankungen wie Spondylitis ankylosans, aber auch mit Virusinfektionen der Atemwege wie COVID-19 in Verbindung gebracht.

Einer der Mechanismen, der die Zusammensetzung der Darmmikrobiota steuert, wird durch Immunglobulin A (IgA)-Antikörper vermittelt, die von Plasmazellen (PC) produziert werden, die sich in der Lamina propria (LP) des Darms befinden. Obwohl bekannt ist, dass die PCs eine heterogene Population innerhalb der LP bilden, die unterscheidbar ist auf Grund der Expression von Ly6C, ist die Beziehung zwischen den verschiedenen Untergruppen bisher ungeklärt. Um zu verstehen, ob die Expression von Ly6C entwicklungsbedingte Unterschiede widerspiegelt, wurde das Transkriptom von $Ly6C^+$ und $Ly6C^-$ IgA^+ Zellen mittels Bulk-RNA-Sequenzierung bestimmt, die eine erhöhte Expression von Sca-1 in $Ly6C^+$ IgA^+ Zellen ergab, was zusätzlich durch eine Durchflusszytometrie-Analyse bestätigt werden konnte. Zusammen mit der verminderten Expression zellzyklusbezogener Gene und der Fähigkeit von $Ly6C^-$ PCs, Ly6C und Sca-1 Expression zu erwerben, zeigen diese Ergebnisse, dass $Sca\text{-}1^+Ly6C^+$-PCs eine differenziertere Untergruppe von IgA-sezernierenden PCs darstellen.

Außerdem wurde der Ursprung der SARS-CoV-2-spezifischen Antikörper bei nicht exponierten Personen bestimmt. Während angenommen wird, dass kreuzreaktive Antikörper von gesunden Personen von Erkältungs-Coronaviren stammen, identifizierten wir *Streptococcus salivarius*, ein Mitglied der intestinalen und oralen Mikrobiota, als Quelle für kreuzreaktive

IgA-Antikörper an Schleimhautoberflächen. Neutralisierende Anti-RBD-IgG-Antikörper, die aus Seren von hospitalisierten COVID-19-Patienten isoliert wurden, binden an *S. salivarius*, und die orale und fäkale Mikrobiota von schweren COVID-19-Fällen war im Vergleich zu gesunden Personen verändert, gekennzeichnet durch eine Abnahme von Streptococcus-Spezies, wie durch 16S rRNA Gen-Sequenzierung nachgewiesen wurde. Diese Ergebnisse zeigen die Beteiligung kommensaler Mikroben an der Induktion kreuzreaktiver SARS-CoV-2 RBD-spezifischer Antikörper an Schleimhautoberflächen.

Schließlich beobachteten wir mittels Mikrobiota-Durchflusszytometrie, dass die fäkale Mikrobiota von AS-Patienten einen verringerten Anteil lebensfähiger Bakterien aufwies, und die Analyse des Kompartiments lebender und toter Bakterien zusätzlich zur fäkalen Gesamtprobe ergab neue, krankheitsassoziierte Bakterientaxa, was die Notwendigkeit einer differenzierten Untersuchung der fäkalen Mikrobiota unterstreicht.

Insgesamt vertiefen die in dieser Arbeit gewonnenen Daten das Verständnis der wechselseitigen Beziehung zwischen der Mikrobiota und dem Immunsystem bei Virusinfektionen der Atemwege und chronischen autoinflammatorischen Zuständen.

Summary

The microbiota comprises all living microorganisms colonizing the external and internal surfaces of the human body, such as the oral cavity and the intestinal tract, with the majority belonging to the kingdom of bacteria. Besides playing a vital role in various aspects affecting human health like providing metabolites by breaking down indigestible fibers, preventing the outgrowth of pathogens and supporting the development of the immune system, the intestinal microbiota is associated with inflammatory diseases like Ankylosing Spondylitis (AS) but also respiratory viral infections like COVID-19.

One of the mechanisms controlling the intestinal microbiota composition is mediated by immunoglobulin A (IgA) antibodies, produced by plasma cells (PCs) residing in the intestinal lamina propria (LP). Even though it is known that PCs build a heterogeneous population within the LP based on the expression of Ly6C, the relationship between the different subsets remains to be clarified. In order to understand if the expression of Ly6C reflects developmental differences, the transcriptome of $Ly6C^+$ and $Ly6C^-$ IgA^+ cells was determined by bulk RNA sequencing, which revealed an increased expression of Sca-1 in $Ly6C^+$ IgA^+ cells, that could be additionally confirmed by flow cytometry analysis. Together with the decreased expression of cell cycle related genes and the ability of $Ly6C^-$ PCs to acquire Ly6C and Sca-1 expression, these results show, that $Sca\text{-}1^+Ly6C^+$ PCs represent a differentiated subset of IgA secreting PCs.

Further, the origin of SARS-CoV-2 specific antibodies in unexposed individuals was determined. While it is suggested, that cross-reactive antibodies from healthy individuals are derived from common cold coronaviruses, we identified *Streptococcus salivarius* a member of the intestinal and oral microbiota as a source for cross-reactive IgA antibodies at mucosal surfaces. Neutralizing anti-RBD IgG antibodies isolated from hospitalized COVID-19 patients sera bind to *S. salivarius* and the oral and fecal microbiota of severe COVID-19 cases was altered compared to healthy

individuals, characterized by a decrease in *Streptococcus* species as revealed by 16S rRNA gene sequencing. These findings show the involvement of commensal microbes in inducing cross-reactive SARS-CoV-2 RBD specific antibodies at mucosal surfaces.

Finally, we observed by microbiota flow cytometry that the fecal microbiota of AS patients displayed decreased frequencies of viable bacteria and the analysis of the live and dead bacteria compartment in addition to the bulk fecal sample revealed novel, disease-associated bacterial taxa, highlighting the need for a differentiated examination of the fecal microbiota.

Altogether, the data obtained in this work deepen the understanding of the mutualistic relationship between the microbiota and the immune system in respiratory viral infection and chronic auto-inflammatory conditions.

Contents

1 Introduction

The external and internal surfaces of the human organism are colonized by a variety of microorganisms, involved in maintaining crucial aspects of the body homeostasis. However, the majority of diseases are considered to be associated with alterations of the microbiota, among them autoimmune disorders with implications on the gastrointestinal tract, the central nervous system and the peripheral joints. Besides influencing aberrant immune responses, commensal microbes may affect protection against viral infections. Thus, it is essential to understand the interplay between the mucosal immune system and the complex microbial community to improve various aspects of human health.

1.1 The intestinal microbiome

The human body is densely populated by a plethora of microorganisms consisting of eukaryotes, bacteria, fungi, archaea and viruses. This microbial community, its characteristic properties and interactions with the environment can be defined as microbiome, and the human microbiome is specified as "the collection of all the microorganisms living in association with the human body" (Berg et al., 2020; Human Microbiome Project, 2007). The term "microbiota" refers to all living members of the microbiome thereby excluding phages, viruses and plasmids (Berg et al., 2020). In this work, "microbiome", "microbiota" and microbial cells refer to bacteria and bacterial cells as they by far outnumber archaea and eukaryotic cells and were the center of this investigation.

Microorganisms colonize internal and external surfaces of the human body including the skin, the oral cavity, the lung and the urogenital and intestinal tract (Dethlefsen et al., 2007). A recent estimation -based on an average male human- concluded that the number of bacteria ($\sim 3.8 \times 10^{13}$ cells) residing in and on the body is fairly equal to the number of human cells ($\sim 3.0 \times 10^{13}$ cells) and the majority of these bacterial cells can be found in

the large intestine (Sender et al., 2016). Although the intestinal microbiota is extremely diverse and consists of more than 1000 bacterial species highly varying between individuals, it is mainly composed of bacteria belonging to five main phyla *Firmicutes*, *Bacteroidetes*, *Actinobacteria, Proteobacteria* and *Verrucomicrobia* (Dethlefsen et al., 2007; Human Microbiome Project, 2012).

Initially, the identification of the microbes colonizing the human organism was based on the comparison of newly isolated strains with published, well described strains on the basis of morphology and phenotype. This approach was limited to culturable bacteria and failed to identify previously unknown bacterial species, before the highly conserved 16S rRNA gene was used as a reliable identifier for bacterial organisms and their taxonomic relationships. Nowadays 16S rRNA gene sequencing is the standard method to determine bacterial taxa in the entire gastrointestinal (GI) tract (Clarridge, 2004; Kroes et al., 1999; Savage, 1977; Schaedler et al., 1965)

The small intestine (SI) is the part of the digestive tract following the stomach and ending in the ileocecal valve, which marks the passage into the large intestine (LI) (Mowat and Agace, 2014). The SI comprises the duodenum, jejunum and ileum and its main physiological function is the absorption of nutrients derived from the digestion of dietary components like proteins, lipids and carbohydrates. In order to maximize the absorption capacity, the SI surface harbors villi that are finger-like projections elongating into the lumen to increase the absorptive surface (Mowat, 2003). Associated with the fast transit time of the upper SI tract, the low pH and the presence of pancreatic enzymes and bile, it is sparsely populated by microbes (Hillman et al., 2017; Kastl et al., 2020; Kurdi et al., 2006). In direction towards the colon the density of bacteria is gradually increasing from 10^{3-5} colony forming units (CFU) per ml in the duodenum to 10^{7-8} CFU/ml in the ileum (Kastl et al., 2020; Sender et al., 2016).

Due to technical challenges it is difficult to reliably determine the microbiota composition of the human SI compartments. In general, the phylum *Proteobacteria* is more abundant in the SI compared to colon or stool

bacteria, whereas bacteria belonging to the phylum *Firmicutes* form a major fraction at both sites (Leite et al., 2020). One of the factors affecting the microbial constitution in the intestine is the concentration of oxygen (O_2). Even though intestinal O_2 concentrations are difficult to determine, it is believed that the duodenum and jejunum harbor low concentrations of oxygen, whereas the ileum and the large intestine are considered to be mostly anaerobe (Friedman et al., 2018; He et al., 1999). A radial oxygen gradient is additional present as O_2 diffusing across the intestinal epithelium is utilized by aerotolerant mucosa-associated bacteria, resulting in an anaerobic lumen, characterized by different bacterial species (Albenberg et al., 2014).

The LI is divided into caecum, ascending colon, transverse colon, descending colon, rectum and anus. Its physiological functions are the reabsorption of water and minerals and the disposal of undigested food particles (Mowat and Agace, 2014). Conversely to the upper small intestinal tract, the transit of the luminal content is slower and the digestive activity smaller, thereby providing optimal growth conditions for bacteria (Muller et al., 2018). This is why the vast majority of the microbes residing in and on the human host are located in the LI (Sender et al., 2016).

Fecal samples are used as a surrogate for colonic content. Even though they cannot reflect the bacterial flora at every single niche in the colon such as the mucosa, the fecal microflora accurately resembles the aggregate bacterial flora of the LI (Hillman et al., 2017; Hold et al., 2002). A variety of factors influence the colonic microbiota composition like genetic variability, age, diet and diseases (David et al., 2014; Durack and Lynch, 2019; Falony et al., 2016; Leeming et al., 2019; Wang et al., 2016). However, the human fecal microbiota consists mainly of the five phyla *Firmicutes* and *Bactroidetes* followed by *Actinobacteria*, *Proteobacteria* and *Verrucomicrobia* (Dethlefsen et al., 2007).

1.2 Microbiota derived fermentation products ensure host homeostasis

The microbiota and human host have a mutualistic relationship. The host provides the commensal microbiota with a habitat and nutrients and in turn benefits from bacterial fermentation products and metabolites.

In order to absorb nutrients, dietary components need to be processed by digestive enzymes. This chemical digestion begins in the oral cavity with amylases in the saliva and is continued in the stomach containing the gastric acid. After the chyme enters the duodenum, it encounters digestive enzymes produced by the pancreas (lipase, protease and amylase) and bile secreted from the gallbladder (Patricia and Dhamoon, 2022). Thus, lipids, proteins and distinct carbohydrates are broken down to some extent, whereas dietary fibers like resistant starches and pectin are not degraded by endogenous enzymes but are fermented by bacteria in the colon. The fermentation products of non-digestible fibers are short chain fatty acids (SCFAs) with butyrate, propionate and acetate considered to be the most relevant (Wong et al., 2006). They beneficially affect various aspects of the human metabolism e.g. intestinal gluconeogenesis, lipogenesis, the cholesterol metabolism and additionally functioning as energy source for colonocytes, thereby ensuring hypoxia at the epithelial surface (De Vadder et al., 2014; Valdes et al., 2018; Wong et al., 2006). Several microbes are equipped with genes enabling them to produce SCFAs and their absence due to low-fiber consumption is associated with cardiovascular diseases, obesity and type 2 diabetes (Lu et al., 2016; Tang et al., 2013; Valdes et al., 2018; Zhao et al., 2018). Obligate anaerobe bacteria belonging to the classes *Clostridia* and *Bacteroidia* express a variety of enzymes for breaking down complex carbohydrates, resulting in SCFAs production. Consequently, their presence in the colonic microbiota community is regarded as favorable over facultative anaerobes belonging to the phylum *Proteobacteria*, which are less potent in carbohydrate consumption (Litvak et al., 2018).

SCFAs directly influence the mucosal immune system. For example butyrate induces the differentiation of colonic regulatory T cells (T_{reg}) and promotes epithelial barrier integrity (Arpaia et al., 2013; Furusawa et al., 2013; Zheng et al., 2017).

Besides complex carbohydrates, the intestinal microbiota metabolizes food derived amino acids like tryptophan and L-carnitine into indoles and trimethylamine (TMA) respectively, which occurs predominantly in the SI (McCarville et al., 2020). The aryl hydrocarbon receptor (AhR) binds the indole ligands, leading to its activation which increases epithelial barrier integrity and IL-22 production by T cells and innate lymphoid cells (ILCs). In inflammatory bowel disease (IBD) patients as well as in experimental colitis models that reconstruct IBD symptoms, a decreased expression of AhR in intestinal tissues was observed (Goettel et al., 2016; Monteleone et al., 2011). The microbiota influences additionally the presence of the amino acids derived neurotransmitters serotonin, catecholamines and gamma-amino butyric acid (GABA) as demonstrated in germ-free mice (McCarville et al., 2020).

Although it is evident that the intestinal microorganisms have a plethora of beneficial effects in terms of digestive support, they have to be prevented from intruding the host organism and their composition has to be tightly controlled in order to impede the outgrowth of virulent pathogens. In this context, immune cells play a key role in homeostasis and the surveillance of barrier tissues.

1.3 The mucosal immune system of the intestine

The intestine represents the largest surface of the body that is in constant contact with microorganisms and thereby potential pathogens and is protected from infections by the mucosal immune system. However, when dysregulated, immune cells have been shown to be involved in the pathogenesis of chronic inflammatory conditions as observed in IBD (Zenewicz et al., 2009).

The intestinal mucosa consists of an epithelial cell (EC) layer, underlying connective tissue called lamina propria and the muscularis mucosa representing the muscle layer of the gastrointestinal tract. Goblet cells in the EC produce mucin glycoproteins that form a mucus layer covering the epithelium. This so called glycocalyx provides a first line of defense as a physical barrier preventing most of the microbiota from direct contact with the EC as well as acting as a scaffold for immunoglobulin A (IgA) antibodies and antimicrobial peptides (AMPs), by that controlling microbial invasion. While in the colon the glycocalyx comprises an inner and outer layer, the SI mucus only builds one layer, due to lower abundance of goblet cells and the instant detachment of the mucin glycoproteins from the epithelial cells by the meprin-β protease (Johansson and Hansson, 2016; Mowat and Agace, 2014). Paneth cells are solely present in the SI and produce AMPs like regenerating islet-derived protein IIIα (REGIIIα), REGIIIγ and α- and β-defensins that shape the microbiota composition (Salzman et al., 2007).

The lamina propria (LP) is localized underneath the ECs, separated by a basal membrane from the epithelium. Blood and lymph vessels and consequently immune cells belonging to the innate and adaptive immune system reside in the lamina propria. The gut associated lymphatic tissue (GALT) consisting of Peyer's Patches (PPs), colonic patches and isolated lymphoid follicles (ILFs), as well as mesenteric lymph nodes (mLNs) are the sites for priming adaptive immune responses in the intestine (Mowat, 2003; Suzuki et al., 2010).

PPs are located in the submucosa of the SI and contain B cell follicles with germinal centers (GCs), surrounded by a T cell area. In contrast to systemic lymph nodes, PPs lack afferent lymphatics and do not obtain antigens via the blood but directly from the lumen of the SI, which is enabled by their specific anatomical properties. The epithelial layer covering the lymphoid structures of the PP is termed follicle-associated epithelium (FAE) and comprises microfold cells (M cells) as the major cell type. These specialized epithelial cells lack microvilli and a glycocalyx and are therefore in direct contact with intestinal antigens, which they transport into the subepithelial

dome (SED). There, dendritic cells, macrophages, T cells and B cells induce immune responses resulting in effector cells residing in the LP (Suzuki et al., 2010).

The organized lymphoid tissues similar to PPs in the LI are called colonic patches. Both structures develop prenatally but exogenous antigen stimuli from the microbiota induce their final differentiation as e.g. PPs in germ-free rodents are smaller and lack GCs (Pollard and Sharon, 1970; Reboldi and Cyster, 2016; Yamanaka et al., 2003).

ILFs are located in the mucosa throughout the SI and LI and consist of B cell follicles, dendritic cells and innate lymphoid cells but lack a distinct T cell zone. ILFs develop after birth and their maturation in the SI is driven by dietary components affecting the regulatory AhR pathway and the microbiota (Buettner and Lochner, 2016; Kiss et al., 2011; Pabst et al., 2006).

The immune reactions occurring in the GALT result in IgA-secreting plasma cells (PCs) localized in the LP. Their main inductive sites are the Peyer's and colonic patches.

1.4 Intestinal Plasma cell development

Naive B cells enter the PPs through high endothelial venules (HEVs), orchestrated by L- selectin, CCR7, CXCR4 and α4β7 integrin (Okada et al., 2002; Reboldi and Cyster, 2016). Expression of CXCR5 on naive B cells allows CXCL13 mediated migration to the follicles (Cyster and Allen, 2019; Okada et al., 2002). Once the B lymphocytes encounter their antigen and receive additional engagement of CD40, CCR6 expression is induced, which enables B cells to migrate to CCL20 secreted by DCs in the SED. There, transforming growth factor β (TGF-β) instructs subsequent IgA class-switching of activated B cells, which return to the follicle and enter the GC (Reboldi et al., 2016).

The GCs are the sites of affinity maturation where B cell proliferation, somatic hypermutation (SHM) and class switch recombination (CSR) occur.

Follicular dendritic cells (FDCs) in the GC, specialized in presenting antigen, can constantly engage with the B cell receptor (BCR) and select for high-affinity B cell receptors, thereby providing signals for CSR (Suzuki et al., 2010). Both processes, SHM and CSR, are dependent on the enzyme activation-induced cytidine deaminase (AID) expressed by B cells (Muramatsu et al., 2000). In order for AID to enable CSR from IgM and IgD to IgA, germline transcription of the constant region α (C_α) gene is necessary. TGF-β produced by GC cells like FDCs, T follicular helper cells (T_{FH}) and B cells is responsible for this induction of transcription (Cazac and Roes, 2000; Cerutti, 2008; Lebman et al., 1990).

Other factors augmenting IgA CSR and IgA production are nitric oxide (NO), a proliferation inducing ligand (APRIL) and B cell-activating factor (BAFF) (Cerutti, 2008; Reboldi and Cyster, 2016).

BAFF and APRIL induce IgA class-switching by directly inducing Cα germline transcription and AID expression through binding to the transmembrane activator and calcium-modulating cyclophilin-ligand interactor (TACI) receptor on B cells even in the absence of T cells, whereas NO induces upregulation of the TGFβ receptor on B cells (Castigli et al., 2005; Cerutti, 2008; Tezuka et al., 2007). Mirroring their role in class switching processes, TACI- and T cell-deficient mice harbor severely decreased numbers of IgA^+ PC in the SI (Grasset et al., 2020).

Furthermore, IL-21 produced by T_{FH} also plays a critical role in promoting IgA CSR as it induces the expression of the AID encoding gene *Aicda* and specifically in combination with TGF-β enhances IgA CSR (Cao et al., 2015; Lycke and Bemark, 2017).

The activated B cell leaves the GC and B cell follicle by downregulating CCR7 and upregulating CXCR4. Increasing expression of Sphingosine-1-phosphate receptor 1 (SiPR1) allows activated B cells to egress from the Peyer's Patch (Gohda et al., 2008). Through efferent lymphatics they migrate to the mesenteric lymph nodes, enter the blood stream via the thoracic duct and ultimately reenter the SI LP where they reside producing IgA. Homing to the intestinal LP is facilitated by expression of CCR10, CCR9

and integrin $\alpha_4\beta_7$, the latter being induced by retinoic acid and TGFβ in the Peyer's Patches (Mora et al., 2006). The ligands for CCR9 and CCR10, namely CCL25 and CCL28, are produced by SI EC and mainly LI EC respectively (Kunkel et al., 2000; Pan et al., 2000). Within the LP, activated B cells fully differentiate into IgA-secreting plasma cells, which is generally marked by downregulation of the transcription factors paired box protein 5 (Pax5) and B-cell lymphoma 6 (Bcl-6), and the interferon-regulatory factor 4 (IRF4)-induced expression of B lymphocyte-induced maturation protein-1 (BLIMP-1) that determines PC development (Nutt et al., 2007; Turner et al., 1994).

Additionally, the transcription factor X-box binding protein 1 (XBP1) is required for PC differentiation and ensures the capacity of the PCs to secrete antibodies, by expanding the endoplasmic reticulum (ER) (Reimold et al., 2001; Shaffer et al., 2004).

Besides the described T cell dependent induction of IgA CSR, T cell independent mechanisms exist. In the absence of T cell-derived CD40 signaling in CD40 KO mice the levels of intestinal IgA are not decreased and mice lacking T cells still harbor IgA^+ PCs (Bergqvist et al., 2006; Macpherson et al., 2000).

Inside the PPs BCR engagement in combination with innate signaling pathways like Toll-like receptors (TLRs) induce IgA CSR in the presence of BAFF, APRIL and TGF-β without involvement of T cells (Pabst, 2012). Apart from PPs, T cell-independent IgA CSR occurs in ILFs. The presence of IgA CSR directly in the LP has also been suggested (Fagarasan et al., 2001).

1.5 Heterogeneity of plasma cell populations in the LP

Intestinal plasma cells are mainly characterized by their ability to produce large amounts of IgA antibodies, which are transported across the EC layer and contribute to the regulation of the microbiota composition. Moreover, they built a heterogeneous population diverse in cytokine production, ontogeny and capacity to protect against infection.

A subset of IgA-secreting PC in the murine SI LP produces inducible nitric oxide synthase (iNOS) and tumor necrosis factor (TNF), which positively correlates with serum IgA concentrations. These PCs can additionally display lymphocyte antigen 6C (Ly6C), Ly6G or CD11c on their surface. Interestingly, the expression of iNOS is microbiota-dependent and the Mammalian Target of Rapamycin (mTOR) promotes the expression of Ly6C (Benhamron et al., 2015; Fritz et al., 2011; Wrammert et al., 2002).
Further, CD11b can be found on PCs in the intestine if microbiota-derived and MyD88-directed signals are present. IL-10 is crucial for maintaining these $CD11b^+$ IgA^+ PCs in the LP, where they show a greater proliferation capacity compared to IgA-secreting PCs lacking CD11b (Kunisawa et al., 2013). In the absence of T cell-signaling no $CD11b^+$, $Ly6C^+$ or $Ly6G^+$ PC can develop, although their development takes place independently of PPs or ILFs (Winsauer et al., 2015).
Recently another PC subset was identified, expressing αE(CD103)β7 (Guzman et al., 2021). Based on the upregulation of Blimp-1 and downregulating of Pax5, Aicda and especially Mki67, they represent terminally differentiated PCs. The amount of IgA transported into the lumen of the SI depends on these CD103-positive PCs, as they directly interact with E-cadherin on polymeric Ig receptor (pIgR) expressing ECs and αE-deficient mice harbored less IgA in their intestinal lumen (Guzman et al., 2021).

1.6 IgA: the major mucosal immunoglobulin

IgA is the main antibody produced at mucosal surfaces (Brandtzaeg, 2009; Chodirker and Tomasi, 1963). Besides the monomeric isoform present in the serum, IgA antibodies can build polymeric structures with 2 monomers that are linked at their fragment crystallizable (Fc) region by the joining (J) chain, produced by the IgA-secreting PC (Brandtzaeg, 1974b; Woof and Russell, 2011). The J chain in combination with the Fc region builds the binding site of the pIgR expressed on the basolateral membrane of intestinal

ECs, thereby enabling the transcytosis of dimeric IgA across the EC layer into the intestinal lumen (Brandtzaeg, 1974a; Johansen et al., 2001; Pabst and Slack, 2020). The extracellular domain of the pIgR is cleaved via proteolysis on the luminal surface, resulting in so-called secretory IgA (SIgA), dimeric IgA covalently bound to the cleaved portion of the pIgR, the secretory component (SC) (Pabst and Slack, 2020).

In humans but not in mice, two isotype forms exist: IgA1 and IgA2. IgA1 is the predominant isoform in the serum (90% IgA1 and 10 % IgA2) and the SI, whereas IgA2 is predominant in the colon (Brandtzaeg and Johansen, 2005). The isotypes differ in their length of the hinge region -which comprises 16 amino acids in IgA1 and 8 amino acids in IgA2- as well as in their glycosylation pattern.

The IgA antibody, the hinge region, the J chain and the SC are sites for decoration with O-linked (hinge region of IgA1) and N-linked glycans. The glycosylation protects the IgA antibody from degradation by proteases and can mediate the association between IgA and the mucus layer (Woof and Russell, 2011).

Binding of SIgA to the microbiota is mediated by complementarity-determining regions (CDRs) of the variable domain of the fragment antigen binding (Fab) region which is referred to as canonical binding and by Fc-mediated interactions, also known as noncanonical. Noncanonical binding occurs, when IgA glycans react with microbial glycan motifs (Royle et al., 2003; Wold et al., 1990).

Hence, a single IgA antibody potentially targets different members of the intestinal microbiota by Fab- and glycan-mediated interactions (Pabst and Slack, 2020).

IgA antibodies mostly bind to antigens displayed on the surface of bacteria, like peptide or glycan structures (Huus et al., 2021; Li et al., 2020). Therefore, diverse subsets of intestinal microbiota can be targeted by monoclonal IgA, if the antigen is shared between different bacteria. This cross-species reactivity could be promoted by protein structures like flagellin, or glycans like lipopolysaccharide (LPS) (Cullender et al., 2013;

Rollenske et al., 2018). Interestingly, recombinantly produced antibodies containing the Fab region of murine intestinal IgA bind various unrelated antigens such as LPS, CpG and insulin indicating a certain degree of polyreactivity. This polyreactivity is also present in germline reversed status and absent of SHM (Bunker et al., 2017). However, the majority of IgA present in the adult intestine is highly mutated, and other studies have shown that cross-species reactivity is indeed depended on SHM (Kabbert et al., 2020; Pabst and Slack, 2020; Rollenske et al., 2018).

1.7 Induction of IgA by the microbiota

The induction of intestinal IgA production and the maturation of the related lymphoid structures are dependent on the commensal microbiota. In this regard, germ-free mice and neonates have strongly reduced amounts of IgA-secreting cells in their intestinal mucosa prior to colonization with commensal microbiota, which was also observed in new born humans and germ-free mice lack intestinal SIgA (Gronlund et al., 2000; Macpherson et al., 2000; Macpherson et al., 2008; Moreau et al., 1978). Consistently, the number and size of GCs in the PPs are drastically reduced by disrupting the intestinal microbiota with antibiotics, and ILFs and GC are absent in germ-free animals (Casola et al., 2004; Fagarasan et al., 2002; Pollard and Sharon, 1970; Suzuki et al., 2010).

The intestinal IgA response in germ-free mice transiently colonized with the mutant *E. coli* strain HA107 is stable even in absence of the initial antigens. This induction of IgA depends on the amount of colonizing microbes and needs to exceed a certain threshold. However, once a complex consistent microbiota is introduced, the HA107-specific SIgA concentrations decrease, suggesting that the IgA response is shaped by predominant microbial antigens present in the intestine (Hapfelmeier et al., 2010).

Mucosa-adhesive bacteria like segmented filamentous bacteria (SFB) induce the production of IgA (Talham et al., 1999). SFB attach to ECs in the terminal ileum of mice where it induces the maturation of ILFs, activate GCs

in PPs and promote the development of Th17 cells (Gaboriau-Routhiau et al., 2009; Ivanov et al., 2009; Lecuyer et al., 2014). In IgA-deficient mice SFB rapidly expand, which is abolished once IgA is reconstituted (Suzuki et al., 2004). Attachment of SFB to the host ECs is crucial to promote IgA production, thus SFB induces a self-limiting immune response (Atarashi et al., 2015). Likewise, *Bacteroides ovatus* is capable of IgA induction in germ-free mice but this ability is strain-specific (Yang et al., 2020).
Interestingly, *Anaeroplasma*-enriched microbiota induce TGF-β expression of intestinal T_{FH} cells, resulting in enhanced intestinal IgA levels (Beller et al., 2020).
Therefore, microbial antigens have a pivotal role in intestinal IgA induction and host defense.

1.8 Mechanisms of IgA-mediated microbiota control

The main function attributed to IgA is to maintain a homeostatic microbiota composition while preventing the outgrowth of pathogens and consequently infections, as well as neutralizing bacteria-derived toxins like cholera toxin (CT) (Macpherson et al., 2008).
"Immune exclusion" describes the IgA-mediated hindrance of bacteria to attach to the EC layer. At high bacterial densities the microbes are cross-linked by IgA antibodies, which leads to agglutination, whereas at low bacterial densities IgA links proliferating bacteria to their own daughter cells; a process that promotes clearance of antigens and pathogenic microorganisms (Hoces et al., 2020; Huus et al., 2021). Therefore, antibody-deficient mice have increased bacterial translocation towards the mLNs, and AID-deficient mice have an expansion of anaerobic bacteria in the SI (Fagarasan et al., 2002; Macpherson and Uhr, 2004). Another mechanism, by which IgA controls the composition of the microbiota is represented by the enchaining of *Salmonella Typhimurium*, protecting against disease during murine infections (Moor et al., 2017). Moreover, binding of IgA to immunogenic structures like LPS on *Salmonella enterica*

decreases its flagella-mediated motility and blocks epitopes on the pathogen required for EC receptor recognition and subsequent invasion (Forbes et al., 2008; Mantis et al., 2011). Additionally, targeting of *E. coli* in gnotobiotic mice by monoclonal IgA antibodies alters bacterial gene expression and motility (Rollenske et al., 2021). Further, SFB attachment to the EC of the terminal ileum is abolished in the presence of IgA (Lecuyer et al., 2014; Suzuki et al., 2004). Altogether, there are several regulatory pathways mediated by IgA which prevent specific microbes from reaching and invading the mucosal surface. Of note, the intestinal microbiota from IBD patients highly coated with IgA displayed colitogenic properties in mice suggesting that IgA is directed against inflammatory bacteria (Palm et al., 2014).

Remarkably, several grams of IgA are produced and secreted daily into the intestinal lumen in absence of infections and a substantial fraction of commensal bacteria are coated by IgA (Conley and Delacroix, 1987; Huus et al., 2021). Hence, IgA maintains and potentially promotes the colonization of commensal microbiota without inflammatory potential.

Even though the exact mechanisms remain elusive, different models and studies suggested potential scenarios. Contrary to SFB, the epithelium-associated species *Bacteroides fragilis* is utilizing IgA for mucus colonization by expressing "commensal colonization factor" (CCF) genes regulating the synthesis of capsular polysaccharides responsible for IgA binding (Donaldson et al., 2018). In addition, it was shown that commensal bacteria induce the expression of polysaccharide utilization loci (PUL) upon binding to IgA. The interaction between glycans on IgA and LPS on *Bacteroides thetaiotaomicron* (*B. theta*) promotes its attachment to the mucus layer. There, *B. theta* induces the expression of Mucus-associated Functional Factor (MAFF), leading to increased intrinsic metabolic activity, which at the same time results in the expansion of Clostridiales members within the mucus layer. This alteration of the microbial composition protected mice from DSS-induced colitis (Nakajima et al., 2018). Furthermore, in *B. theta* monocolonized mice, IgA-targeting suppresses the expression of the

capsular polysaccharide synthesis 4 (CPS4) locus, while inducing the expression of CPS5, potentially leading to immune evasion (Peterson et al., 2007). Together, intestinal bacteria adapt their polysaccharide expression in response to IgA binding.

Besides this direct utilization of IgA antibodies, more general models have been proposed, suggesting that IgA antibodies and their glycans form biofilms with the commensal bacteria and the mucus layer, thereby enabling inter-species interactions resulting in survival advantages. In vitro, human secretory IgA promotes biofilm formation with a commensal flora and *E.coli* (Bollinger et al., 2003). The host secretion of e.g., IgA and mucus, maintains the diversity of adhesive microbes in a simulation-based model and potentially selects for particular bacteria. Depending on intestinal fluid dynamics and the bacterial growth rate a mucosa-associated biofilm could promote or be detrimental for adhesive bacterial colonization (Hoces et al., 2020; McLoughlin et al., 2016). Notably, the intestinal fluid dynamics, such as flow rates, are increased under inflammatory conditions, thereby affecting microbiota composition (Bassotti et al., 2004).

1.9 Influence of the intestinal microbiota on ankylosing spondylitis

The intestinal microbiota plays a crucial role in maintaining the body homeostasis by influencing a variety of physiological processes. However, the majority of auto-inflammatory diseases are associated with changes in the microbiota composition. The disruption of the bacterial community in comparison to the composition of healthy individuals can be defined as dysbiosis. For several inflammatory diseases affecting the GI tract, such as Crohn's disease (CD) and Ulcerative colitis (UC) but also for the inflammatory pathology of joints and the central nervous system, e.g. rheumatoid arthritis (RA), multiple sclerosis (MS) and ankylosing spondylitis (AS), associations to a dysregulated microbiota have been reported (Maeda and Takeda, 2017; Mauro et al., 2021; Petersen and Round, 2014).

However, whether the inflammatory condition are cause or consequence of a dysbiosis remains to be clarified.

Inflammatory diseases affecting the spine and peripheral joints, in the absence of rheumatoid factor are collectively described as Spondyloarthritis (SpA). AS is an axial SpA with inflammatory sites at the spine and sacroiliac joints, resulting in compromised reconstruction of the bone, and thus ankylosis. Several risk alleles have been identified associated with IL-23, IL-17 and TLR4 signaling pathways (Mauro et al., 2021). However, among the discovered risk genes, the major histocompatibility complex class I (MHCI) variant, human leukocyte antigen B27 (HLA-B27), accounts for up to 30% of genetic predisposition and ≤90% of individuals suffering from AS are HLA-B27$^+$ (Braun and Sieper, 2007). In this context, it has been shown that the intestinal microbiota is altered in healthy individuals that carry HLA-B27 (Asquith et al., 2019). Additionally, the fecal microbiota of transgenic rats expressing human HLA-B27 differs from their littermates and a major fraction of these rats develop intestinal inflammation and spondylitis which is diminished under germ-free conditions and dependent on the microbiota composition (Onderdonk et al., 1998; Taurog et al., 1994). Various mechanisms on how HLA-B27 enhances disease progression have been postulated. Among them, that HLA-B27 preferentially presents bacterial peptides in the intestine which resemble self-peptides, resulting in inflammation in the spine or sacroiliac joints, highlighting again the interaction between the immune system and intestinal microbes for the occurrence of AS (Diaz-Pena et al., 2020).

Further, several other risk factors have been described and comorbidities of AS include uveitis, psoriasis and IBD (Mauro et al., 2021). AS strongly correlates with subclinical intestinal inflammations, which are able to develop into IBD (De Vos et al., 1989; De Vos et al., 1996).

Various studies have reported alterations in the intestinal microbiota of AS patients compared to healthy individuals but no AS-specific composition could be determined. An increase in *Prevotella copri* and a decrease in *Bacteroides* species in AS fecal samples was reported collectively in different

reports, however other studies did not confirm these findings (Klingberg et al., 2019; Wen et al., 2017; Yin et al., 2020; Zhang et al., 2019a; Zhou et al., 2020a).

The mechanisms how the microbiota affects AS are not completely understood but it was suggested, that intestinal bacteria-derived molecules could induce an inflammatory reaction. A peptide from the nitrogenase of *Klebsiella pneumonaie* and a peptide found in the DNA primase from *Chlamydia trachomatis* are similar to peptides derived from HLA-B27, thereby potentially leading to autoimmune reactions involving HLA-B27 (Ramos et al., 2002; Schwimmbeck and Oldstone, 1988).

1.10 Molecular mimicry: implications in autoimmunity

The microorganisms residing in the GI comprise millions of genes which represent a plethora of putative antigens (Tierney et al., 2019; Yang et al., 2009). Some of these antigens resemble self-structures and this molecular mimicry can potentially lead to autoimmune responses at various body sites.

The principle of molecular mimicry was initially described in the early 1980s. A monoclonal antibody specific for the large T protein of the simian virus 40 (SV40) also recognized an unidentified host protein (Lane and Hoeffler, 1980). A similar cross-reactivity was found for different monoclonal antibodies binding to the phosphoprotein of the measles virus and the herpes simplex virus (HSV) protein and the human intermediate filament protein vimentin, which is part of the cytoskeleton (Fujinami et al., 1983). Implications of such cross-reactivity for autoimmune diseases was reported in myasthenia gravis (MG). MG is characterized by autoantibodies directed against the acetylcholine receptor (AChR). The type 1 glycoprotein D of HSV contains a sequence homologous to a sequence found in the α-subunit of the AChR, and anti-AChR antibodies from the serum of MG patients were found to be cross-reactive to HSV (Schwimmbeck et al., 1989).

Antigens derived from intestinal bacteria similar to self-antigens can influence autoimmune reactions outside the gut. The bacterial aquaporin-Z protein shares homologous regions with the human aquaporin-4 protein, which is a target of auto-reactive antibodies in the chronic inflammatory disease neuromyelitis optica (NMO). Immunization of mice with aquaporin-Z resulted in an auto-immune reaction directed against aquaporin-4 and subsequent inflammation of the murine brain (Ren et al., 2012). A β-galactosidase (β-gal) from the commensal *B. theta* is similar to a peptide of the myosin heavy chain 6 (MYH6) that is targeted by autoreactive T cells in myocarditis. In a mouse model of spontaneous autoimmune myocarditis, *B. theta* expressing the β-gal peptide similar to MYH6 promoted disease progression towards an inflammatory cardiomyopathy (Gil-Cruz et al., 2019).

In general, cross-reactivity is not necessarily leading to autoimmune reactions. Instead, the intestinal microbiota can also confer protection against microbial and viral respiratory infections. In this context, mice treated with antibiotics are more susceptible to infection with influenza and *Pseudomonas aeruginosa* pinpointing towards a beneficial role of the microbiota during these infections (Ichinohe et al., 2011; Robak et al., 2018). Underlining this concept, the administration of intestinal microbiota-specific monoclonal IgA antibodies prior to *Pseudomonas aeruginosa* exposure diminished their susceptibility for infection, suggesting a protective effect of cross-reactive antibodies (Robak et al., 2018).

Moreover, bacterial antigens recognized by antibodies derived from intestinal PCs are not only present on host cells, but also displayed by viruses. Antibodies derived from the blood plasma of acute HIV-1-infected patients directed against the virus envelope protein (gp41) have been shown to cross-react to commensal bacteria. Importantly, these cross-reactive antibodies originate in the intestine and are also found in uninfected individuals (Trama et al., 2014).

With the emergence of the Coronavirus Disease 2019 (COVID-19) pandemic, we investigated to which extend the commensal microbiota

influence immune responses towards Severe acute respiratory syndrome (SARS) coronavirus 2 (SARS-CoV-2).

1.11 SARS-CoV-2: a respiratory virus leading to gastro-intestinal manifestations

SARS-CoV-2 is a β-coronavirus comprising a single-strand of positive-sense RNA enveloped by a nucleoprotein (N), decorated with E and M transmembrane proteins and the Spike (S) glycoprotein (Klein et al., 2020). The S protein contains a receptor-binding domain (RBD) responsible for the interaction with angiotensin-converting enzyme 2 (ACE2), the receptor enabling SARS-CoV-2 to enter the host via respiratory surfaces (Hoffmann et al., 2020). ACE2 is expressed in the upper respiratory tract, on alveolar epithelial cells in the lung but also in the heart, kidney, liver and ileum (Zou et al., 2020). Once SARS-CoV-2 has entered the organism it can reach and replicate at various body sites including the GI tract. Besides infecting cells of the respiratory tract, SARS-CoV-2 is also able to infect intestinal enterocytes expressing high levels of ACE2 and viral RNA can be detected in fecal samples of hospitalized COVID-19 patients (Lamers et al., 2020; Xiao et al., 2020). Further, intestinal manifestations like diarrhea co-occur with SARS-CoV-2 infection and the intestinal microbiota of severe COVID-19 cases is altered compared to healthy individuals (Hung et al., 2021; Zuo et al., 2020). Hence, the intestinal mucosal immune system and the microbiota might be affected by COVID-19 pathogenesis.

Antibodies binding SARS-CoV-2 RBD block its interaction with ACE2, thereby preventing viral infection (Ju et al., 2020). SARS-CoV-2 virulence is additionally inhibited upon antibody binding to other epitopes derived from the S protein, specifically the N-terminal domain (NTD) (Liu et al., 2020). Serum antibodies like IgG, IgM and IgA are beneficial for clearance of the virus and act via ablation of virus reproduction. Thus, early response antibody concentrations correlate with the severity of the disease course (Dispinseri et al., 2021).

In order to prevent the initial infection, SARS-CoV-2-specific antibodies at mucosal surfaces like IgA1, IgA2 and IgM could be crucial (Mao et al., 2022; Renegar et al., 2004). In this regard, severely diseased COVID-19 patients lack IgA2 antibodies specific to SARS-CoV-2, implicating their potential relevance for disease progression (Ferreira-Gomes et al., 2021).
Interestingly, likewise to HIV-1 envelope cross-reactive antibodies, unexposed individuals harbor antibodies specific for SARS-CoV-2. In particular, predominantly serum IgG reactive to the S2 subunit of the S protein and RBD was detected (Majdoubi et al., 2021; Ng et al., 2020).
Even though it is assumed that these antibodies are derived in response to common cold coronaviruses, the original antigen source leading to the induction of cross-reactive RBD-specific secretory IgA antibodies is still unidentified.

2 Aims

The aim of this thesis was to understand the impact of the microbiota on immune responses present upon viral infections and auto-inflammatory conditions.

In order to firstly clarify the mechanisms of microbiota control, the heterogeneous population of IgA-secreting PCs of the murine SI was characterized.

Further, the involvement of the fecal microbiota in enhancing SARS-CoV-2 immunity was investigated, as SARS-COV-2 cross-reactive antibodies are present in unexposed healthy individuals but their origin has not been identified yet. Lastly, to closely examine the influence of intestinal microbes on the emergence and progression of AS, the composition of the proliferating live and compromised dead microbiota compartment was assessed with the pivotal goal to reveal novel disease-associated bacterial taxa, which may serve as Biomarkers.

Aims

3 Materials and Methods

3.1 Microbiota Flow Cytometry

3.1.1 Live/Dead microbiota staining

Fecal material from AS patients and healthy individuals was weighed and suspended in PBS (10 µl/µg) and passed through a 30 µM filter. After a centrifugation step (5 min, 13.000 rpm, 4°C) the supernatant was collected and sterile filtered through a 0.22 µM syringe top filter and stored at -20 °C for later use. The bacterial pellet was re-suspended in 25 ml PBS and the OD was adjusted to 0.5 and subsequently centrifuged for 10 min at 4000 rpm and 4°C. The pellet was re-suspended in 1 ml of PBS and 200 µl were used per staining on a 96 well plate, whereas the remaining sample was stored in 1 ml of 40% glycerol in LB medium mixture at -80°C, with 1 ml containing approximately an OD of 0.8. Following another centrifugation step, the bacterial pellets were re-suspended in 50 µl PBS containing SytoBC (1:125, v/v) and incubated for 15 min at 4°C. Another washing step was performed (3000 rpm, 5 min, 4°C) prior to incubating the bacteria with 1:1000 DAPI in PBS (v/v) for 15 min at 4°C. The samples were washed once more and measured using a BD Influx cell sorter. The quality of each acquisition was assured by the alignment of lasers, laser delays and laser intensities by Sphero™ Rainbow Particles. For sorting, the drop delay was determined prior with Accudrop Beads. Samples were acquired with an event rate below 15,000 events and sorted with an event rate below 10,000 events and analyzed using FlowJo v10 analysis software.

From the post-sorted fraction 200 µl were incubated with SytoBC (1:400, v/v) and DAPI (1:400, v/v) simultaneously for 10 min at 4°C and measured to determine the purity of the sort.

If possible, a number of 18,000,000 live and dead cells were sorted and centrifuged for 10 min at 4000 rpm. The pellet was re-suspended in 750 µl

PBS and divided into three aliquots, centrifuged at 14000 rpm for 5 min and stored at -80°C once the supernatant was removed.

Table 1. Reagents to determine live microbiota fraction

Reagent	**Source**	**Identifier**
SytoBC	Life Technologies	Cat. No. #S34855
DAPI	In house	N/A
PBS	In house	N/A
LB	In house	N/A
Glycerol	Roth	Cat. No. #3783.1
Sphero™ Rainbow Particles	BD Biosciences	Cat. No. #559123
Accudrop Beads	BD Biosciences	Cat. No. #345249
BD Influx	BD Biosciences	https://www.bdbiosciences.com/en-us/products/instruments/flow-cytometers/research-cell-sorters/bd-influx
FlowJo V10		

3.1.2 Microbiota viability assay

Fecal material from AS patients and healthy individuals was weighed, suspended in PBS (10 µl/µg), filtered through a 30 µM filter and spun down (5 min, 13.000 rpm, 4°C). The bacterial pellet was re-suspended and the OD at 660 nm adjusted to 0.4 (Multiskan FC photometer) in 200 µl of PBS and transferred to a 96 well plate. After a centrifugation step at 3000 rpm for 5 min at 4°C, the bacterial pellet was re-suspended in 50 µl PBS containing SytoBC (1:500, v/v) and incubated for 15 min at 4°C. Another washing step was performed (3000 rpm, 5 min, 4°C) prior to incubating the bacteria with 1:4000 DAPI in 50 µl PBS (v/v) for 15 min at 4°C. The samples were washed once more, re-suspended in 200 µl PBS and sorted using a BD Influx cell sorter. Ten cells of the $SytoBC^{+}DAPI^{-}$ or $SytoBC^{+}DAPI^{-}$ population were sorted per well containing 100 µl of PYG medium, resulting in 32

replicates for each population. After 48 hours of incubation under anaerobic conditions (oxygen < 25 ppm) at 37°C, the OD of each well was determined. The mean OD of the wells only containing PYG medium were used as blank and subtracted from the OD of each well containing sorted bacteria.

3.1.3 Staining of fecal microbiota and bacteria cultures

To reduce glycerol toxicity while thawing, 1 mL of autoclaved and sterile-filtered PBS was added to the frozen fecal microbiota or bacteria culture stocks. Samples were centrifuged at 13.000 rpm for 10 min twice, the supernatant removed and the pellets re-suspended in PBS and an OD 0f 0.04 was used for each staining. All stainings of microbiota samples were performed in a DNase containing buffer (PBS/ 0.2 % BSA/25 µg/µL DNase). Staining for human immunoglobulins was performed in 100 µL with 1:50 (v/v) of the detection antibodies: anti-human IgM Brilliant Violet 650, anti-human IgG PE/ Dazzle™ 594, anti-human IgA1 Alexa Fluor, anti-human IgA2 Alexa Fluor 488. The samples were incubated for 30 minutes at 4 ° C and 1 mL of a 5 µM Hoechst 33342 solution was added directly and incubated for another 30 min at 4 °C. For the detection of Spike protein-similar structures the samples were first incubated in 50 µL containing 0.5 µg SARS-CoV-2 Spike Neutralizing Antibody or Neutralizing Antibody isolated from COVID-19 patients for 15 min at 4 °C then washed with PBS and stained again in 50 µL of the anti-Rabbit Alexa 647 or anti-human IgG PE/ Dazzle™ 594 (2µg/ml) which was then topped up with 5 µM Hoechst 33342 solution. After Hoechst 33342 staining samples were washed with PBS and centrifuged at 13,000 x g for 5 min. After removal of the supernatant, the samples were re-suspended in PBS/ 0.2 % BSA. The samples were transferred to 5 mL round bottom tubes for acquisition. In order to determine the binding of salivary IgA to bacterial cultures, the saliva was spun down (13.000 rpm, 10 min, 4°C). The supernatant was passed through a 0.22 µM filter and incubated with the bacterial culture for 15 min at 4°C. After washing (3000 rpm, 5 min, 4°C) the bacterial pellet

was re-suspended with PBS containing 5 µM Hoechst 33342, anti-human IgA1 Alexa Fluor and anti-human IgA2 Alexa Fluor 488 (1:50, v/v). The incubation for 15 min at 4°C was followed by another washing step (3000 rpm, 5 min, 4°C) before cells were re-suspended in 200 µl PBS and measured with the Influx cytometer.

Table 2. Reagents for microbiota staining

Reagent	**Source**	**Identifier**
DNase	Sigma Aldrich	Cat. No. #10104159001
anti-human IgM BV650 (MHM-88)	Biolegend	Cat. No. #314526
anti-human IgG PE/ Dazzle™ 594 (HP6017)	Biolegend	Cat. No. #409324
anti-human IgA1 Alexa Fluor 647 (B3506B4)	Southern Biotech	Cat. No. #9130-31
anti-human IgA2 Alexa Fluor 488 (A9604D2)	Southern Biotech	Cat. No. #9140-30
Hoechst 33342	Thermo Fischer	Cat. No. #62249
SARS-CoV-2 (2019-nCoV) Spike Neutralizing Antibody, Rabbit Mab (HA14JL2302)	Sino Biological	Cat. No: #40592-R001
SARS-CoV-2 (2019-nCoV) Spike Neutralizing Antibody, human Mab	Kreye et al. 2020	N/A
anti-Rabbit Alexa 647	Jackson ImmunoResearch	Cat. No. #111-606-144

3.2 Bacteria culture

PYG medium and plates were prepared as described by the DSMZ (German Collection of Microorganisms and Cell Cultures). 300,000 events were sorted into 1 ml of PYG medium and directly transferred to a COY anaerobic chamber (oxygen< 25 ppm). Sorted bacteria were plated on PYG, BHI (Brain heart infusion broth) and Fastidious agar plates and bacteria were

grown for 24 hours. Colonies were picked and PYG medium, BHI broth and Schaedler broth were inoculated with colonies from the respective plates. The next day, DNA was isolated and the remaining bacteria were frozen in 40% glycerol LB medium in liquid nitrogen or – 80 °C.

Table 3. Bacteria culture reagents

Reagent	Source	Identifier
PYG medium	DSMZ	https://www.dsmz.de/microorganisms/medium/pdf/DSMZ_Medium104.pdf
Breain Heart Infusion broth	Sigma Aldrich	Cat. No. #53286-100G
Fastidious agar plates	Thermo Scientific	Cat. No. #12957138
Schaedler Broth	Roth	Cat. No. #5772.1

3.3 Sequencing from bacterial colonies

For the identification of the bacterial species bound to the neutralizing anti-RBD antibodies, the DNA from 200 µl of the grown bacteria was isolated using ethanol precipitation. The isolated DNA was subsequently amplified by the 16S rDNA specific primers LPW57 and LPW58 (as used in (Woo et al., 2000)). In brief, bacterial DNA was amplified with Taq-polymerase (0.005 u/µl), 3.12 mM MgCl2, 1 X GenTherm buffer, 0.25 mM dNTP mix and LPW57 and LPW 58 (1µM) for 35 amplification cycles in a thermocycler. The DNA product was verified by gel electrophoresis and purified with the NuceloSpin Gel and PCR Clean-up Kit. The concentration of the purified PCR product was adjusted to 5 ng/µl in 15 µl and send to Sanger sequencing by Eurofins Genomics. Sequence identity was determined with the Nucleotide Basic Local Alignment Search Tool (BLAST) provided by NCBI.

Table 4. Reagents for bacterial culture sequencing

Reagent	Source	Identifier
LPW57	TIB Molbiol	5'-AGTTT GATCCTGGCTCAG-3'
LPW58	TIB Molbiol	5'-AGGCCCGGGAACGTATTCAC-3'
Taq-polymerase	Rapidozym	Cat. No. #GEN-003-1000
MgCl2	Rapidozym	N/A
GenTherm buffer	Rapidozym	N/A
dNTP mix	Thermo Scientific	Cat. No. #R0192
NuceloSpin Gel and PCR Clean-up Kit	Macherey-Nagel	Cat. No. #740609.50

3.4 Preparation of oral swabs for 16 S rRNA sequencing

Swabs were prepared for 16 S rRNA sequencing with an adapted protocol of the Quick-DNA™ Fecal/Soil Microbe Miniprep Kit. Swabs were obtained from clinics on –80 °C and kept frozen until further use. The swab stick was either already stored in buffer or Bead Bashing™ buffer was added to cover the swab brush. Up to 750 µL of the buffer solutions where transferred to a BashingBead™ Lysis Tube and rigorously mixed at 13,000 rpm at 37 °C. Following the kits protocol the supernatant was harvested after centrifugation at 13,000 x g for 5 min and once more filtered by a Zymo-Spin™ III-F Filter. The DNA containing solution was then treated with Genomic Lysis Buffer and the containing DNA was put on a DNA binding Zymo-Spin™ IICR Column repeatedly until the entire sample volume was loaded. The bound DNA was washed with DNA Pre-Wash Buffer and g-DNA Wash Buffer. The washed DNA was eluted in 50 µL DNA Elution buffer and once more further purified by filtration through the Zymo-Spin™ III-HRC Filter. 2.5 µL of each of the prepared samples was directly loaded to the amplicon PCR of the Illumina Nextera NGS protocol described in 3.5.

Table 5. Reagents for 16S rRNA preparation of swab samples

Reagent	Source	Identifier
Quick-DNA™ Fecal/Soil Microbe Miniprep Kit	Zymo Research	Cat. No. # D6010

3.5 16S sequencing of fecal bacteria

The 16 S rRNA was performed as described in the "16S Metagenomic Sequencing Library Preparation" for the Illumina MiSeq System. In brief, the V3/V4 region was amplified directly from the sorted samples or from a 1:10 dilution from bulk fecal material, which was suspended in PBS (10 µg/µl). To guarantee an amplification of bacterial DNA, the reaction was performed for 35 instead of 25 cycles. After the amplicon PCR the genomic DNA was removed by AmPure XP Beads with a 1:1.25 ratio of sample to beads (v/v). Next the purity and the size of the amplicons were determined on a 1.5 % agarose gel and, if suitable, subjected to the index PCR using the Nextera XT Index Kit v2 Set C/D. Once the indices were added to the amplicons by PCR, the samples were cleaned again with AmPure XP Beads in a 1: 0.8 ratio of sample to beads (v/v). Samples were then analyzed by capillary gel electrophoresis with a Fragment Analyzer 5200 and evaluated concerning correct size and purity with the NGS standard sensitivity fragment analysis kit. Of all suitable samples a pool of 2 nM was generated and loaded to the Illumina MiSeq 2500 system.

Raw data were processed and de-multiplexed using MiSeq Reporter Software. Forward and reverse reads were combined using PANDAseq 2.11 with a minimum overlap of 25 bases (Masella et al., 2012) and classified using "classifier.jar" 2.13 from the Ribosomal Database Project with a confidence cutoff of 50% (Cole et al., 2014; Wang et al., 2007). The copy number adjusted counts were agglomerated to bacterial genera, rarefied to the smallest size and alpha diversity were estimated using phyloSeq 1.34 (McMurdie and Holmes, 2013). Principle coordinate analysis were performed using Bray–Curtis dissimilarity distance using vegan 2.5-7.

The linear discriminant analysis were performed using LEfSe, based on copy number adjusted counts normalized to 1M reads.
Non-metric Multidimensional Scaling was performed using Bray–Curtis dissimilarity distance using phyloSeq 1.38 based on relative abundancies.
Random forest analysis was performed using microbial 0.0.20 based on raw read values
(https://cran.r-project.org/web/packages/microbial/index.html).
Raw sequence data were deposited at the NCBI Sequence Read Archive (SRA) under the accession number PRJNA738291.

Table 6. 16S rRNA sequencing reagents

Reagent	Source	Identifier
KAPA HiFi HotStart ReadyMix	Roche	Cat. No. #7958927001
Nextera XT Index Kit v2 Set C	Illumina	Cat. No. #FC-131-2003
AmPure XP Beads	Beckman Coulter	Cat. No. #A63881
Fragment Analyzer 5200	Agilent	Cat. No. #M5310AA
NGS Fragment Kit	Agilent	Cat. No. #DNF-473-0500
MiSeq Reagent Kit v3	Illumina	Cat. No. #MS-102-3003

3.6 Enzyme-linked immunosorbent assay

To determine the SARS-Cov-2-specific antibody titers, 96-well plates were coated overnight with either 1 µg/ml recombinant SARS-CoV-2 (2019-nCoV) Spike Protein (RBD, His Tag) or recombinant SARS-CoV-2 Nucleocapsid His Protein or SARS-CoV-2 Spike RBM (receptor binding motif), 480-496 aa. Plates were washed, blocked and the administration of sera and fecal supernatants were done as previously described (Ferreira-Gomes et al., 2021). To detect RBD-specific IgA, a biotinylated anti-human IgA antibody was applied, followed by an incubation for 1 h at 37°C. After washing 6 times with PBST, avidin-HRP was added and after 1 hour incubation at RT and 5 times washing with PBST, Tetramethylbenzidine (TMB) Substrate was added. The reaction was stopped by addition of 2N

H2SO4. Optical densities were measured on Spectramax (Molecular devices).

Table 7. Reagents for ELISA

Reagent	**Source**	**Identifier**
Goat Anti-Human Ig-UNLB	Southern Biotech	Cat. No. #2010-01
Goat Anti-Human IgA-UNLB	Southern Biotech	Cat. No. #2050-01
PBST	In house	N/A
PBS/BSA	In house	N/A
IgA1	Genway	Cat. No. #E04696
IgM	Sigma	Cat. No. #18260
IgA2	Genway	Cat. No. #50D1F7
IgG	Janssen Biotech	
anti-human IgG-AP	ICN/Cappel	Cat No. #59289
anti-human IgM-AP	Sigma	Cat. No.#A3437-.25ML
anti-human IgA-AP	Sigma	Cat. No. #A2043
anti-human IgA1-AP (B3506B4)	Southern Biotech	Cat. No. #9130-04
anti-human IgA2-AP (A9604D2)	SouthernBiotech	Cat. No. #9140-04
pNPP	Sigma	Cat. No. #N2770
NaOH	Carl Roth	Cat. No #6771.1
SARS-CoV-2 (2019-nCoV) Spike Protein (RBD, His Tag)	Sino biological	Cat. No. #40592-V08B-100
SARS-CoV-2 Nucleocapsid His Protein, CF (;)	RnD Systems	Cat. No. #10474-CV
SARS-CoV-2 Spike RBM, 480-496 aa	Eurogentec	Cat. No: #As-656-19
anti-human IgA antibody	Southern Biotech	Cat. No. #2050-08
avidin-HRP	Invitrogen	Cat. No. #88-7324-88
TMB Substrate	Invitrogen	Cat. No. #88-7324-88
H2SO4	Carl Roth	Cat. No. # 9316.1

3.7 Purification of fecal IgA antibodies

Human IgA was purified from fecal supernatants with Peptide M/ Agarose as described by the manufacturer. Peptide M/ Agarose was used to prepare a column which was equilibrated with 20 mM sodium phosphate buffer (pH 7). Subsequently the 0.2 µM filtered fecal supernatant was applied on the column at least three times. The fecal IgA was eluted from the column after a washing step with 20 mM sodium phosphate buffer, with 0.1 M Glycin-HCl. The elution was neutralized with 1 M Tris/HCl and concentrated via dialysis. Finally, the IgA concentration was determined with a NanoDrop 2000C or ELISA.

Table 8. Reagents for the purification of IgA antibodies

Reagent	Source	Identifier
Peptide M/Agarose	InvivoGen	Cat. No. #gel-pdm-2
Gycin/HCl	In house	N/A
Tris/HCl	In House	N/A
NanoDrop 2000C	Thermo Scientific	Cat. No. # ND-2000

3.8 Flow cytometric assay for analysis of anti-Spike protein responses

HEK293T cells were transfected with a plasmid expressing wild-type SARS-CoV-2 S protein. Next day, the proportion of transfected cells was determined by staining with anti-SARS-CoV-2 Spike Glycoprotein S1 antibody for 30 min, wash cells once with PBS/ 0.2 % BSA and subsequent staining with anti-human IgG PE/ Dazzle™ 594. Further transfected cells were collected and incubated with sera or fecal supernatants for 30 min, washed twice with PBS/BSA and stained with anti-human IgM Brilliant Violet 650, anti-human IgG PE/ Dazzle™ 594, anti-human IgA1 Alexa Fluor 647, anti-human IgA2 Alexa Fluor 488. Cells were washed with PBS/ 0.2 % BSA and either measured directly, dead cell exclusion by DAPI or stained for dead cells with Zombie Violet™ in PBS for 5 min at room temperature and

fixed in 4 % paraformaldehyde solution overnight at 4°C. Samples were acquired on a FACSCanto or a MACS Quant 16 and analyzed using FlowJo v10 analysis software.

Table 9. Reagents for anti-Spike protein responses

Reagent	Source	Identifier
anti-SARS-CoV-2 Spike Glycoprotein S1 (CR3022)	Abcam	Cat. No. #ab273073
Zombie Violet™	Biolegend	Cat. No. #423113
FACSCanto	BD Biosciences	N/A
MACS Quant 16	Miltenyi	Cat. No. # 130-109-803

3.9 Flow cytometric assay for analysis of ACE2-RBD interaction

HEK293T cells were transfected with a plasmid expressing human ACE2 protein. Next day, the proportion of transfected cells was determined by staining with biotinylated RBD for 30 min. The cells were washed once with PBS/ 0.2 % BSA and subsequently stained with streptavidin-FITC. Further transfected cells were collected and incubated with biological samples for 30 min, washed twice with PBS/BSA and incubated with biotinylated RBD for 30 min, washed once with PBS/ 0.2 % BSA and subsequently stained with streptavidin-FITC. Cells were washed with PBS/ 0.2 % BSA measured directly. Dead cell exclusion was done using DAPI. Samples were acquired on a FACSCanto and analyzed using FlowJo™ v10 Software (BD Life Sciences) analysis software.

Table 10. Reagents for FACS analysis of ACE2-RBD interaction

Reagent	Source	Identifier
SARS-CoV-2 (2019-nCoV) Spike RBD-His Recombinant Protein,Biotinylated	Sino biologicals	Cat. No. : #40592-V08H-B
eBioscience™ Streptavidin FITC Conjugate	Thermo Fisher	Cat. No. #11-4317-87
DAPI	In house	N/A
FACSCanto	BD Biosciences	https://www.bdbiosciences.com/en-ca/products/instruments/flow-cytometers/clinical-cell-analyzers/facscanto
FlowJo™	BD Life Sciences	https://www.flowjo.com/solutions/flowjo
HEK 293 T cells	In house	N/A

3.10 Isolation of small intestinal lamina propria cells

Isolation of lamina propria cells from the small intestine was performed as described before (Weigmann et al., 2007) with small modifications. In brief, the intestine was isolated and SI Peyer's Patches and fat were removed. The tissue was opened and thoroughly washed in cold PBS to remove feces and mucus. Small intestinal tissue was then weighed and cut in pieces of 1 cm size and transferred to a pre-digestion solution consisting of Gibco™ Roswell Park Memorial Institute (RPMI) 1640 GlutaMAX™ Medium supplemented with 10% FCS/PS/ME, containing 5 mM EDTA and incubated for 20 min at 37°C. After intensively shaking the samples, the intraepithelial lymphocytes (IEL) and epithelial cell (EC) containing supernatant was discarded, fresh pre-digestion solution was added and the procedure was repeated.

The remaining tissue was minced with scissors and scalpel followed by digestion with Dispase II and Collagenase D (1 mg/ml) for 20 minutes at 37°C at 220 rpm in a shaking incubator. Samples were vortexed intensively and the cell-containing supernatant was collected. Solid tissue remains were digested again followed by homogenization with a 19G needle. The cell suspension was passed through a 70 µM filter and washed once more.
Animal procedures were performed according to the German animal protection laws and approved by the "Landesamt für Gesundheit und Soziales".

Table 11. Cell suspension reagents

Reagent	Source	Identifier
Gibco™ RPMI 1640, GlutaMAX™	Thermo Fisher	Cat. No. #61870010
EDTA	Roth	Cat. No. #8040.1
Collagenase D	Merck	Cat. No. #COLLD-RO
DNase I	Merck	Cat. No. #10104159001
Dispase® II	Merck	Cat. No. #D4693

3.11 Mice immunization

Grown bacteria were collected, washed three times with PBS and heat-inactivated at 65 C for 1 hr. Heat inactivated bacteria were resuspended with final OD600 equals 1.0. C57Bl/6 mice were injected with 200 µl of heat-killed bacteria i.p. From oral gavage, live bacteria stocks were grown, washed with PBS several times, OD600 was adjusted to 1, 200 µl of live bacteria was gavaged every second day. All animal procedures were performed in accordance with Russian regulations of animal protection.

3.12 *In vitro* cell culture

Murine IgA-secreting cells from the small intestinal lamina propria were sorted according to Sca-1 and Ly6C expression. After washing the sorted fraction at 1500 rpm, cells were re-suspended in RPMI medium

supplemented with 10% FCS/PS/ME and counted via Neubauer chamber. Up to 300.000 cells were subsequently cultured in 200 µl of 10% FCS/PS/ME in the presence of BAFF (50 ng/ml) and IL-6 (20 ng/ml).

3.13 Flow Cytometry

A maximum of 10^6 viable cells were washed and re-suspended in 50 µl PBS/BSA containing an anti Fcγ-Receptor antibody (12 µg/ml) to prevent unspecific binding. After 10 minutes incubation on ice, the samples were washed and re-suspended in 50 µl PBS/BSA and surface molecule specific, fluorochrome coupled antibodies (Table 12) were added in concentrations determined by titration as optimal. To exclude dead cells a fixable viability dye was added and the cells were kept at 4°C in the dark for 15 minutes of incubation. The cells were washed and re-suspended in an appropriate amount of PBS/BSA and measured with a BD FACSCanto II.

Table 12. Antibodies used for immunofluorescence surface staining

Reagent	Source	Identifier
Fixable Viability Dye eFluor™ 780	Thermo Fisher	Cat. No. #65-0865-18
CD45-FITC (30-F11)	Thermo Fisher	Cat. No. #11-0451-85
CD45-PerCP-Cy5 (30-F11)	Biolegend	Cat. No. #103130
IgA-Dylight650	Bethyl	Cat. No. #A90-103D5
Ly-6C-Pe-Cy7 (HK1.4)	Thermo Fisher	Cat. No. #25-5932-82
Sca-1 APC (D7)	Thermo Fisher	Cat. No. # 17-5981-82
Anti-FcγR (2.4G2/75)	In house	N/A

3.14 Human Donors

The recruitment of study subjects was conducted in accordance with the Ethics Committee of the Charité (EA4/014/20, EA1/068/17, EA1/200/16, EA 1/144/13 with EA 1/075/19, EA 2/066/20) and was in compliance with the Declaration of Helsinki.

4 Results

4.1 Ly6C$^+$ IgA$^+$ B cells express the surface protein Sca-1

The population of IgA-producing B cells in the SI LP of mice is heterogeneous and characterized by the differential expression of surface molecules such as Ly6C. In order to more closely examine the differences between Ly6C+ and Ly6C- IgA-producing B cells, a transcriptomic profile was determined using bulk RNA sequencing. A total of 81 genes significantly differed ($p<0.05$) between the two groups (Figure 1). Among them, 42 genes (approximately 52%) encode for immunoglobulin proteins, of which expression was uniquely increased in Ly6C$^+$ cells suggesting that these cells produce higher amounts of IgA antibodies (Figure 1 B). Additional to the immunoglobulin coding genes, Ly6C$^+$ IgA-secreting cells contained increased transcripts of genes *Ly6i* and *Ly6a* encoding the surface proteins Ly6I and Ly6A-2/6E-1, the latter also known as "Stem cell antigen 1" (*Sca-1*) a molecule reported to be expressed by BM, splenic and PP PCs (Figure 1 A) (Wilmore et al., 2017).

Strikingly, five of the six genes highly expressed ($p< 0.01$) in Ly6C$^-$ cells were involved in DNA replication. "Cell division control protein 6 homolog" (*Cdc6*) affects the initiation of DNA replication, "DNA replication licensing factor Minichromosome maintenance protein complex (MCM) 3, 5 and 7" are components of the MCM2-7 complex that builds a helicase and "Histone chaperone ASF1B" is involved in DNA replication-dependent nucleosome assembly. The gene *H2-Dmb2* encodes the MHC class II H2-M beta 2 chain and is therefore involved in antigen presentation.

To validate the results obtained by RNA sequencing, we next determined the presence of the surface proteins MHCII and Sca-1 on SI LP IgA secreting cells (Figure 2). We observed no significant differences in MHCII surface expression between Ly6C$^+$ and Ly6C$^-$ cells (Figure 2 A). However, the majority of Ly6C$^+$ cells were Sca-1 positive, whereas the fraction of Sca-1$^+$ cells in the Ly6C$^-$ population was decreased (Figure 2 B).

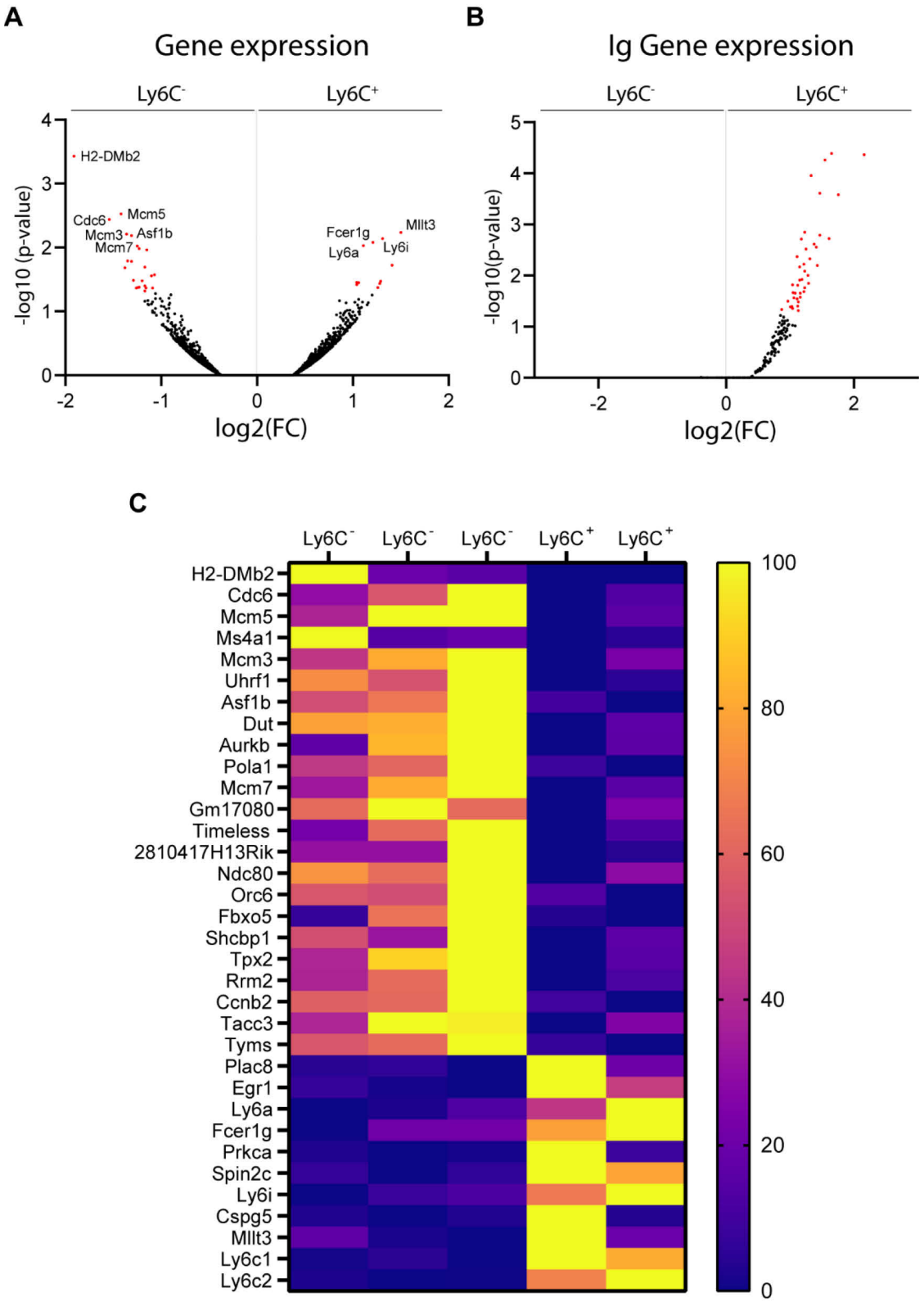

Figure 1. Transcriptome profile of Ly6C$^+$ plasma cells differs from Ly6C$^-$ subset. **(A)** Volcano plots depicting the gene expression in Ly6C$^+$ and Ly6C$^-$ IgA producing cells from the small intestinal lamina propria. Immunoglobulin encoding genes are shown separately in **(B)**. Significantly different expressed genes are shown in red ($p<0.5$) and in (A) labeled with their corresponding name ($p<0.01$)**. (C)** Heatmap of the normalized counts of genes, shown as red in (A). Each column represents a single replicate. The color code depicts percentage of the maximum score per gene.

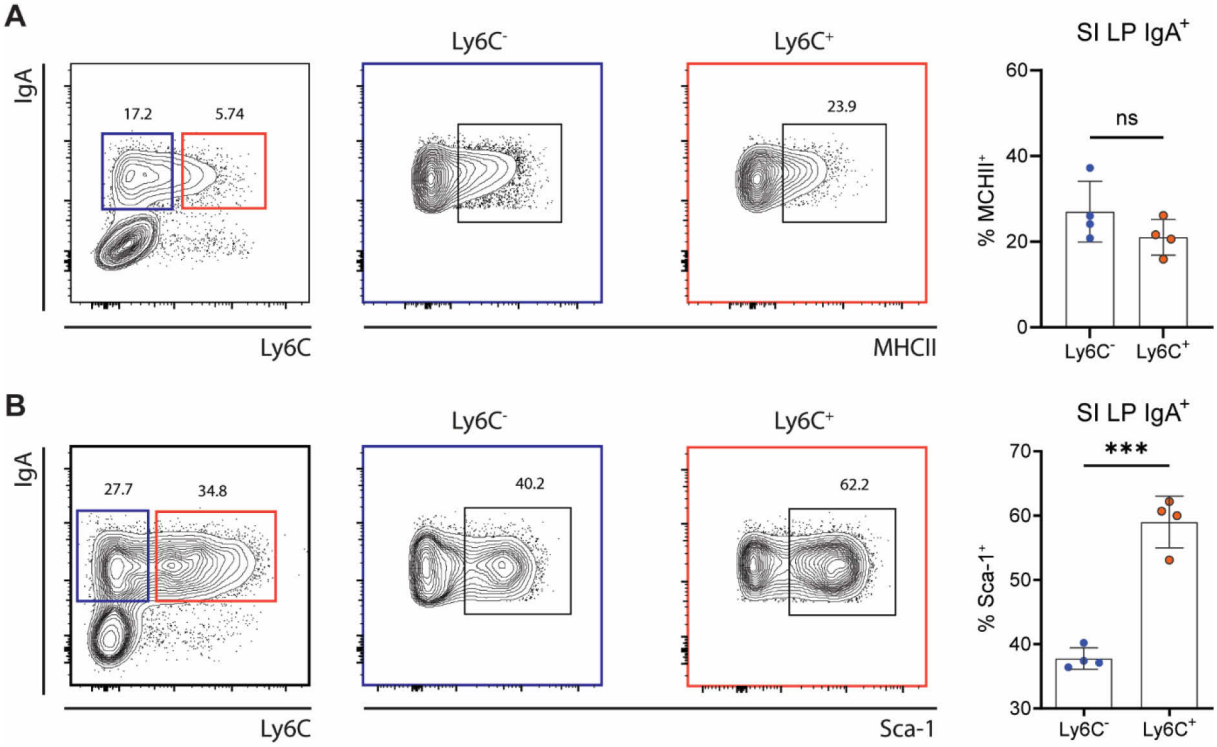

Figure 2. The majority of Ly6C$^+$ cells express the surface protein Sca-1. (A) Representative flow cytometry plot and quantified frequencies of MHCII$^+$ cells among IgA$^+$ Ly6C$^-$ (blue) and IgA$^+$Ly6C$^+$ (red) cells from the SI LP. Each dot represents one mouse. ns, not significant as calculated by Mann-Whitney test. **(B)** Representative flow cytometry plot and quantified frequencies of Sca-1$^+$ cells among IgA$^+$Ly6C$^+$ (red) cells from the SI LP is increased compared to Ly6C$^-$ cells (blue). *, $p<0.05$, **, $p<0.01$, ***, $p<0.001$, as calculated by unpaired t-test with Welch's correction, ns, not significant. Data are representative of one experiment.

Collectively, these data show that Ly6C$^+$ plasma cells express increased transcripts of genes encoding immunoglobulin proteins, whereas plasma cells lacking Ly6C expression are characterized by high levels of transcripts associated with DNA replication, leading to the suggestion that Ly6C$^+$ cells might resemble a matured subset of plasma cells.

Furthermore, the expression of the surface protein Sca-1 is increased in Ly6C$^+$ IgA$^+$ cells and thereby identifies a subset of Sca-1$^+$ plasma cells, in addition to the established markers Ly6C, CD11b and Ly6G.

4.2 Robust Sca-1 expression by PCs can be acquired

As the expression of Ly6C is present in PCs which contain decreased amounts of replication associated transcripts and its expression is absent on the surface of IgA-secreting cells in the PPs but present in the LP, we hypothesized that the expression of Sca-1 is also inducible. In order to test this, IgA$^+$ cells from the SI LP were isolated based on their Ly6C and Sca-1 expression, specifically Ly6C$^-$Sca-1$^-$, Ly6C$^+$Sca-1$^-$, Ly6C$^-$Sca-1$^+$ and Ly6C$^+$Sca-1$^+$ and were cultured in the presence of BAFF and IL-6 for five days *in vitro* (Figure 3).

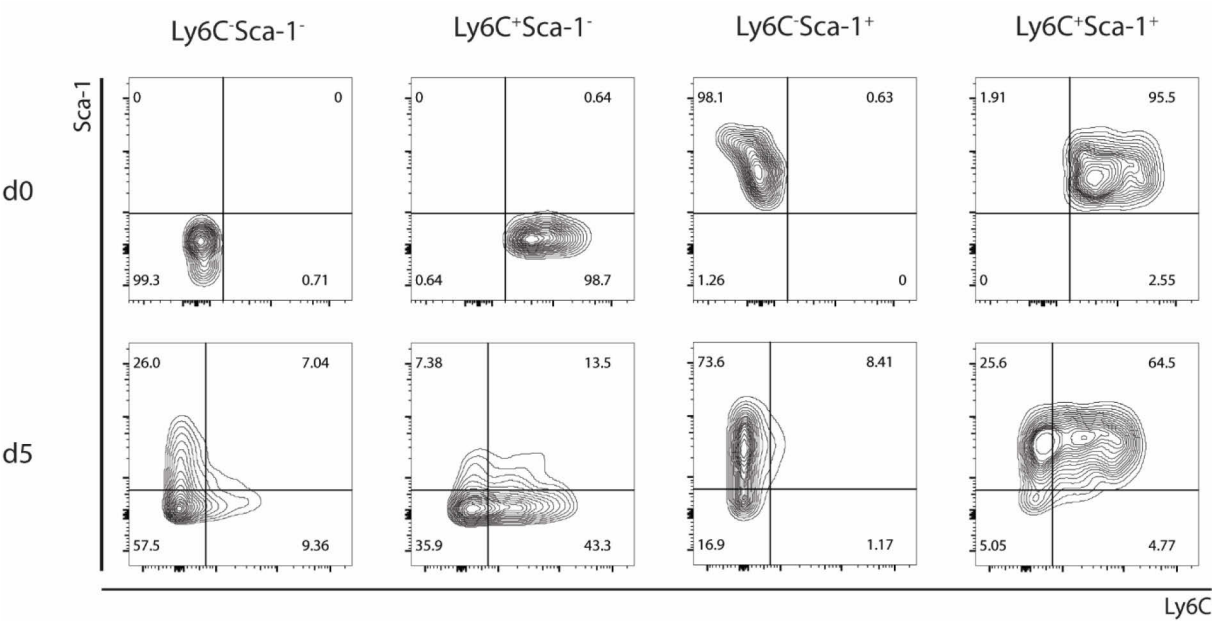

Figure 3. IgA$^+$ secreting B cells acquire Sca-1 expression *in vitro*. IgA-producing cells from the SI LP expressing Ly6C (Ly6C$^+$Sca-1$^-$), Sca-1 (Ly6C$^-$Sca-1$^+$), both (Ly6C$^+$Sca-1$^+$) or no marker (Ly6C$^-$Sca-1$^-$) were cultured for five days (lower panel) in the presence of BAFF and IL-6. Representative flow cytometry plots represent consistent data from two independent experiments.

Among the Ly6C$^-$Sca-1$^-$ cells 9.36% acquired uniquely Ly6C expression, whereas 26% started expressing Sca-1 only. The Ly6C$^+$Sca-1$^-$ cells maintained their Ly6C expression while additionally gaining Sca-1 (13.5%) production or losing Ly6C while gaining Sca-1 expression (7.38%). Notably, Sca-1 expression on single positive Ly6C$^-$Sca-1$^+$ cells remained mostly stable (73.6%) and 8.41% additionally acquired Ly6C expression.

Double positive Ly6C$^+$Sca-1$^+$ cells more efficiently kept their Sca-1 expression but downregulated the production of Ly6C.
These data highlight the plasticity of IgA-secreting PCs in the SI LP. As the expression of Sca-1 is acquired independently of previous acquisition of Ly6C and thereafter stays unchanged, it potentially characterizes a matured cell population.

4.3 Anti-RBD specific IgA antibodies are present in fecal supernatants of healthy individuals and severe COVID-19 patients

Several lines of evidence indicate that IgA antibodies secreted by intestinal PCs, induced by microbial antigens can cross-react with self-structures as well as viral surface molecules. In order to investigate whether commensal-derived antigens are the source of SARS-CoV-2 cross-reactive antibodies, we assessed the reactivity of IgA from fecal supernatants of 9 severe COVID-19 cases from the Charité intensive care unit and 12 aged-matched, healthy, uninfected individuals (severe COVID-19: 68 years ± 19.5; healthy donors: 60 years ± 8.5). The presence of fecal IgA specific to SARS-CoV-2 RBD was determined by incubating fecal supernatants with immobilized RBD. Four out of nine hospitalized COVID-19 patients had fecal IgA antibodies specific to SARS-CoV-2 RBD, whereas two out of 12 uninfected individuals harbored RBD specific IgA in their fecal supernatants (Figure 4 A, B). As the presence of cross-reactive antibodies decreases with age and age in general is a major risk factor for a severe disease course, the existence of fecal anti-RBD IgA antibodies in young (29 years ± 13) unexposed individuals was additionally investigated (Figure 4 C). Nine out of 19 young healthy donors displayed RBD specific fecal IgA, thereby showing a significant increase of this fraction compared to older healthy donors and severe COVID-19 cases (Figure 4 D).

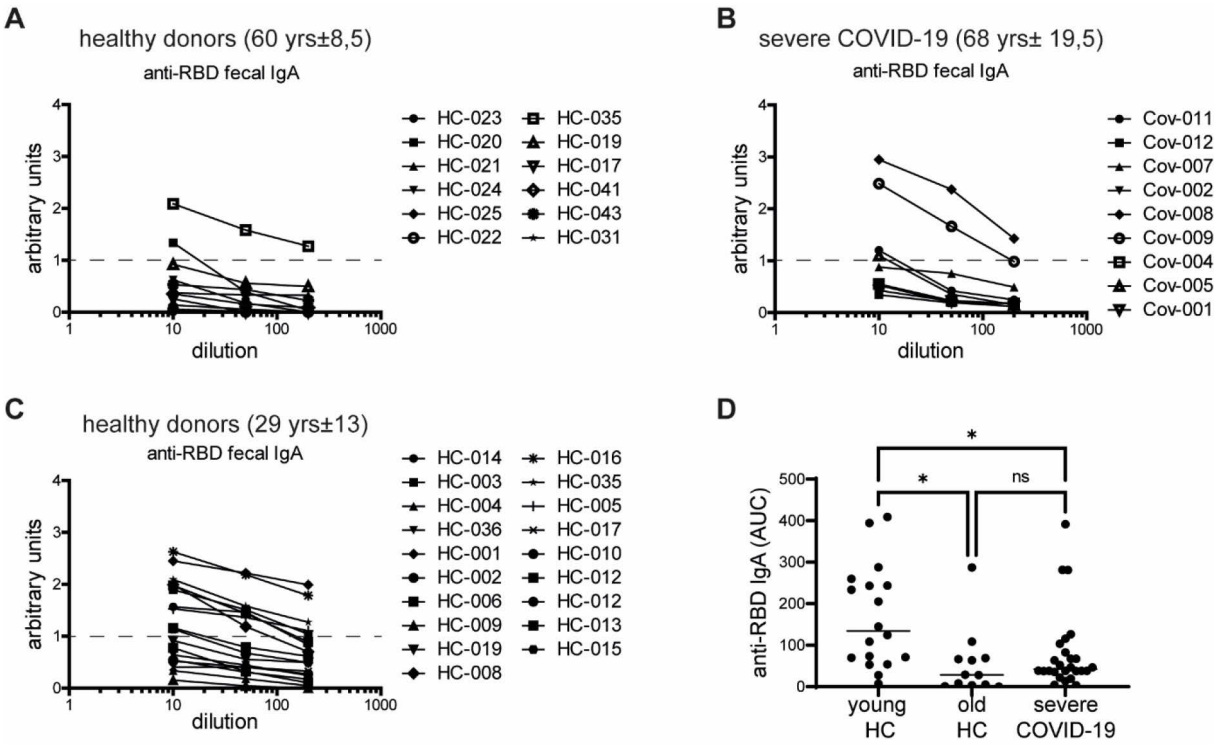

Figure 4. Presence of cross-reactive fecal anti-RBD IgA antibodies in healthy individuals declines with age. Levels of RBD-specific IgA from fecal supernatants of age-matched healthy (**A**) and severe COVID-19 (**B**) individuals as determined by ELISA. (**C**) Levels of RBD-specific IgA from fecal supernatants of young, healthy individuals. (**D**) Area under the curve (AUC) values of the measurements depicted in A-C. *, $p<0.05$, **, $p<0.01$, ***, $p<0.001$, as calculated by Kruskal-Wallis test with Dunn's multiple comparisons; ns, not significant.

In order to determine their neutralizing capacity, IgA was isolated from fecal supernatants of severe COVID-19 cases and healthy individuals harboring anti-RBD-specific IgA antibodies. Therefore, human ACE2-expressing HEK293T cells were incubated with biotinylated RBD, which was subsequently detected with fluorescent streptavidin. The reduction of this signal in presence of purified fecal IgA was measured and the inhibition of binding of the RBD protein to the ACE2 receptor was calculated (Figure 5 A, B). Mucosal IgA from five healthy individuals but from only one severe COVID-19 patient was able to decrease the ACE2-RBD binding. None of the tested antibodies could inhibit the interaction completely, even when used with minimal dilution of 1:1 suggesting that the amount of RBD-specific neutralizing antibodies, or their affinity is low in the feces of healthy donors. Further, the majority of tested IgA did not inhibit the binding of RBD to

ACE2, indicating additionally the presence of non-neutralizing, RBD-specific IgA antibodies.

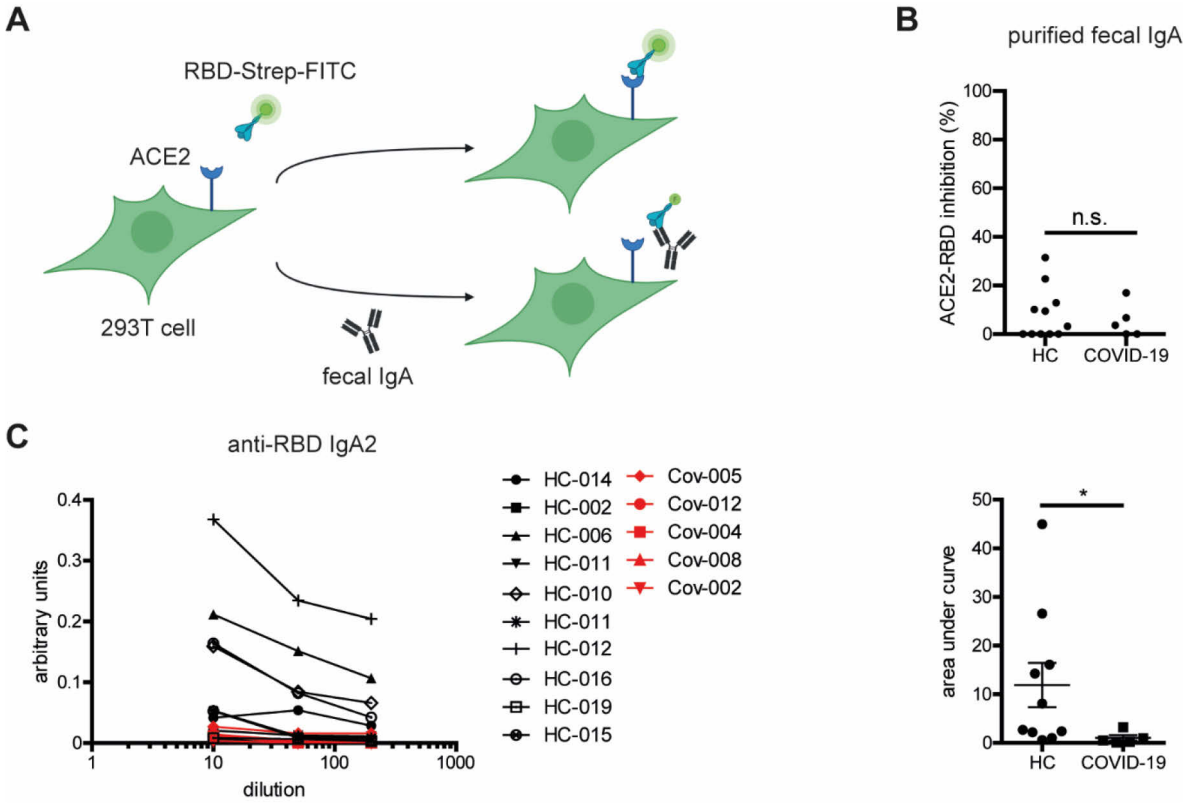

Figure 5. Purified fecal IgA from healthy individuals inhibits ACE2-RBD interaction by binding to RBD. (**A**) Scheme of the experimental setup for the *in vitro* neutralizing assay. The binding capacity of fluorescent labelled RBD to human ACE2 expressed by 293T cells was determined. (**B**) Inhibition of binding from RBD to ACE2 by IgA purified from fecal supernatants of healthy individuals and severe COVID-19 patients. (**C**) Levels and AUC values of anti-RBD IgA2 isolated from fecal supernatants of healthy and severe COVID-19 individuals. *, p<0.05, **, p<0.01, ***, p<0.001, as calculated by unpaired t-test; ns, not significant.

To further characterize the nature of RBD-specific fecal IgA, the subclasses of the antibodies was determined (Figure 5 C). Healthy donors harbored anti-RBD IgA2 in their feces, while severe COVID-19 patients lacked these antibodies. Thus, the previously described non-RBD-specific IgA2 antibodies in severe COVID-19 are present in serum and feces (Ferreira-Gomes et al., 2021).

These data point out that healthy individuals harbor RBD specific IgA antibodies in their feces which decrease with age, and a fraction of these antibodies is able to inhibit an ACE2-RBD interaction, suggesting neutralizing capacity.

4.4 Mucosal IgA-bound commensal bacteria differ between anti-RBD IgA$^+$ and IgA$^-$ healthy individuals

To understand why healthy individuals contain RBD-specific IgA antibodies in their feces, the properties of the microbiota was further analyzed as it is a crucial factor for the induction of mucosal IgA production. Commensal microbes play an important role in shaping the host IgA response and are additionally targeted by it (Atarashi et al., 2015). Therefore, healthy individuals were divided into two groups based on the presence of mucosal anti-RBD IgA (HC RBD-IgA$^+$ and HC RBD-IgA$^-$). The coating of fecal bacteria by IgA1 and IgA2 was quantified by flow cytometry showing no difference in the percentage of IgA1- and IgA2-coated bacteria between RBD-IgA$^+$ and RBD-IgA$^-$ healthy donors (Figure 6 A). Next, the bacteria bound by IgA1 and IgA2 were isolated by fluorescence-activated cell sorting (FACS) and the taxonomic composition was determined by 16S rRNA gene sequencing. To identify differently occurring bacterial taxa from RBD-IgA$^+$ and RBD-IgA$^-$ healthy individuals, a Linear discriminant (LDA) combined with effect size (LefSE) analysis was performed. Bacteria bound by IgA from RBD-IgA$^+$ donors were enriched for *Parabacteroides*, *Sporobacter*, *Bilophila*, and *Vagococcus*, while in RBD-IgA$^-$ donors the IgA-coated fraction was enriched for *Pseudomonas*, *Dorea*, *Soonwooa*, *Lachnospira* and *Bacillus* genera (Figure 6 B).

These data show, that the IgA-coated bacteria fraction differs between healthy individuals harboring or lacking anti-RBD IgA antibodies, suggesting that the presence of mucosal RBD-specific antibodies may be associated with the recognition of distinct commensal microbiota.

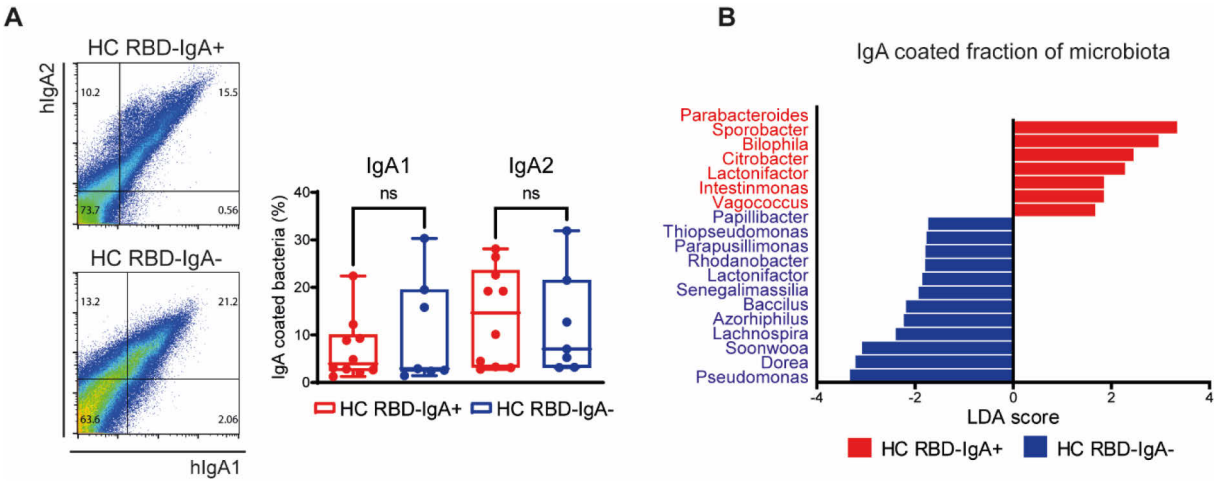

Figure 6. IgA-coated fecal bacteria differ between HC RBD-IgA$^+$ and HC RBD-IgA$^-$ individuals. (**A**) Representative FACS plots of fecal microbiota coating with IgA1 and IgA2 from HC RBD-IgA$^+$ and HC RBD IgA$^-$ individuals (left). Quantification of IgA1- and IgA2-coated bacteria (right). (**B**) LefSE analysis depicting differently abundant bacterial genera in HC RBD-IgA$^+$ versus HC RBD-IgA$^-$ donors. ns, not significant as calculated by unpaired t-test.

4.5 Anti-RBD neutralizing antibodies bind to fecal microbiota of healthy individuals

The occurrence of RBD-specific IgA in the feces of healthy individuals and its connection to the particular IgA response towards the microbiota led to the suggestion that intestinal microbes express surface structures partially resembling the SARS-CoV-2 RBD motif of the Spike protein, resulting in cross-reactive antibodies. In order to test this, anti-RBD neutralizing antibodies were used to detect bacteria presenting RBD-like structures using polyclonal anti-serum derived from rabbit immunization (rabbit anti-RBD) and 15 monoclonal antibodies derived from hospitalized COVID-19 patients. The monoclonal antibodies were cloned from peripheral blood antibody-secreting (2 out of 15) and SARS-CoV-2 Spike-specific memory B cells (13 out of 15) that were previously selected based on strong RBD binding and a high SARS-CoV-2 neutralizing capacity (Kreye et al., 2020). Fecal microbiota from anti-RBD IgA-positive and -negative healthy donors was incubated with the respective antibodies and binding was determined using fluorescently labeled anti-rabbit IgG and anti-human IgG secondary antibodies (Figure 7 A, B). Both, rabbit- and human-derived antibodies

bound to distinct fecal bacteria. Out of 15 antibodies cloned from hospitalized COVID-19 patients, two showed no microbiota reactivity (HK CV07-287, HL CV07-250), and nine recognized bacteria irrespective of pre-existing RBD-specific mucosal antibodies (Table 13). Two clonally related antibodies, CV07-200 and CV07-283, differed in their binding pattern (Figure 7 C). Additionally, the simultaneous staining with rabbit and human antibodies revealed similar as well as varying recognition of bacteria (Figure 7 D).

Therefore it can be stated, that the majority of the examined anti-RBD neutralizing antibodies bind to commensal bacteria of healthy individuals.

Table 13. Frequencies of fecal bacteria bound by neutralizing antibodies

clone	RBD-IgA$^+$		RBD-IgA$^-$		
	HC-001	HC-003	HC-011	HC-009	HC-043
HK CV38-113	0	1.65	0.72	1.14	2.09
HK CV07-287	0	0	0	0	0
HL CV07-270	2.1	6.59	5.46	5.31	5.11
HK CV-X2-106	0	1.06	0	0	0
HL CV07-283	0.74	0.89	0	0	0
HL CV07-262	0.64	0.64	0	0	0
HL CV07-250	0	0	0	0	0
HL CV07-222	0.55	1.37	0	0	0
HK CV-X1-126	1.04	0.86	2.36	1.95	2
HL CV07-200	1.68	1.51	0	0	0.32
HL CV07-315	0.85	1.03	2.14	1.04	1.56
HK CV38-221	1.9	0.86	0	0	2.5
HK CV38-139	1	1.42	2.94	1.75	2.94
HK CV05-163	2.15	5.15	3.46	2.66	1.61
HL CV07-255	1.87	2.76	0	1.28	0.44
Rab. anti-RBD	1.01	3.82	0.17	0.9	0.32

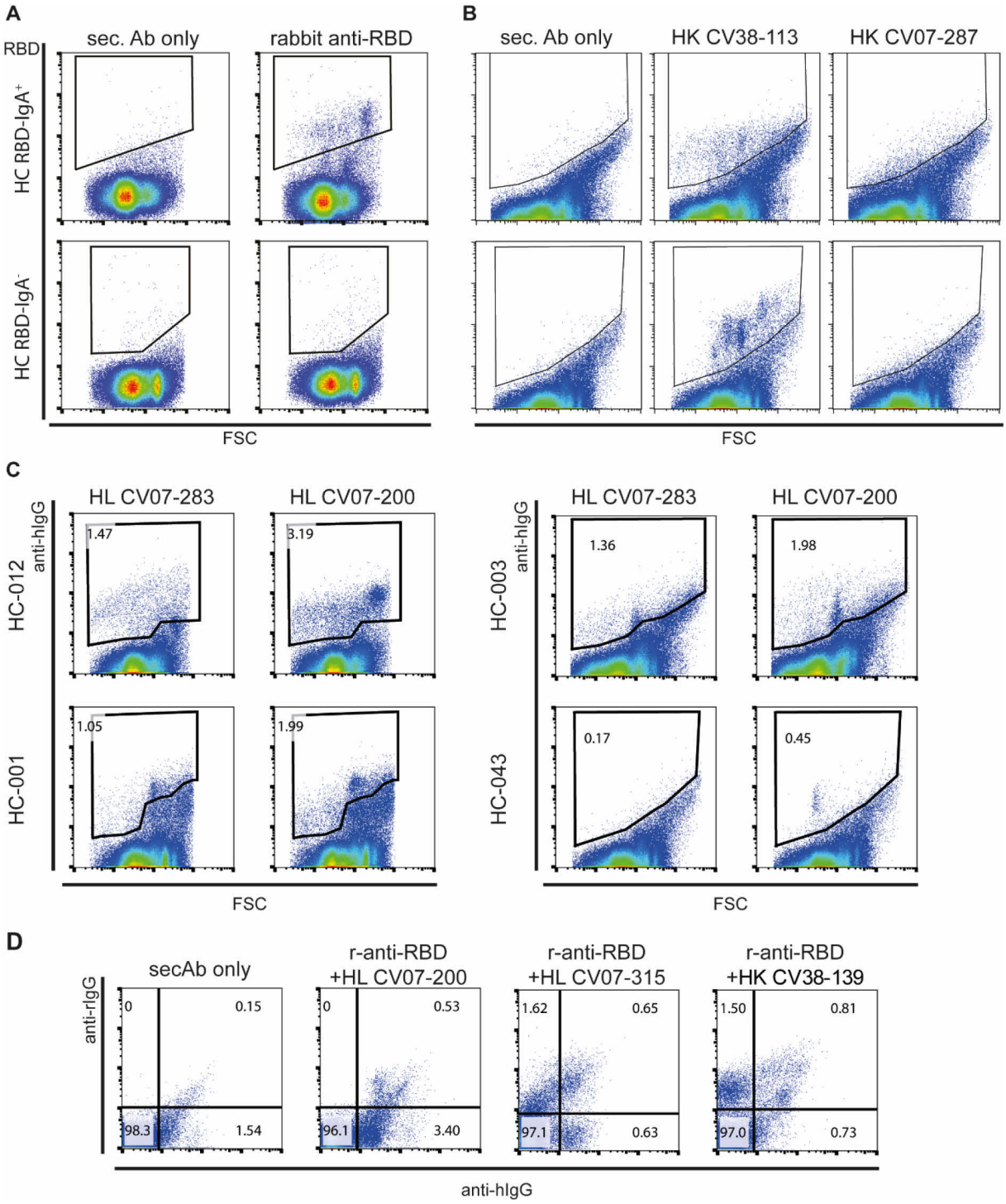

Figure 7. RBD-specific neutralizing antibodies bind to fecal bacteria from healthy individuals. (A) Flow cytometric plots of anti-RBD neutralizing antibodies derived from rabbit immunization and isolated from severe COVID-19 patients. **(B)** Binding to fecal bacteria of healthy donors harboring (HC RBD-IgA$^+$) or lacking (HC RBD-IgA$^-$) RBD specific IgA in their feces. **(C)** Recognition pattern of fecal bacteria from various healthy donors from clonally related human anti-RBD antibodies HL CV07-283 and HL CV07-200. **(D)** Simultaneous staining of fecal microbiota with rabbit and human anti-RBD neutralizing antibodies.

4.6 RBD-specific neutralizing antibodies recognize various fecal bacteria of healthy individuals

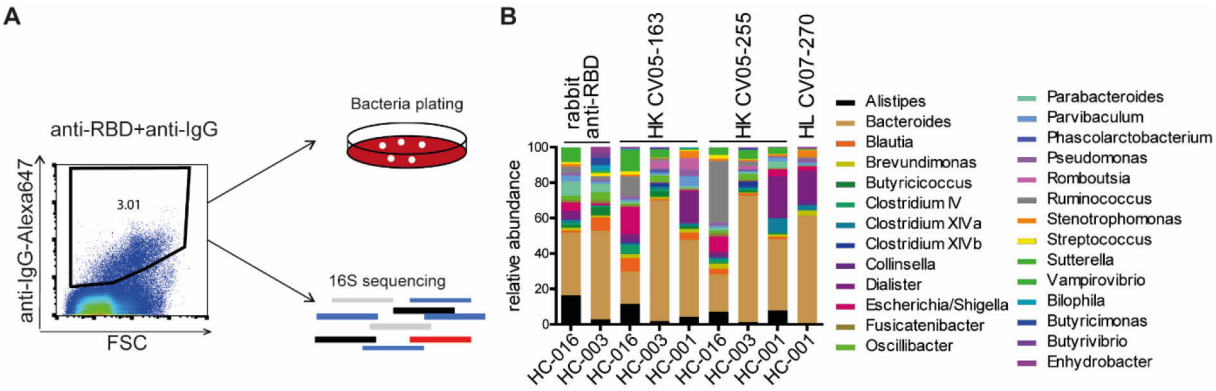

Figure 8. Anti-RBD neutralizing antibodies bind various fecal bacteria. (A) Scheme of the strategy used to identify commensal bacteria bound by RBD-specific neutralizing antibodies. FAC-sorted bacteria were identified by 16S rRNA gene sequencing and cultured. **(B)** Relative abundances of fecal bacteria taxa of different healthy donors bound by rabbit anti-RBD, HK CV05-163, HK CV05-255 and HL CV07-270.

To identify which bacterial species induce cross-reactive antibodies, we sorted the bacteria recognized by the neutralizing antibodies. Therefore, fecal material from three healthy donors (HC-001, HC-003 and HC-016) were stained with four antibodies separately (rabbit anti-RBD, HK CV05-163, HK CV05-255 and HL CV07-270) and the 16S rRNA gene was sequenced (Figure 8). Despite the individual differences in the microbiota composition, we enriched *Bacteroides*, *Escherichia/ Shigella and* Dialister with the antibodies in all donors, revealing a certain specificity for distinct bacterial taxa (Figure 8 B). *Streptococcus* was identified in all donors by all antibodies except for the human monoclonal antibody HL CV07-270.

Thus, antibodies specific for RBD bind to similar bacterial species of healthy donors positive for fecal anti-RBD antibodies.

Using FACS we isolated bacteria bound by anti-RBD-specific antibodies. The sorted bacteria grew on various selective media such as BHI, PYG and blood agar under anaerobic conditions. Single colonies were sent for NGS and the sequence identity was determined with BLAST.

Among the isolated bacteria were several strains belonging to the genera *Streptococcus*, *Bacillus*, *Bifidobacterium*, *Enterococcus and Escherichia*. The human antibody HL CV07-315 also uniquely bound to *Acidaminococcus intestinalis* and *Veillonella parvula* (Table 14.). One of the isolated species from fecal material was *Streptococcus salivarius* a commensal of the oral microflora with probiotic properties (Burton et al., 2006).

Together, these results show that RBD-specific antibodies do not only neutralize SARS-CoV-2 but also recognize various fecal commensals from healthy individuals.

Table 14. Bacterial strains isolated with neutralizing antibodies

Bacterial strain	Rabbit anti-RBD	HL CV07-270	HK CV-X1-126	HL CV07-200	HL CV07-315	HK CV05-163	HL CV07-255
Streptococcus salivarius	X	X			X		X
Sterptococcus australis/ Rubneri	X						X
Streptococcus Parasanguinis		X			X		X
Escherichia Coli	X	X			X	X	X
Bacillus safensis	X			X	X		
Bacillus cereus				X	X		
Escherichia fergusonii	X	X			X		
Bifidobacterium pseudocatenulatum		X					X
Bifidobacterium longum							X
Enterococcus Hirae		X					X
Enterococcus faecalis			X		X		
Acidaminococcus intestinalis					X		
Veillonella parvula					X		

4.7 Isolated bacterial species from healthy individuals bind to anti-RBD neutralizing antibodies

To verify whether the isolated strains display RBD-like structures on their surface, we stained them with anti-RBD neutralizing antibodies (Figure 9). *Bacillus sp*. and *E. Fergusonii* bound the neutralizing antibodies. The commercially available probiotic *Streptococcus salivarius* strain K12 was recognized by the rabbit-derived antibody. *Bifidobacterium pseudocatenulatum* bound the human anti-RBD antibodies. Only a fraction of the bacteria could be stained with the anti-RBD antibodies which might be explained by different growth states of the bacteria thereby resulting in a heterogeneous distribution of the RBD-like surface molecules within the population.

In summary, it could be validated that the isolated bacteria species express a structure on their surface similar to RBD.

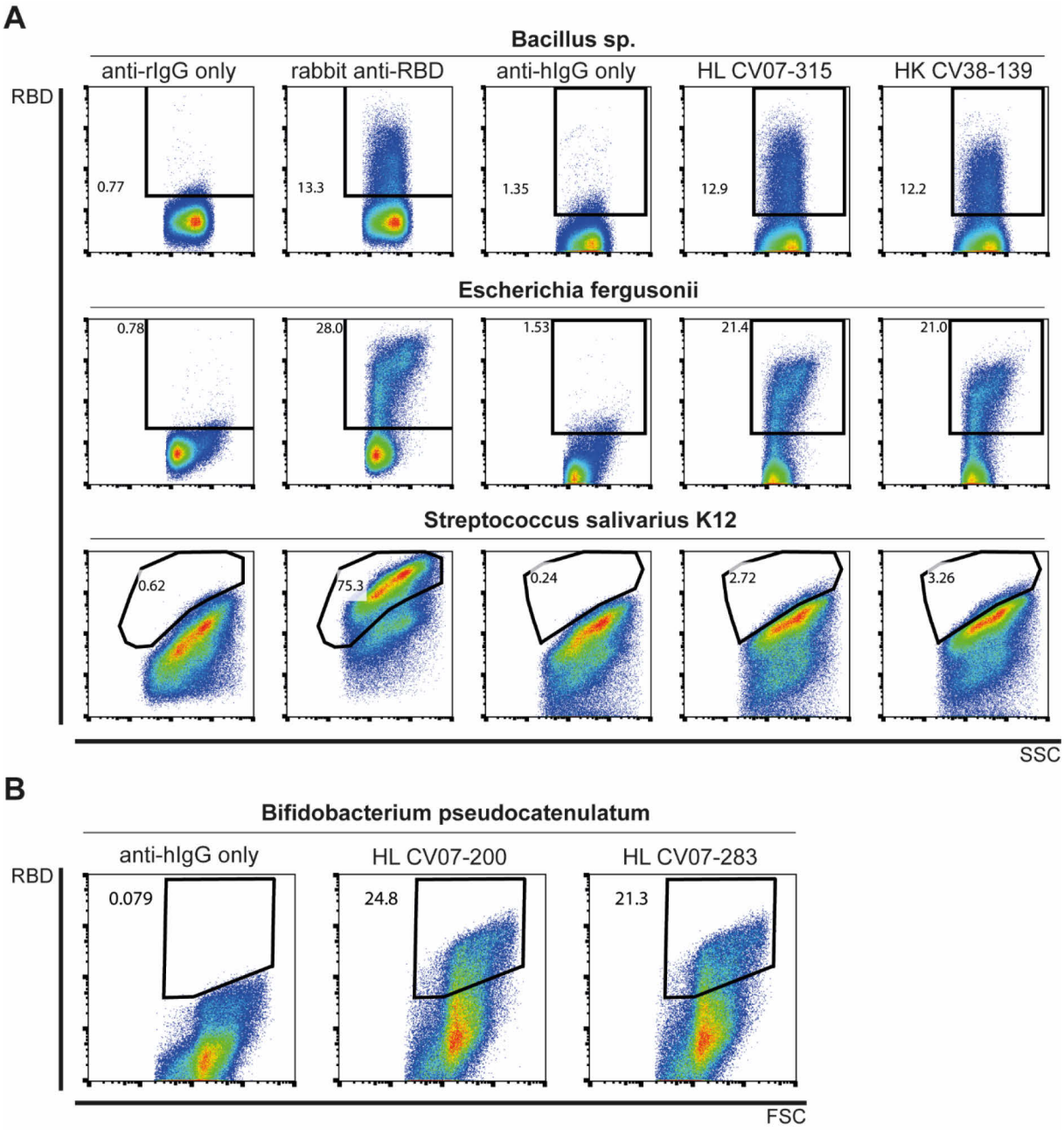

Figure 9. Isolated bacterial strains are recognized by anti-RBD neutralizing antibodies. (A) Flow cytometry plots of *Bacillus sp.*, *E. Fergusonii* and *S. Salivarius* K12 stained with rabbit and human (HL CV07-315, HK CV38-139) anti-RBD antibodies. **(B)** Flow cytometry plots of *Bifidobacterium pseudocatenulatum* stained with human neutralizing antibodies HL CV07-200 and HL CV07-283.

4.8 Salivary IgA from healthy donors recognize specific bacterial strains

As SARS-CoV-2 enters the host via the respiratory route and *Streptococcus salivarius* is a commensal of the oral microflora, we determined the reactivity of salivary IgA antibodies towards the identified bacterial species. Therefore, *Streptococcus salivarius* K12 and *Bifidobacterium pseudocatenulatum* were incubated with saliva from healthy individuals previously identified to harbor (HC RBD-IgA$^+$) or lack (HC RBD-IgA$^-$) anti-RBD IgA in their fecal supernatants. Additionally, we used *Bacillus subtilis* as a negative control, because it was not among the isolated RBD-resembling bacteria.

Salivary IgA2 antibodies recognized *Streptococcus salivarius* and, to a lower extent, *Bifidobacterium pseudocatenulatum* (Figure 10 A). The mean fluorescence intensities (MFI) were significantly higher in individuals who were positive for fecal anti-RBD IgA, whereas the IgA1 antibodies did not differ in their binding ability between the groups (Figure 10 B). *Bacillus subtilis* was bound by less IgA antibodies independent of isotype and no differences could be observed between HC RBD-IgA$^+$ and HC RBD-IgA$^-$ individuals.

Thus, the isolated bacterial species which are bound by anti-RBD neutralizing antibodies are recognized to a greater extent by salivary IgA2 from healthy individuals harboring fecal anti-RBD IgA.

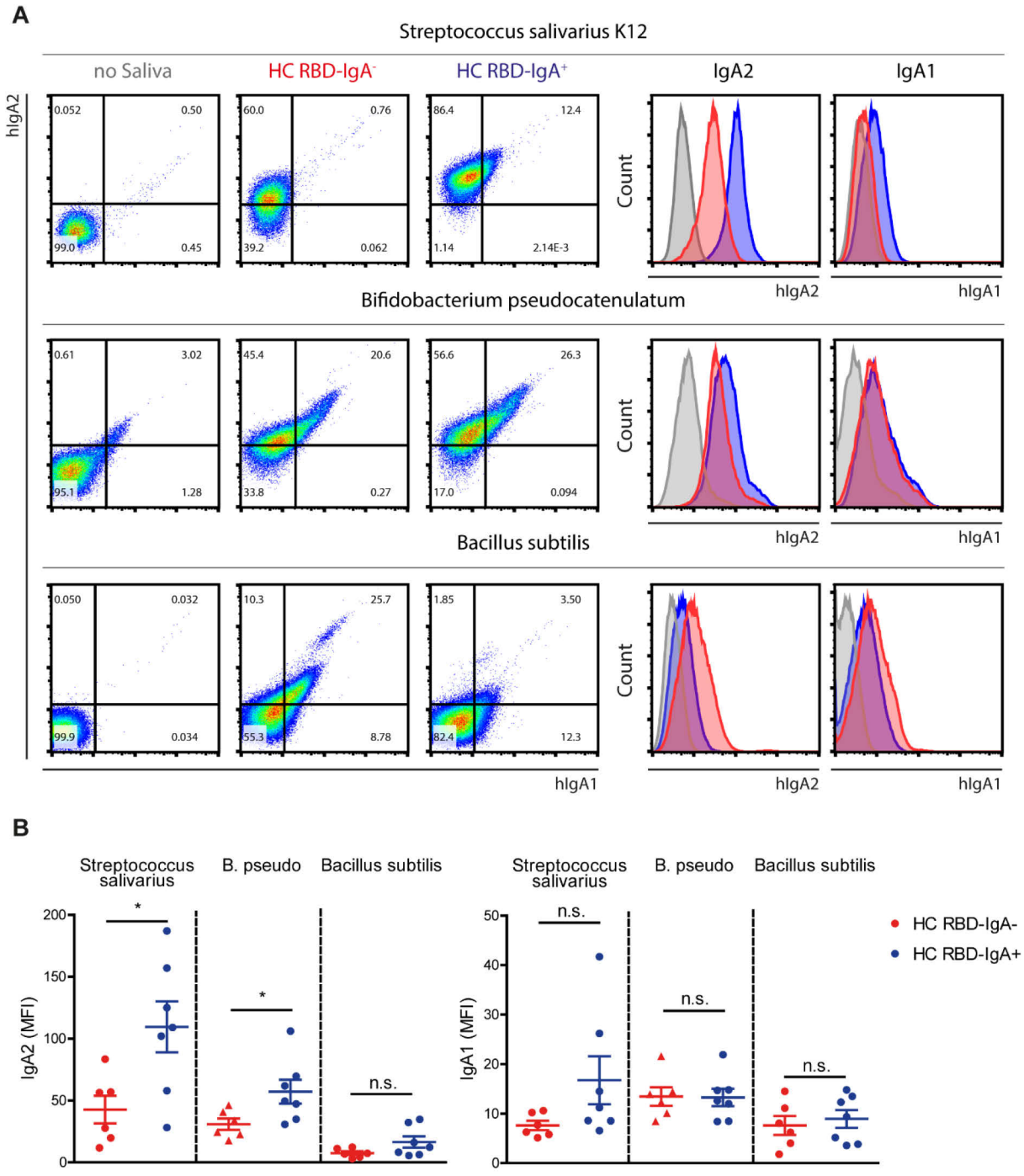

Figure 10. Salivary IgA antibodies from HC RBD-IgA$^+$ donors bind to isolated bacterial strains. (A) Representative Flow cytometry plots and MFI histograms of *S. Salivarius, B. Pseudocatenulatum* and *B. Subtilis* incubated with saliva of healthy individuals and stained with fluorochrome labelled anti-human IgA1 and IgA2 antibodies. **(B)** MFI values of *S. Salivarius*, *B. Pseudocatenulatum* and *B. Subtilis* incubated with saliva from HC RBD-IgA$^+$ and HC RBD-IgA$^-$ individuals. *, $p<0.05$, as calculated by unpaired t-test; n.s., not significant.

4.9 *Streptococcus salivarius* and *Bifidobacterium pseudo-catenulatum* induce RBD specific antibodies in mice

In order to assess whether the isolated bacteria species can induce antibodies reactive to RBD, C57BL/6 mice were once intraperitoneally injected with heat-killed bacteria and the serum was analyzed 14 days post-injection. *Streptococcus salivarius* but not *Bifidobacterium pseudo-catenulatum* was able to induce anti-RBD IgG in the serum of mice (Figure 11 A). Taking into account that these bacteria are part of the oral and intestinal microflora, we also fed mice via oral gavage with the two species and determined the induction of anti-RBD IgA antibodies in their fecal supernatants after 14 days and thereby the mucosal immune response. Oral feeding of mice with *S. salivarius* or *B. pseudo* led to fecal IgA antibodies reactive to RBD (Figure 11 B). Interestingly, only the fecal anti-RBD IgA antibodies induced by *S. salivarius* blocked the ACE2-RBD binding (Figure 11 C), determined by the same assay as depicted in Figure 5.
In brief, administration of *S. salivarius* intraperitoneally or via the oral route induces anti-RBD IgG and IgA antibodies respectively.

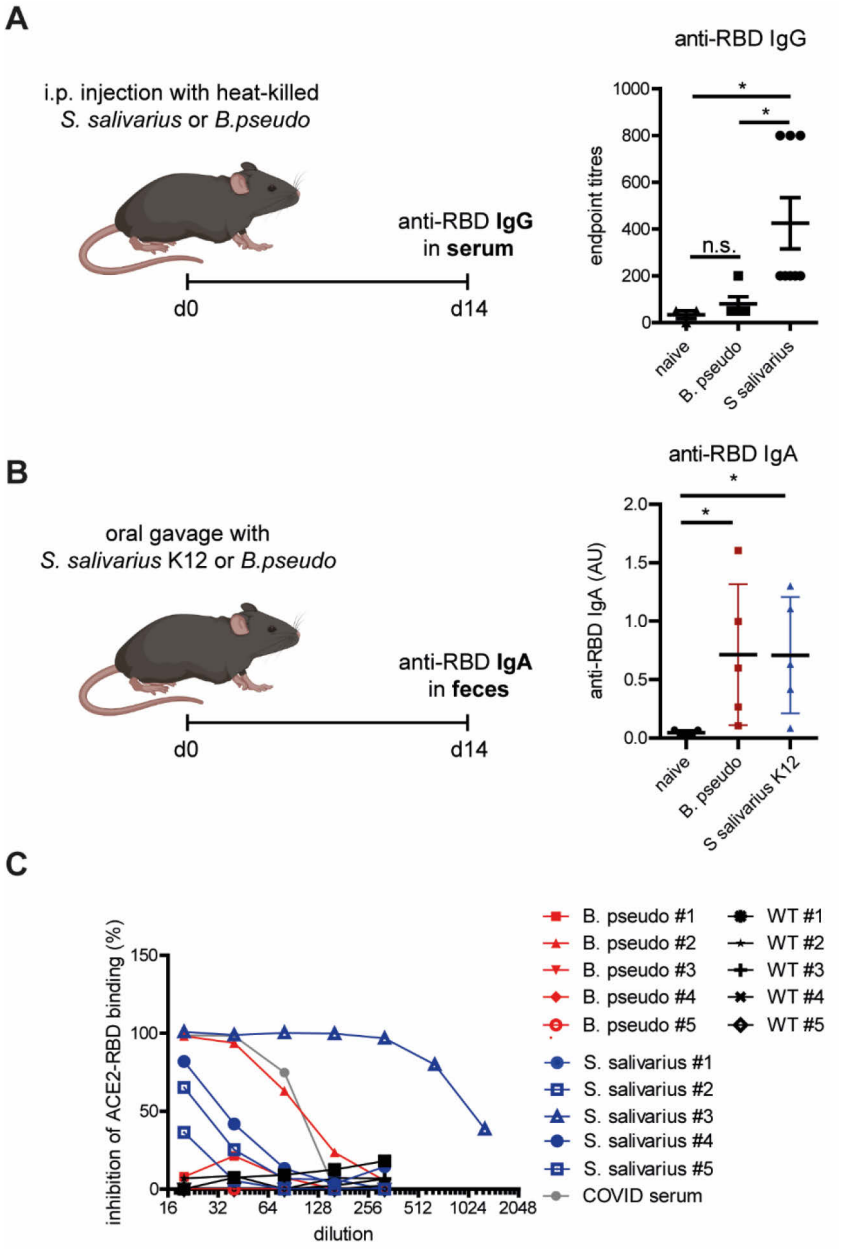

Figure 11. *S. salivarius* and *B. pseudo* induce RBD-reactive antibodies. (**A**) Mice were injected i.p. with heat-killed *S. salivarius* or *B. pseudo* and the anti-RBD IgG antibody titers were measured in serum after 14 days. (**B**) anti-RBD IgA antibodies in fecal supernatants of mice orally supplemented with *S. salivarius* und *B. pseudo*. (**C**) Inhibition of RBD binding to ACE2 by fecal supernatants from B. Two-way ANOVA with Bonferroni's correction was applied for (**A**)**.** Kruskal-Wallis test with Dunn's multiple comparisons was used for (**B**). *, p<0.05, **, p<0.01, ***, p<0.001, n.s., not significant.

4.10 Oral microbiota composition of severe COVID-19 cases is dysbiotic

Streptococcus salivarius is a commensal bacteria residing in the human oral cavity and induced fecal anti-RBD IgA antibodies in mice by oral gavage. SARS-CoV-2 infects the human host mainly through the respiratory route, and thus it was hypothesized that the absence of *S. salivarius* could affect the COVID-19 disease course. To identify potential differences in the oral microbiota, we performed 16S rRNA gene sequencing of saliva samples and buccal swaps of healthy individuals, patients with a flu-like illness and mild and severe COVID-19 patients, hospitalized in the intensive care unit. A principal coordinate analysis (PCoA) based on Bray-Curtis dissimilarity revealed that the oral microbiota of severe COVID-19 patients differed from healthy individuals, mild COVID-19 cases and patients with flu-like illness (Figure 12 A). This was also reflected by a trend of decreased microbiota diversity depicted as Shannon and Simpson index (Figure 12 B).

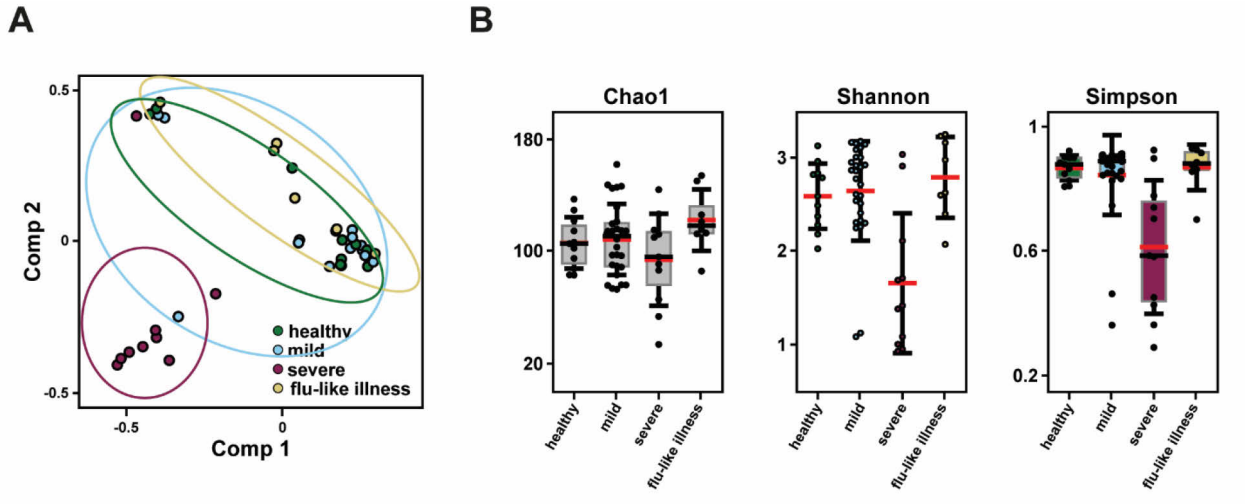

Figure 12. Oral microbiota composition of severe COVID-19 patients is dysbiotic. **(A)** PCoA of the oral microbiota from healthy individuals, flu-like illness, as well as mild and severe COVID-19 patients. (**B**) Species richness calculated as Chao1 index and microbiota diversity calculated as Shannon and Simpson index of the oral microbiota of healthy individuals, flu-like illness, as well as mild and severe COVID-19 patients. . Kruskal-Wallis test with Dunn's multiple comparisons was used to determine no significant differences.

In order to reveal which bacterial species are differently abundant in the oral microbiota of hospitalized COVID-19 patients a LefSE measurement was performed. Several genera were enriched in severe COVID-19 in comparison with healthy donors, flu-like illness and mild COVID-19 patients, among them *Pseudomonas*, *Enterococcus* and *Staphylococcus* (Figure 13 A).

To directly quantify differences between the investigated groups, the relative abundance of various bacterial genera of the oral cavity was determined. Interestingly, *Streptococcus*, the genera inducing cross-reactive antibodies specific to RBD, was significantly reduced in the oral cavity of patients severely suffering from COVID-19. This was not observed for the *Bifidobacterium* genus, even though *Bifidobacterium pseudocatenulatum* induced as well fecal anti-RBD specific antibodies (Figure 13 B). The oropharynx of hospitalized COVID-19 patients was therefore characterized by increased abundancies of *Enterococci* and *Staphylococci* genera. Of note, hospitalized patients were only partly treated with antibiotics, therefore these changes in the oral microbiota composition cannot be explained by usage of antibiotics at the intensive care unit.

In summary, these data suggest that the oral microbiota of severe COVID-19 cases differs from mild cases, healthy individuals and patients with flu-like symptoms and is characterized by a decrease in the genus *Streptococcus* and an increase in the genera *Enterococcus* and *Staphylococcus*.

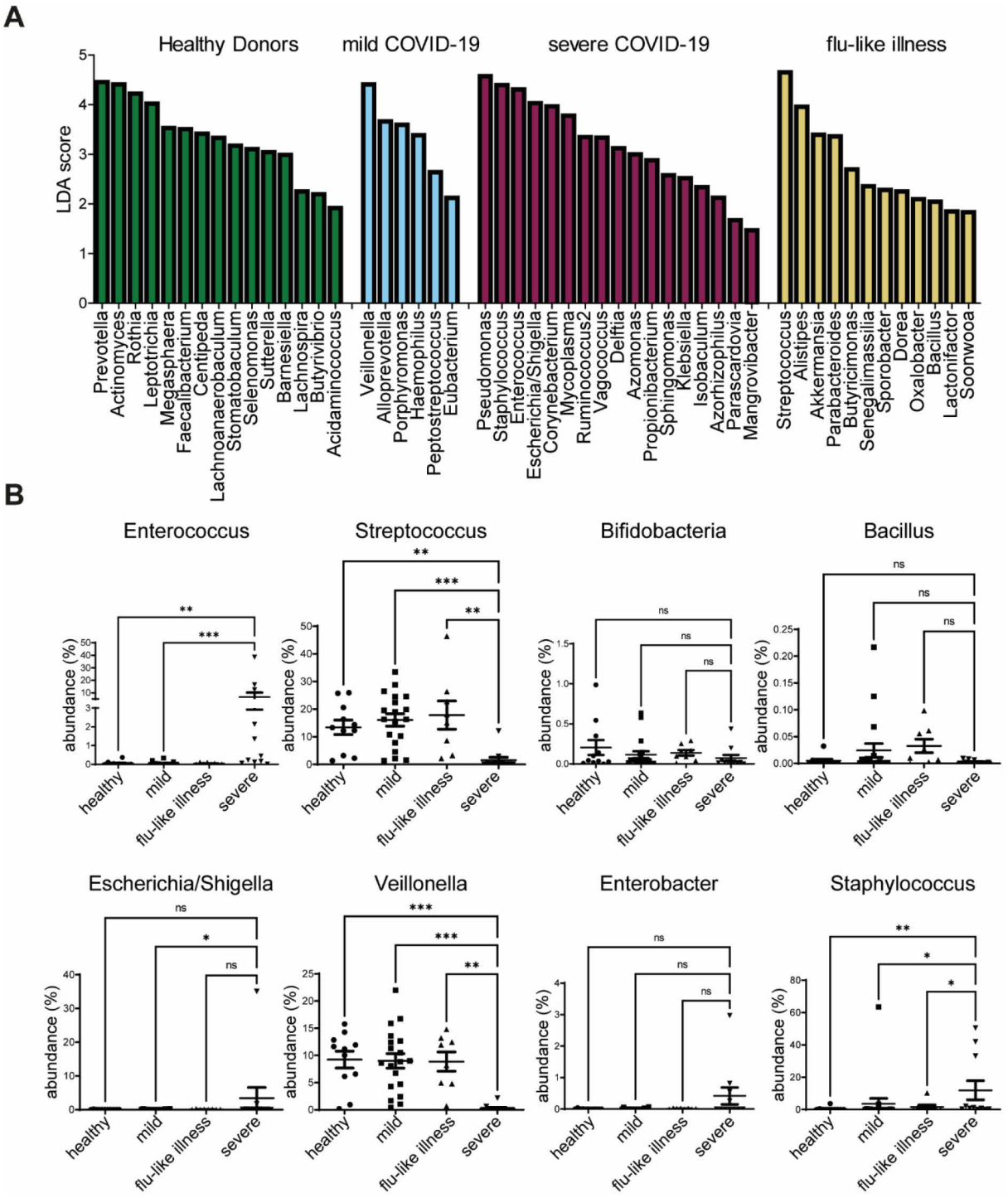

Figure 13 Severe COVID-19 induces changes in the oral microbiota. (A) LDA scores of genera as calculated by LefSE measurements of the oral microbiota from healthy individuals, flu-like illness patients and mild and severe COVID-19 patients. (**B**) Relative abundance of selected genera of the oral microbiota from healthy individuals, flu-like illness patients and mild and severe COVID-19 patients. Kruskal-Wallis test with Dunn's multiple comparisons was used. *, $p<0.05$, **, $p<0.01$, ***, $p<0.001$, ns, not significant.

4.11 Alterations in the fecal microbiota of hospitalized COVID-19 patients

In order to determine whether the differences in the oral microbiota are also present in the fecal microbiota composition, we analyzed and compared the fecal microbiota composition of severe COVID-19 patients and healthy individuals by 16S rRNA gene sequencing.

Fecal microbiota of severe COVID-19 patients did not differ from healthy donors, shown by PCoA based on Bray-Curtis dissimilarity distance (Figure 14 A). The bacterial composition of six severe COVID-19 donors built a distinct cluster, hinting towards heterogeneity inside the cohort.

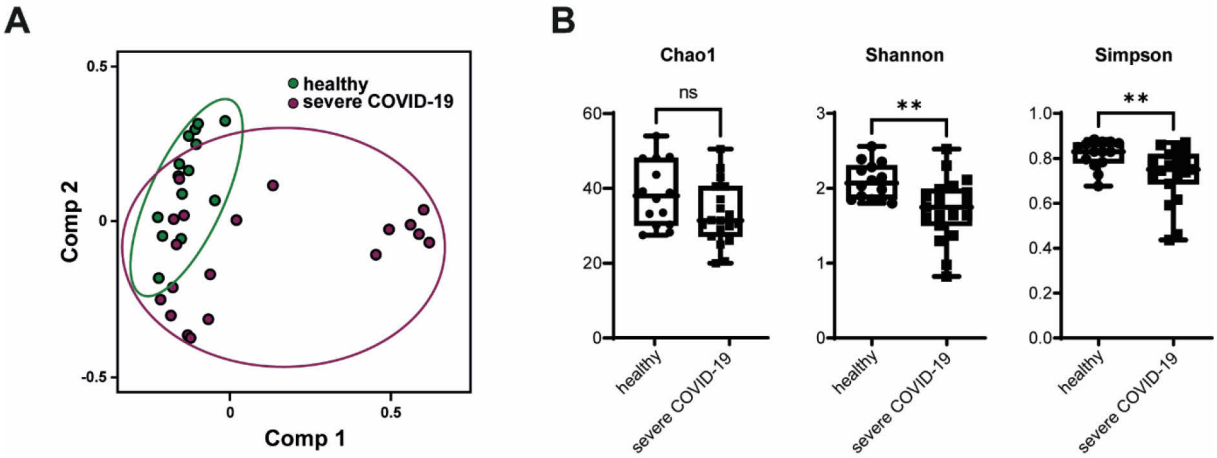

Figure 14 Fecal microbiota diversity is reduced in severe COVID-19 patients. (**A**) PCoA based on Bray-Curtis dissimilarity distance of the fecal microbiota from healthy individuals and severe COVID-19 patients. (**B**) Bacterial richness (Chao1 index) and diversity (Shannon and Simpson index) of fecal microbiota from healthy donors and hospitalized COVID-19 patients. **, $p<0.01$, as calculated by unpaired t-test; n.s., not significant.

LefSE analysis of the fecal bacterial composition resulted in several genera differently abundant in severe COVID-19 patients. In accordance with the observations from oral microbiota, *Enterococcus*, *Staphylococcus* and *Pseudomonas* genera were enriched in hospitalized COVID-19 patients, whereas *Streptococcus* and *Bifidobacterium* were more abundant in healthy donors, based on LDA scores (Figure 15 A).

The identification of altered abundances of bacterial genera in the feces was similar to the results obtained from the oropharynx. *Streptococcus* was significantly increased in healthy individuals in contrast to *Bifidobacterium*. *Enterococcus* was enriched and -opposed to the oral microbiota- *Staphylococcus* was not increased in severe COVID-19 patients (Figure 15 B).

Taken together, these data indicate that severe COVID-19 alters the fecal microbiota, resulting in decreased bacterial diversity and decreased abundance of *Streptococcus* and outgrowth of *Enterococcus*.

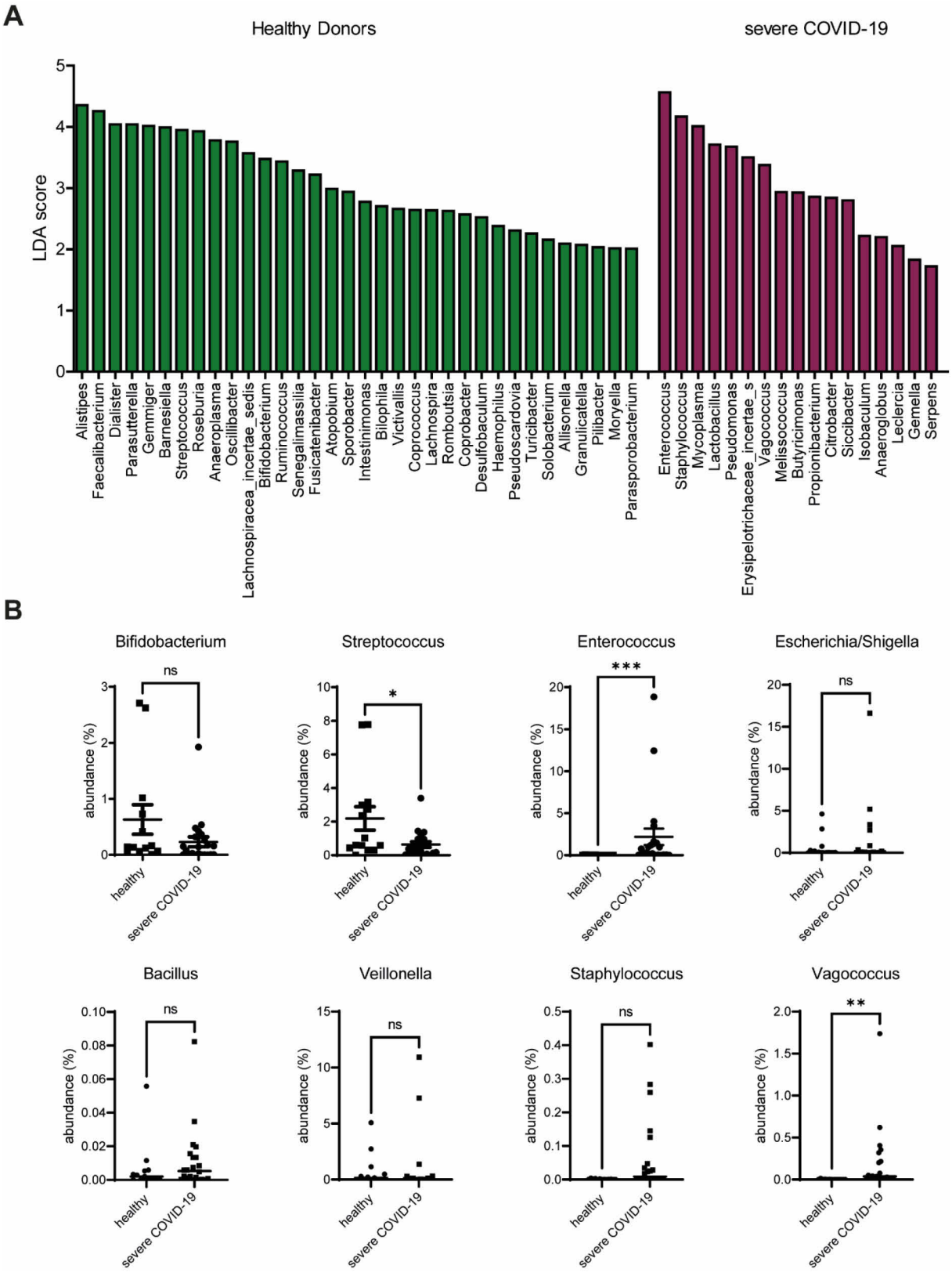

Figure 15 Fecal microbiota in hospitalized COVID-19 patients is altered compared to healthy individuals. (**A**) Linear discriminant analysis (LDA) scores from LefSE analysis of fecal bacterial genera from healthy individuals and severe COVID-19 patients. (**B**) Abundance of selected genera of the fecal microbiota from healthy donors and hospitalized COVID-19 patients. *, $p<0.05$, **, $p<0.01$, ***, $p<0.001$, as calculated by unpaired t-test; n.s., not significant.

In addition to viral infections, immune responses towards the fecal microbiota impact on chronic inflammatory diseases affecting peripheral sites outside the gastrointestinal tract as observed in RA, MS and AS (Maeda and Takeda, 2017; Schepici et al., 2019; Zhang et al., 2019b).
On this account, we next wanted to understand the alterations of the fecal microbiota composition associated with AS.

4.12 Immunoglobulin-coating of fecal bacteria is not altered in AS

To understand the interaction of the fecal microbiota with the mucosal immune system, the coating of fecal bacteria with intestinal-derived IgA1, IgA2 and IgG was determined. Interestingly, no differences in the coating of the total microbiota neither with IgA1, IgA2 nor IgG was observed between HC individuals and AS patients (Figure 16).

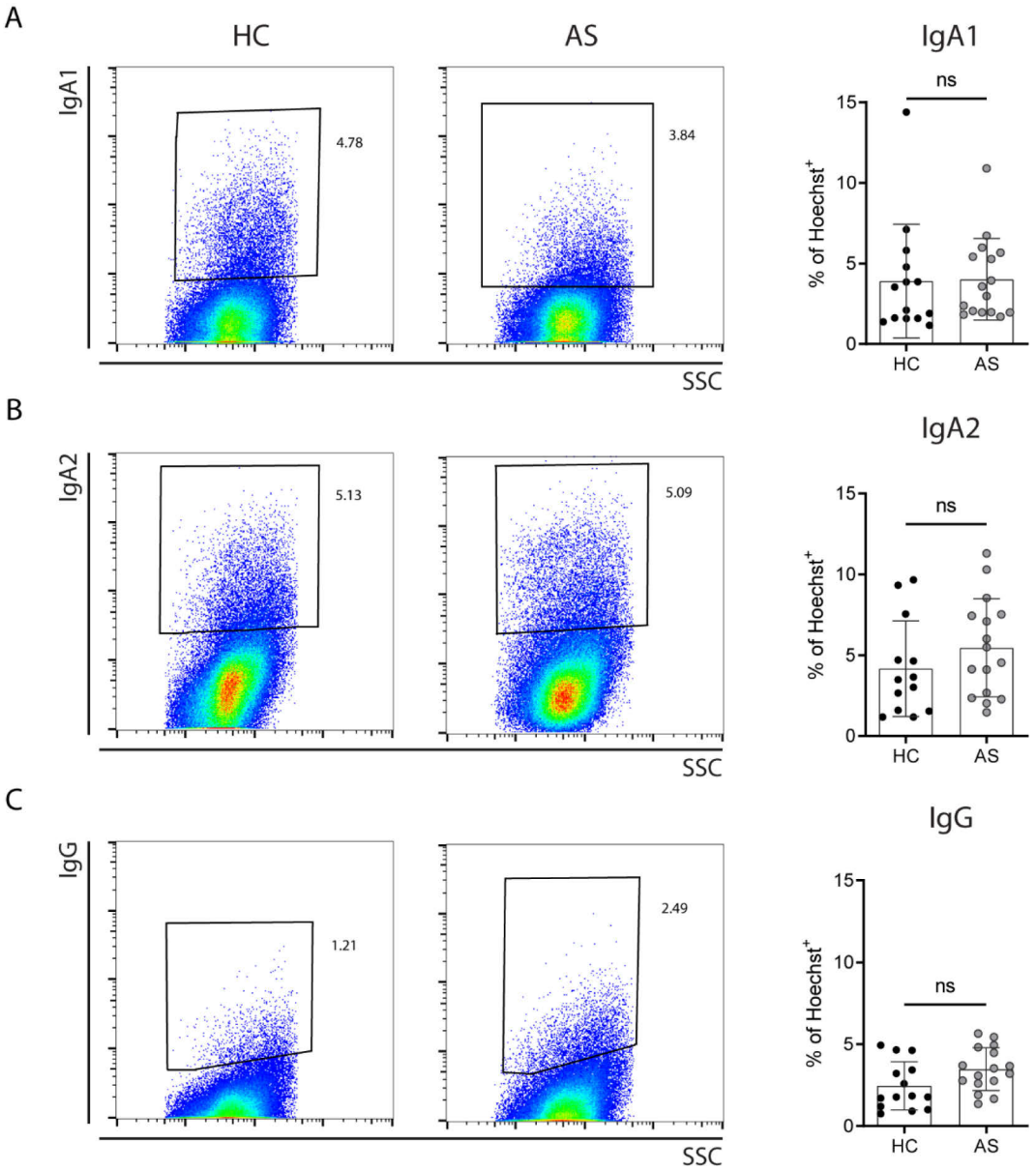

Figure 16. Coating of fecal bacteria by immunoglobulins is not altered in AS. Representative flow cytometry plots and quantification of **(A)** IgA1-, **(B)** IgA2- and **(C)** IgG-coated fecal bacteria in healthy individuals (HC) and AS patients. ns, not significant as calculated by unpaired t-test with Welch's correction.

4.13 AS patients show decreased frequency of SytoBC$^+$DAPI$^-$ bacteria in feces

It was previously reported that AS patients have an increased abundance of *Bacteroidetes* in the terminal ileum compared to healthy individuals, whereas the fecal microbiota composition was decreased in *Bacteroidetes* and increased in *Actinobacteria* species (Costello et al., 2015; Wen et al., 2017). In order to understand which bacteria actively influence the disease state, we investigated the living fraction of the fecal bacteria. To this end, we used the DNA dyes propidium iodide (PI) and SytoBC allowing us to simultaneously discriminate between live, injured and dead bacterial cells (Ben-Amor et al., 2005). The combination of both dyes enabled us to differentiate between "live" or intact bacteria, which are positive for SytoBC and negative for DAPI (SytoBC$^+$DAPI$^-$) and "dead" or compromised bacteria which are penetrated by both fluorophores (SytoBC$^+$DAPI$^+$).

Fecal samples from patients suffering from AS were markedly decreased in frequencies of live, SytoBC$^+$DAPI$^-$ bacteria compared to healthy individuals (Figure 17 A).

To verify the viability of the two identified compartments, the SytoBC$^+$DAPI$^-$ and SytoBC$^+$DAPI$^+$ bacterial populations of HCs and AS patients were sorted into PYG medium and kept under anaerobic conditions for two days before the optical density (OD) was assessed. SytoBC$^+$DAPI$^-$ bacterial cells from HC and AS fecal samples proliferated in contrast to their SytoBC$^+$DAPI$^+$ counterparts (Figure 17 B).

Thus, these chronic inflammations of the CNS are associated with decreased proportions of fecal SytoBC$^+$DAPI$^-$ bacteria, reflecting a decrease in the live bacteria compartment.

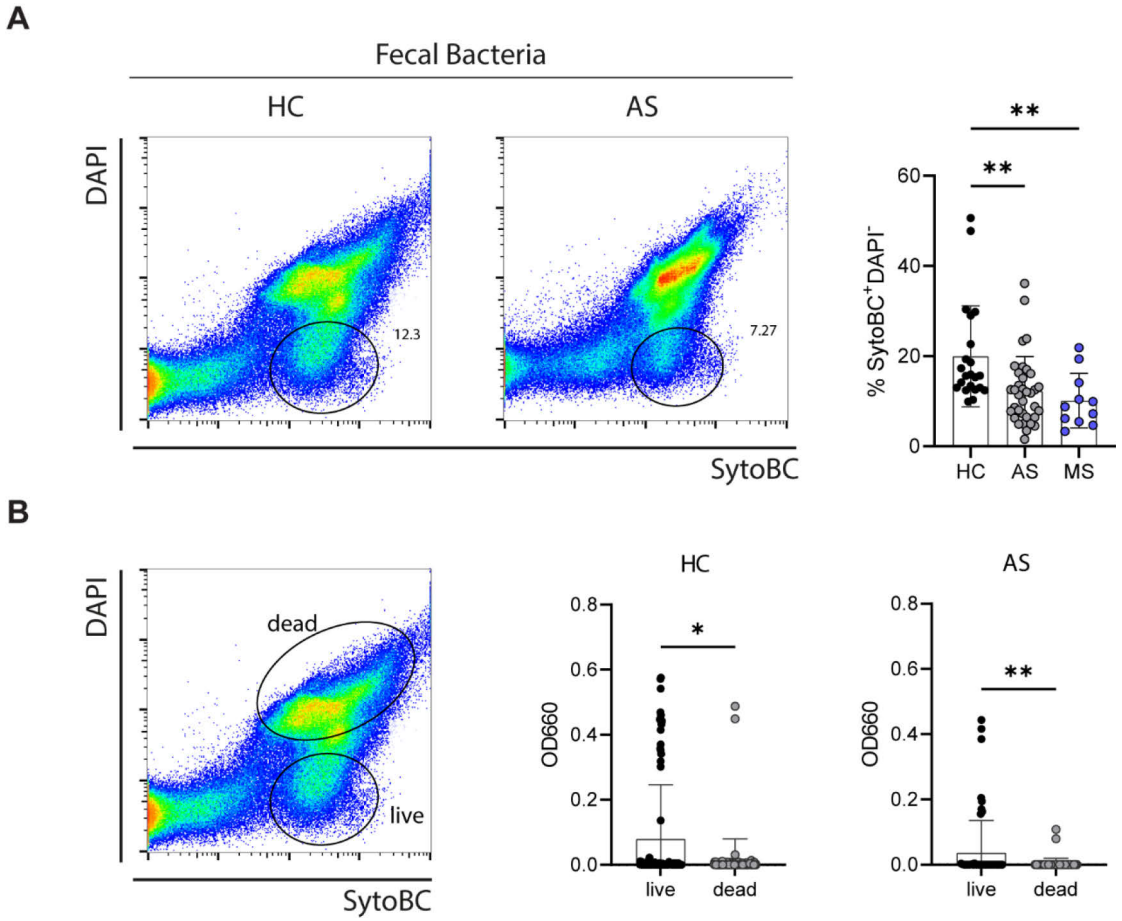

Figure 17. Live fraction of fecal bacteria is decreased in AS patients. (A) Representative flow cytometry plots of fecal samples from HC and AS patients stained with DAPI and SytoBC. The $SytoBC^{+}DAPI^{-}$ population is defined as live bacteria. **(B)** Gates depicting the live and dead bacteria fraction and OD values at 660nm from the respective sorted cells after a two days culture in PYG medium. Values represent three healthy donor samples and two AS patient samples. *, $p<0.05$, **, $p<0.01$, ***, $p<0.001$, ns, not significant as calculated by Kruskal-Wallis test with Dunn's multiple comparisons (A) and Mann-Whitney test (B).

4.14 Distinct microbiota populations reveal novel disease-associated bacteria

In order to identify the bacterial taxa comprising the live and dead compartment, the SytoBC^{+}DAPI^{-} and SytoBC^{+}DAPI^{+} population were sorted and analyzed by 16S rRNA gene sequencing. The fecal microbiota composition between healthy individuals and AS patients did not differ as revealed by a Non-metric Multidimensional Scaling (NMDS) based on Bray-Curtis distance but the analysis of the live and dead bacterial compartment resulted in a slightly increased separation of the HC and AS groups compared to the bulk fecal samples (Figure 18 A, C, E). The alpha diversity of the SytoBC^{+}DAPI^{+} compartment from AS patients was decreased as calculated by Shannon and Simpson index, which was neither observed in the unsorted sample nor the SytoBC^{+}DAPI^{-} population (Figure 18 B, D, F).
A random forest analysis resulted in mean decrease accuracy (MDA) values depicting bacterial taxa predictive for AS or healthy status (Figure 19 A). Analysis of the naive fecal sample resulted in 14 genera identified to be differently present in AS and HC of which only three were shared with the dead bacterial fraction and two with the live compartment (Figure 19 B). Interestingly, only the genus *Devosia* was predictive for AS in all three bacterial compartments and its relative abundance was significantly increased in AS naive fecal samples and the SytoBC^{+}DAPI^{-} and SytoBC^{+}DAPI^{+} fraction (Figure 19 C).
Therefore, the analysis of the live and dead fecal microbial compartment reveals novel disease-associated bacteria which could not be identified by 16S rRNA gene sequencing of the total fecal sample.

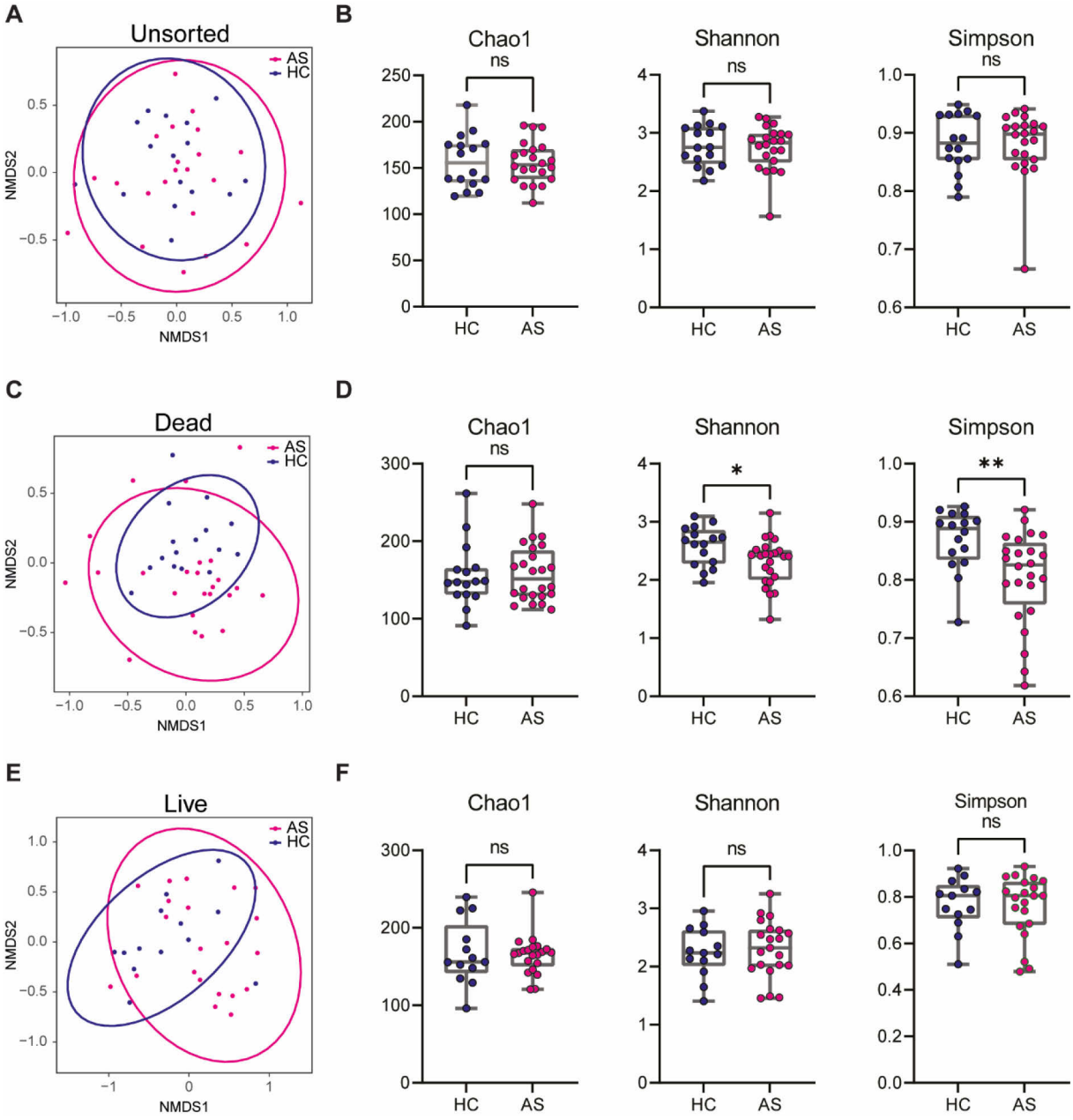

Figure 18. Fecal microbiota composition of AS patients does not differ from healthy individuals independent of bacterial fraction. NMDS plots of the naive fecal sample (**A**) and the dead (**C**) and live (**E**) fraction of AS patients and healthy individuals based on Bray-Curtis distance. Bacterial richness (Chao1 index) and diversity (Shannon and Simpson index) of the naive fecal microbiota (**B**), the dead (**D**) and live (**F**) from HC and AS patients. *, $p<0.05$, **, $p<0.01$, ***, $p<0.001$, ns, not significant as calculated by Mann-Whitney test.

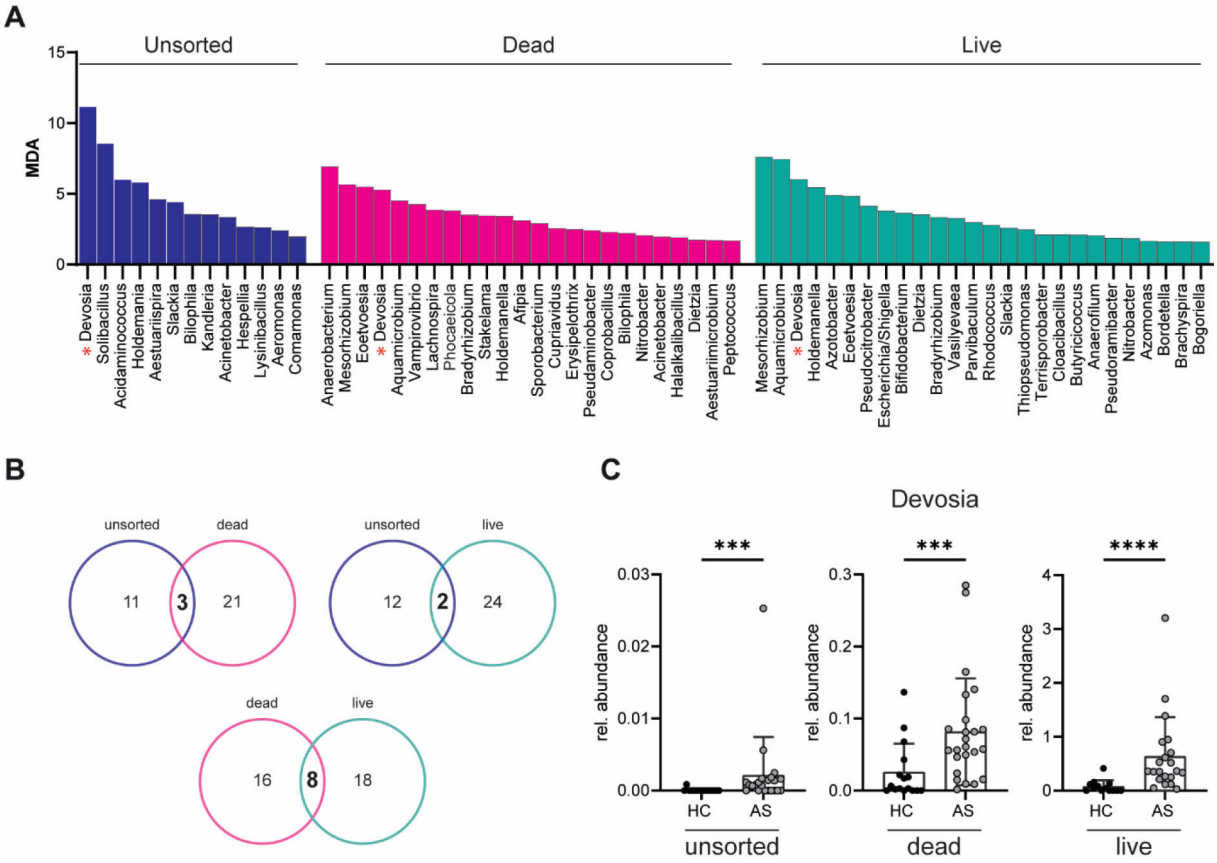

Figure 19. Disease-associated bacteria from sorted fractions differ from bulk sample. (**A**) MDA scores of bacterial taxa from the unsorted, the dead and the live compartment calculated by Random forest. Depicted with a red asterix is the genus *Devosia*. (**B**) Venn plots of taxa identified by RF across distinct compartments. (**C**) Relative abundance of the genus *Devosia* in the naive, dead and live bacterial fraction of healthy individuals and AS patients. ***, p<0.001, ****, p<0.0001 as calculated by Mann-Whitney test.

The relative abundances of the bacterial taxa with high MDA values in the SytoBC^{+}DAPI^{-} and SytoBC^{+}DAPI^{+} compartments were compared between AS patients and healthy individuals (Figure 20). Indeed, the discriminant taxa *Anaerobacterium*, *Vampirovibrio* and *Phocaeicola* were increased in the SytoBC^{+}DAPI^{+} population of healthy donors compared to AS patients, whereas in the SytoBC^{+}DAPI^{-} population they were equally abundant (Figure 20 A). Differences for the genera *Azotobacter*, *Pseudocitrobacter*, *Escherichia/Shigella* and *Bifidobacterium* were observed in the live but not the dead bacteria compartment as predicted by MDA scores (Figure 20 B). *Bifidobacterium* was the sole genus increased in AS patients live fecal bacteria.

The bacterial taxa *Mesorhizobium*, *Eoetvesia*, *Aquamicrobium* and *Holdemanella* were decreased in healthy individuals in both SytoBC^{+}DAPI^{-} and SytoBC^{+}DAPI^{+} populations (Figure 20 C).

Thus, the composition of live and dead fecal bacteria of AS patients differs in their abundance of distinct bacterial taxa, thereby revealing novel disease-associated bacteria.

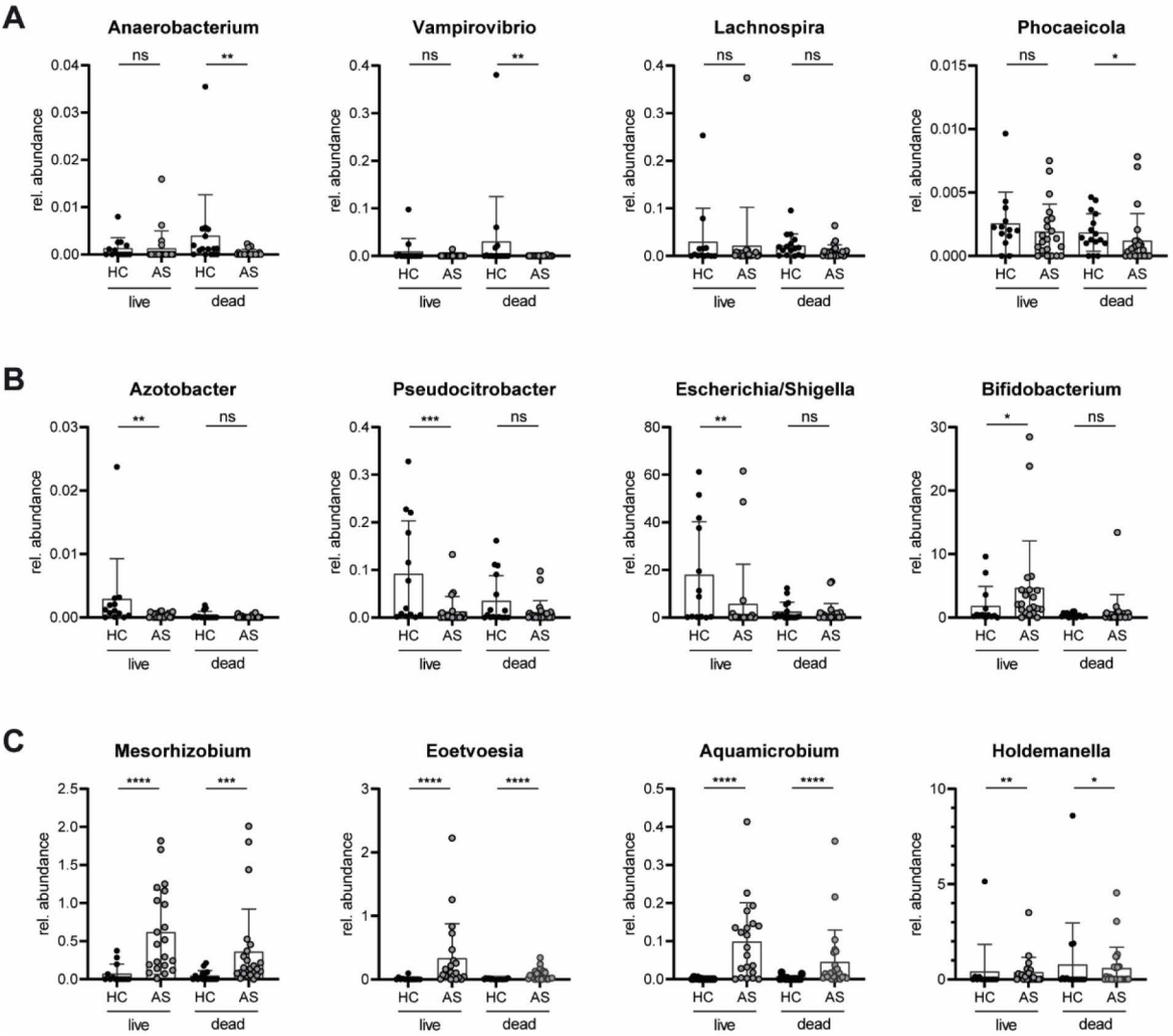

Figure 20. Different abundant bacteria in HC and AS SytoBC^{+}DAPI^{-} and SytoBC^{+}DAPI^{+} fractions. Relative abundancies of selected taxa identified by RF as discriminant for HC or AS in the dead fraction (**A**), the live fraction (**B**) or in both (**C**). *, p<0.05, **, p<0.01, ***, p<0.001, ns, not significant as calculated by Mann-Whitney test.

5 Discussion

Ly6C$^+$ IgA$^+$ PCs are characterized by increased expression of Sca-1

Small intestinal LP IgA-secreting PCs build a heterogeneous population distinct in cytokine production and expression of surface molecules like Ly6C. Even though it was previously shown, that Ly6C$^+$ PCs are absent in T cell-deficient mice and develop independent of ILFs and PPs, it has not been clarified how their transcriptomic profile and their developmental stage differs from PCs lacking Ly6C expression (Winsauer et al., 2015).

Therefore, the transcriptome of murine SI Ly6C$^+$ PCs was compared to Ly6C$^-$ PCs. Notably, Ly6C$^+$ PCs were characterized by an increased expression of immunoglobulin heavy and light chain genes as well as the surface protein Sca-1, whereas the expression of genes associated with DNA replication and the MHC class II H2-M beta 2 chain gene were increased in PCs lacking Ly6C. Consistent with the upregulated Ig secretion and progressive loss of MHCII expression during PC development (Kallies et al., 2004), this data indicate, that Ly6C$^+$ PCs represent a more matured or aged subpopulation of IgA secreting cells, which can be further differentiated by the expression of Sca-1. Antibody-secreting CD138$^+$ cells in the BM, the spleen and the PPs display Sca-1 on their surface, thus it is possible that Sca-1$^+$ IgA$^+$ PCs residing in the LP can acquire Sca-1 expression already in the PPs (Wilmore et al., 2017). However, IgA-secreting PCs from the LP obtained Sca-1 *in vitro* independent of Ly6C expression, suggesting that it represents a surface antigen of matured PCs, which can be acquired upon survival and activation signals such as IL-6 and BAFF, additionally to the known inducers of Sca-1 expression on B cells, namely IFN-γ and TNF (Malek et al., 1989).

Interestingly, it has been recently reported that age-associated B cells accumulating in the meningeal dura mater express Sca-1. These cells are significantly decreased in seven to 12 -week-old mice compared to seven to 25-months-old mice (Brioschi et al., 2021). Whether this age-associated increase of Sca-1$^+$ PCs is also present in the SI LP and what their

contribution in controlling the microbiota composition is, should be in the focus of future studies.

Unpublished previous work in our group has revealed that Ly6C is absent on B cells from PPs and that Ly6C$^+$ PCs accumulate over time in the SI LP of young mice (data not shown). Recently, newly generated IgA-secreting plasma blasts were found in the liver and were described to express Ly6C originating from PPs (Moro-Sibilot et al., 2016). This indicates that the expression of Ly6C is initiated after egress from the PPs and maintained by PCs that encountered intestinal antigens. Stimulation of splenic B cells with LPS induces Ly6C expression that is diminished once CD40 is simultaneously engaged (Wrammert et al., 2002) but other microbial stimuli and potentially signals provided by T cells (Winsauer et al., 2015) – besides BAFF and IL-6-which might lead to the induction of Ly6C expression still need to be determined. Additionally, it should be clarified, which potential function Ly6C exerts on PCs, as the data obtained in this work mostly suggest the role of a marker to characterize different PC subsets.

Fecal IgA antibodies cross-reactive to the RBD of SARS-CoV-2 are present in unexposed individuals

The presence of SARS-CoV-2-reactive antibodies in unexposed individuals has been attributed to previous infections with common cold coronaviruses but the origin of these systemic cross-reactive antibodies has not been proven. Here, we report the existence of secretory IgA antibodies at mucosal surfaces of healthy, uninfected individuals that bind to the RBD of the SARS-CoV-2 S-protein.

Unexposed donors harbor S-protein-binding IgG antibodies in their sera. Even though it has been assumed that these antibodies were derived from previous immune responses towards seasonally spreading human coronaviruses, they could also be detected in individuals without recent virus infection as determined by reverse transcription-quantitative PCR (Ng et al., 2020). All of the healthy donors investigated in our work were seronegative for RBD-specific antibodies but a fraction still displayed

intestinal IgA targeting RBD indicating a separation of the systemic and mucosal immune response. Interestingly, the prevalence of cross-reactive antibodies peaks in children and adolescents (6-16 years) and declines with age (Ng et al., 2020). Likewise, the presence of RBD-binding IgG antibodies correlates with younger age (Selva et al., 2021) consistent with the absence of mucosal cross-reactive IgA binding to RBD in aged individuals observed in this work. As age is a major risk factor for the development of severe COVID-19 (Zhou et al., 2020b), the neutralizing capacity of these cross-reactive antibodies should be determined.

Besides antibodies, pre-existing cross-reactive $CD4^+$ T cells have been detected in healthy donors, which are reactive to the spike protein of SARS-CoV-2 as well as endemic coronaviruses (Braun et al., 2020). However, in COVID-19 patients these cross-reactive T cells are absent among the SARS-CoV-2-specific $CD4^+$ T cell compartment, suggesting that these pre-existing low-avidity T cells do not confer protection against SARS-CoV-2 infection and potentially are another risk factor during COVID-19 in older individuals (Bacher et al., 2020). The questions arise whether cross-reactive T cells reside at mucosal tissues and if they are involved in the initiation of the immune response leading to cross-reactive secretory IgA, which seems likely concerning the contribution of T cells in the generation of IgA, e.g. in the PPs.

Streptococcus salivarius induces RBD-specific antibodies

Streptococcus salivarius, a member of the intestinal and oral microbiota was among the identified bacteria pointing towards a putative role for the induction of neutralizing anti-RBD antibodies. Sera derived from COVID-19 infected patients bind to *S. salivarius* and Western blot analysis of the bacterial lysate with subsequent mass-spectroscopy, cloning and overexpression in *E. coli* revealed an uncharacterized protein RSSL-01370 as an antibody target (data not shown). Furthermore, oral administration of *S. salivarius in vivo* in mice induced fecal RBD-binding IgA antibodies,

that inhibit RBD-ACE2 interactions. Epitope-mapping of IgA antibodies induced by *S. salivarius* against peptides derived from the S-Protein of SARS-CoV-2 revealed binding to a peptide sequence corresponding to the receptor binding motif (RBM) of RBD (data not shown). Hence, the commensal bacteria *S. salivarius* of the oropharyngeal microbiota induces cross-reactive antibodies that recognize structures in the RBD of the SARS-CoV-2 S-protein.

Such bacteria-induced antibodies additionally targeting viral proteins have also been reported for HIV-1. Specifically the HIV-1 envelope proteins gp41 and gp120 are bound by antibodies cross-reacting with intestinal bacteria (Jeffries et al., 2016; Trama et al., 2014). Interestingly, immunization of humans with a vaccine containing gp120 and gp41 components has resulted in HIV-1 reactive, but not neutralizing antibodies (Williams et al., 2015). In line with that, it should be determined whether the identified, RBD-like protein from *S. salivarius* alone is capable of inducing an immune response resulting in RBD binding and potentially neutralizing antibodies.

The oral and fecal microbiota composition of severe COVID-19 patients is altered

Especially in the context of vaccination strategies against SARS-CoV-2 this elaboration is of high relevance as mainly systemic neutralizing IgG antibodies are induced upon vaccination (Goel et al., 2021; Ramasamy et al., 2021; Sahin et al., 2020). In order to efficiently prevent an infection with SARS-CoV-2, neutralizing antibodies at the nasal and oral mucosal surfaces may be necessary. After immunization with two doses of mRNA-based vaccines, salivary IgG antibodies binding to RBD can be detected while no or only a moderate IgA response has been reported (Azzi et al., 2022; Becker et al., 2021). Despite fecal IgA binding to RBD, we detected salivary IgA antibodies reactive to *S. salivarius* in unexposed healthy donors. Thus, our ongoing study investigates if an oral supplementation of *S. salivarius* in combination with a SARS-CoV-2 vaccine results in

neutralizing secretory IgA antibodies at relevant sites for virus entry, namely the oral cavity.

Consequently, the composition of the oral microbiota may serve as a risk factor for the development of severe COVID-19. The microbiota potentially affects the protection against virus infection by modulating the expression of the ACE2 receptor (Geva-Zatorsky et al., 2017), inducing type I IFN responses in the lung (Bradley et al., 2019) and initiating TGF-β mediated IgA CSR (Beller et al., 2020; Ferreira-Gomes et al., 2021).

We observed that the oral microbiota of hospitalized COVID-19 cases was decreased in *Streptococcus* species irrespective of antibiotic treatment compared to healthy individuals, mild COVID-19 cases and patients with flu-like symptoms. This could reflect that a diminished abundance of salivary *Streptococcus* species renders individuals more susceptible to a severe COVID-19 disease course or that the severe disease results in this alteration of the microbial composition. Both scenarios are possible and may exist concomitantly. It should not be neglected that differences in the oral microbiota can also arise from the invasive ventilation of patients at the intensive care unit as it has been previously reported (Llorens-Rico et al., 2021). However, the abundance of *Streptococcus* was not affected by the type of oxygen support, thereby reflecting a disease-specific phenomenon.

Additionally to alterations in the oral microbiota, changes in the fecal microbiota of severe COVID-19 patients were detected. Previous studies have shown that hospitalized COVID-19 cases display changes in their microbiota composition (Yeoh et al., 2021; Zuo et al., 2020) but no bacterial signature has been proposed, probably to heterogeneity of the patient cohorts and different medical therapies. In general, it has been observed that acute COVID-19 is associated with opportunistic pathogens, whereas immunomodulatory bacteria are depleted (Zuo et al., 2020). Our findings of an increase in *Enterococc*i and *Staphylococci* and depletion of *Veillonella* and *Streptococci* species in severe COVID-19 cases are compatible with that view.

It should be kept in mind that the described differences in bacterial taxa are based on relative abundances. Therefore, it cannot be excluded, that the observed alterations could represent a decrease in *Streptococci* species as well as an increase in other species. In order to more accurately analyze the differences in microbiota composition, the actual bacterial cell number should be determined, as the usage of relative abundance might lead to different results (Vandeputte et al., 2017).

Decreased frequency of live bacteria in feces from AS patients compared to healthy individuals

Alterations in the intestinal microbiota are also present in patients suffering from AS, an inflammatory disease of the spine and sacroiliac joints. Bacteria like *Prevotella corpri* and *Bacteroides species* have been described among various reports to be altered in the fecal microbiota of AS patients but these findings are not consistent with other studies (Klingberg et al., 2019; Wen et al., 2017; Yin et al., 2020; Zhang et al., 2019a; Zhou et al., 2020a). It was proposed that the presentation of microbial antigens on HLA-B27 can lead to autoimmune reactions via the principle of molecular mimicry; however, the detailed mechanisms explaining the impact of the microbiota on disease development and progression remain to be determined (Ramos et al., 2002; Schwimmbeck and Oldstone, 1988). In order to identify intestinal microbes actively involved in AS, the compartment of live and dead or compromised fecal bacteria of AS patients and healthy individuals was investigated, thereby providing more detailed information than solely analyzing native fecal samples. The observed reduction of SytoBC^{+}DAPI^{-} (live) bacteria in patients with AS and MS could be explained by the overall inflammatory milieu, resulting in increased mucosal immune responses. The coating of fecal bacteria with IgA and IgG is a parameter indirectly reflecting intestinal inflammation as it is increased in IBD and correlates with disease activity (Lin et al., 2018). In AS the bacterial coating with IgA and IgG is similar to healthy feces, thus arguing at least against differences in

immunoglobulin-mediated immune responses leading to a decrease in live bacteria.

Another reason for the increase in compromised or dead bacteria in fecal samples from AS patients could be the prevalence of strictly anaerobe bacteria, which rapidly die once exposed to oxygen. Even though this is contrary to the notion, that inflammatory dysbiosis is characterized by an outgrowth of facultative anaerobic bacteria (Rigottier-Gois, 2013). However, the taxon significantly enriched in all fractions of AS fecal microbiota is *Devosia*, a genus of gram-negative, aerobic bacteria (Nakagawa et al., 1996). Further, the genus *Anaerobacterium* is increased in the dead bacteria compartment of healthy individuals, additionally arguing against the hypothesis, that the decrease in live fecal bacteria is a result of higher abundance of anaerobic microbes in AS patients. In line with that, the aerobic genus *Mesorhizobium* (Laranjo et al., 2014) is increased in the live and dead bacteria fraction of AS patients. In order to completely rule out an influence of strictly anaerobe bacteria on these findings, a more detailed, systematical analysis should be performed.

Even though the biological reasons resulting in the increased fraction of dead fecal bacteria in AS patients were not yet clarified, the discovered differences in flow cytometry profiles could be used for AS diagnosis. Additional work needs to be done to verify this predictive potential, which is of great relevance as the diagnosis delay of AS can be approximately 10 years (Dincer et al., 2008).

Compartmentalization in live and dead bacteria reveals novel disease-associated bacterial taxa

To determine the influence of certain bacterial species in the intestinal microbiota on a disease state, their abundance serves as an important factor. Nevertheless, the presence of gut microorganisms alone does not implicate their functional activity, which provides additional information about their actual effect on the disease (Schirmer et al., 2018). Consistent with that, it is favorable to differentiate between live and dead bacteria

concerning the major source of potentially disease mediating metabolites and antigens. The compartmentalization of fecal bacteria in SytoBC^{+}DAPI^{+} dead and SytoBC^{+}DAPI^{-} live bacteria revealed novel disease-associated bacteria taxa like *Anaerobacterium*, *Mesorhizobium, Eoetvoesia, Holdemanella* and *Azotobacter,* which would have been unidentified by analyzing the native feces. In which way the species comprising these genera influence AS onset and progression or whether their prevalence is a cause of the disease, remains to be determined. Further, it needs to clarified how the composition of the live and dead compartment is changing over time as at some point the dead bacteria was a living component of the microbiota. If the death rate of a certain microbe constantly exceeds its growth rate, it will be excluded from the bacterial community and thus be undetectable.

Some of the differentially abundant bacteria like *Devosia*, *Mesorhizobium* and *Eoetvoesia* are known to be present in soil or wastewater (Felfoldi et al., 2014; Jarvis et al., 1997; Talwar et al., 2020) and are not primarily associated with the human intestinal microbiota, which might hint towards a potential contamination.

Devosia was the only taxon commonly increased in AS fecal samples compared to healthy donors. The genus comprises gram-negative bacteria, predominantly present in toxin-contaminated soil habitats and characterized by genes encoding for peptide permeases (Talwar et al., 2020). How *Devosia* species may impact AS is completely speculative but it is worth mentioning that a strain has been isolated from cerebrospinal fluid (CSF) (Nicholson et al., 2015), suggesting that it could play a role in immune responses outside the intestine.

6 References

Albenberg, L., T.V. Esipova, C.P. Judge, K. Bittinger, J. Chen, A. Laughlin, S. Grunberg, R.N. Baldassano, J.D. Lewis, H. Li, S.R. Thom, F.D. Bushman, S.A. Vinogradov, and G.D. Wu. 2014. Correlation between intraluminal oxygen gradient and radial partitioning of intestinal microbiota. *Gastroenterology* 147:1055-1063 e1058.

Arpaia, N., C. Campbell, X. Fan, S. Dikiy, J. van der Veeken, P. deRoos, H. Liu, J.R. Cross, K. Pfeffer, P.J. Coffer, and A.Y. Rudensky. 2013. Metabolites produced by commensal bacteria promote peripheral regulatory T-cell generation. *Nature* 504:451-455.

Asquith, M., P.R. Sternes, M.E. Costello, L. Karstens, S. Diamond, T.M. Martin, Z. Li, M.S. Marshall, T.D. Spector, K.A. le Cao, J.T. Rosenbaum, and M.A. Brown. 2019. HLA Alleles Associated With Risk of Ankylosing Spondylitis and Rheumatoid Arthritis Influence the Gut Microbiome. *Arthritis Rheumatol* 71:1642-1650.

Atarashi, K., T. Tanoue, M. Ando, N. Kamada, Y. Nagano, S. Narushima, W. Suda, A. Imaoka, H. Setoyama, T. Nagamori, E. Ishikawa, T. Shima, T. Hara, S. Kado, T. Jinnohara, H. Ohno, T. Kondo, K. Toyooka, E. Watanabe, S. Yokoyama, S. Tokoro, H. Mori, Y. Noguchi, H. Morita, Ivanov, II, T. Sugiyama, G. Nunez, J.G. Camp, M. Hattori, Y. Umesaki, and K. Honda. 2015. Th17 Cell Induction by Adhesion of Microbes to Intestinal Epithelial Cells. *Cell* 163:367-380.

Azzi, L., D. Dalla Gasperina, G. Veronesi, M. Shallak, G. Ietto, D. Iovino, A. Baj, F. Gianfagna, V. Maurino, D. Focosi, F. Maggi, M.M. Ferrario, F. Dentali, G. Carcano, A. Tagliabue, L.S. Maffioli, R.S. Accolla, and G. Forlani. 2022. Mucosal immune response in BNT162b2 COVID-19 vaccine recipients. *EBioMedicine* 75:103788.

Bacher, P., E. Rosati, D. Esser, G.R. Martini, C. Saggau, E. Schiminsky, J. Dargvainiene, I. Schroder, I. Wieters, Y. Khodamoradi, F. Eberhardt, M. Vehreschild, H. Neb, M. Sonntagbauer, C. Conrad, F. Tran, P. Rosenstiel, R. Markewitz, K.P. Wandinger, M. Augustin, J. Rybniker, M. Kochanek, F. Leypoldt, O.A. Cornely, P. Koehler, A. Franke, and A. Scheffold. 2020. Low-Avidity CD4(+) T Cell Responses to SARS-CoV-2 in Unexposed Individuals and Humans with Severe COVID-19. *Immunity* 53:1258-1271 e1255.

Bassotti, G., G. de Roberto, F. Chistolini, F. Sietchiping-Nzepa, O. Morelli, and A. Morelli. 2004. Twenty-four-hour manometric study of colonic propulsive activity in patients with diarrhea due to inflammatory (ulcerative colitis) and non-inflammatory (irritable bowel syndrome) conditions. *Int J Colorectal Dis* 19:493-497.

Becker, M., A. Dulovic, D. Junker, N. Ruetalo, P.D. Kaiser, Y.T. Pinilla, C. Heinzel, J. Haering, B. Traenkle, T.R. Wagner, M. Layer, M. Mehrlaender, V. Mirakaj, J. Held, H. Planatscher, K. Schenke-Layland, G. Krause, M. Strengert, T. Bakchoul, K. Althaus, R. Fendel, A. Kreidenweiss, M. Koeppen, U. Rothbauer, M. Schindler, and N. Schneiderhan-Marra. 2021. Immune response to SARS-CoV-2 variants of concern in vaccinated individuals. *Nat Commun* 12:3109.

Beller, A., A. Kruglov, P. Durek, V. von Goetze, K. Werner, G.A. Heinz, J. Ninnemann, K. Lehmann, R. Maier, U. Hoffmann, R. Riedel, K. Heiking, J. Zimmermann, B. Siegmund, M.F. Mashreghi, A. Radbruch, and H.D. Chang. 2020. Specific microbiota enhances intestinal IgA levels by inducing TGF-beta in T follicular helper cells of Peyer's patches in mice. *Eur J Immunol* 50:783-794.

Ben-Amor, K., H. Heilig, H. Smidt, E.E. Vaughan, T. Abee, and W.M. de Vos. 2005. Genetic diversity of viable, injured, and dead fecal bacteria assessed by fluorescence-activated cell sorting and 16S rRNA gene analysis. *Appl Environ Microbiol* 71:4679-4689.

Benhamron, S., S.P. Pattanayak, M. Berger, and B. Tirosh. 2015. mTOR activation promotes plasma cell differentiation and bypasses XBP-1 for immunoglobulin secretion. *Mol Cell Biol* 35:153-166.

Berg, G., D. Rybakova, D. Fischer, T. Cernava, M.C. Verges, T. Charles, X. Chen, L. Cocolin, K. Eversole, G.H. Corral, M. Kazou, L. Kinkel, L. Lange, N. Lima, A. Loy, J.A. Macklin, E. Maguin, T. Mauchline, R. McClure, B. Mitter, M. Ryan, I. Sarand, H. Smidt, B. Schelkle, H. Roume, G.S. Kiran, J. Selvin, R.S.C. Souza, L. van Overbeek, B.K. Singh, M. Wagner, A. Walsh, A. Sessitsch, and M. Schloter. 2020. Microbiome definition re-visited: old concepts and new challenges. *Microbiome* 8:103.

Bergqvist, P., E. Gardby, A. Stensson, M. Bemark, and N.Y. Lycke. 2006. Gut IgA class switch recombination in the absence of CD40 does not occur in the lamina propria and is independent of germinal centers. *J Immunol* 177:7772-7783.

Bollinger, R.R., M.L. Everett, D. Palestrant, S.D. Love, S.S. Lin, and W. Parker. 2003. Human secretory immunoglobulin A may contribute to biofilm formation in the gut. *Immunology* 109:580-587.

Bradley, K.C., K. Finsterbusch, D. Schnepf, S. Crotta, M. Llorian, S. Davidson, S.Y. Fuchs, P. Staeheli, and A. Wack. 2019. Microbiota-Driven Tonic Interferon Signals in Lung Stromal Cells Protect from Influenza Virus Infection. *Cell Rep* 28:245-256 e244.

Brandtzaeg, P. 1974a. Mucosal and glandular distribution of immunoglobulin components: differential localization of free and bound SC in secretory epithelial cells. *J Immunol* 112:1553-1559.

Brandtzaeg, P. 1974b. Presence of J chain in human immunocytes containing various immunoglobulin classes. *Nature* 252:418-420.

Brandtzaeg, P. 2009. Mucosal immunity: induction, dissemination, and effector functions. *Scand J Immunol* 70:505-515.

Brandtzaeg, P., and F.E. Johansen. 2005. Mucosal B cells: phenotypic characteristics, transcriptional regulation, and homing properties. *Immunol Rev* 206:32-63.

Braun, J., L. Loyal, M. Frentsch, D. Wendisch, P. Georg, F. Kurth, S. Hippenstiel, M. Dingeldey, B. Kruse, F. Fauchere, E. Baysal, M. Mangold, L. Henze, R. Lauster, M.A. Mall, K. Beyer, J. Rohmel, S. Voigt, J. Schmitz, S. Miltenyi, I. Demuth, M.A. Muller, A. Hocke, M. Witzenrath, N. Suttorp, F. Kern, U. Reimer, H. Wenschuh, C. Drosten, V.M. Corman, C. Giesecke-Thiel, L.E. Sander, and A. Thiel. 2020. SARS-CoV-2-reactive T cells in healthy donors and patients with COVID-19. *Nature* 587:270-274.

Braun, J., and J. Sieper. 2007. Ankylosing spondylitis. *Lancet* 369:1379-1390.

Brioschi, S., W.L. Wang, V. Peng, M. Wang, I. Shchukina, Z.J. Greenberg, J.K. Bando, N. Jaeger, R.S. Czepielewski, A. Swain, D.A. Mogilenko, W.L. Beatty, P. Bayguinov, J.A.J. Fitzpatrick, L.G. Schuettpelz, C.C. Fronick, I. Smirnov, J. Kipnis, V.S. Shapiro, G.F. Wu, S. Gilfillan, M. Cella, M.N. Artyomov, S.H. Kleinstein, and M. Colonna. 2021. Heterogeneity of meningeal B cells reveals a lymphopoietic niche at the CNS borders. *Science* 373:

Buettner, M., and M. Lochner. 2016. Development and Function of Secondary and Tertiary Lymphoid Organs in the Small Intestine and the Colon. *Front Immunol* 7:342.

Bunker, J.J., S.A. Erickson, T.M. Flynn, C. Henry, J.C. Koval, M. Meisel, B. Jabri, D.A. Antonopoulos, P.C. Wilson, and A. Bendelac. 2017. Natural polyreactive IgA antibodies coat the intestinal microbiota. *Science* 358:

Burton, J.P., P.A. Wescombe, C.J. Moore, C.N. Chilcott, and J.R. Tagg. 2006. Safety assessment of the oral cavity probiotic Streptococcus salivarius K12. *Appl Environ Microbiol* 72:3050-3053.

Cao, A.T., S. Yao, B. Gong, R.I. Nurieva, C.O. Elson, and Y. Cong. 2015. Interleukin (IL)-21 promotes intestinal IgA response to microbiota. *Mucosal Immunol* 8:1072-1082.

Casola, S., K.L. Otipoby, M. Alimzhanov, S. Humme, N. Uyttersprot, J.L. Kutok, M.C. Carroll, and K. Rajewsky. 2004. B cell receptor signal strength determines B cell fate. *Nat Immunol* 5:317-327.

Castigli, E., S.A. Wilson, S. Scott, F. Dedeoglu, S. Xu, K.P. Lam, R.J. Bram, H. Jabara, and R.S. Geha. 2005. TACI and BAFF-R mediate isotype switching in B cells. *J Exp Med* 201:35-39.

Cazac, B.B., and J. Roes. 2000. TGF-beta receptor controls B cell responsiveness and induction of IgA in vivo. *Immunity* 13:443-451.

Cerutti, A. 2008. The regulation of IgA class switching. *Nat Rev Immunol* 8:421-434.

Chodirker, W.B., and T.B. Tomasi, Jr. 1963. Gamma-Globulins: Quantitative Relationships in Human Serum and Nonvascular Fluids. *Science* 142:1080-1081.

Clarridge, J.E., 3rd. 2004. Impact of 16S rRNA gene sequence analysis for identification of bacteria on clinical microbiology and infectious diseases. *Clin Microbiol Rev* 17:840-862, table of contents.

Cole, J.R., Q. Wang, J.A. Fish, B. Chai, D.M. McGarrell, Y. Sun, C.T. Brown, A. Porras-Alfaro, C.R. Kuske, and J.M. Tiedje. 2014. Ribosomal Database Project: data and tools for high throughput rRNA analysis. *Nucleic Acids Res* 42:D633-642.

Conley, M.E., and D.L. Delacroix. 1987. Intravascular and mucosal immunoglobulin A: two separate but related systems of immune defense? *Ann Intern Med* 106:892-899.

Costello, M.E., F. Ciccia, D. Willner, N. Warrington, P.C. Robinson, B. Gardiner, M. Marshall, T.J. Kenna, G. Triolo, and M.A. Brown. 2015. Brief Report: Intestinal Dysbiosis in Ankylosing Spondylitis. *Arthritis Rheumatol* 67:686-691.

Cullender, T.C., B. Chassaing, A. Janzon, K. Kumar, C.E. Muller, J.J. Werner, L.T. Angenent, M.E. Bell, A.G. Hay, D.A. Peterson, J. Walter, M. Vijay-Kumar, A.T. Gewirtz, and R.E. Ley. 2013. Innate and adaptive immunity interact to quench microbiome flagellar motility in the gut. *Cell Host Microbe* 14:571-581.

Cyster, J.G., and C.D.C. Allen. 2019. B Cell Responses: Cell Interaction Dynamics and Decisions. *Cell* 177:524-540.

David, L.A., C.F. Maurice, R.N. Carmody, D.B. Gootenberg, J.E. Button, B.E. Wolfe, A.V. Ling, A.S. Devlin, Y. Varma, M.A. Fischbach, S.B. Biddinger, R.J. Dutton, and P.J. Turnbaugh. 2014. Diet rapidly and reproducibly alters the human gut microbiome. *Nature* 505:559-563.

De Vadder, F., P. Kovatcheva-Datchary, D. Goncalves, J. Vinera, C. Zitoun, A. Duchampt, F. Backhed, and G. Mithieux. 2014. Microbiota-generated metabolites promote metabolic benefits via gut-brain neural circuits. *Cell* 156:84-96.

De Vos, M., C. Cuvelier, H. Mielants, E. Veys, F. Barbier, and A. Elewaut. 1989. Ileocolonoscopy in seronegative spondylarthropathy. *Gastroenterology* 96:339-344.

De Vos, M., H. Mielants, C. Cuvelier, A. Elewaut, and E. Veys. 1996. Long-term evolution of gut inflammation in patients with spondyloarthropathy. *Gastroenterology* 110:1696-1703.

Dethlefsen, L., M. McFall-Ngai, and D.A. Relman. 2007. An ecological and evolutionary perspective on human-microbe mutualism and disease. *Nature* 449:811-818.

Diaz-Pena, R., P. Castro-Santos, J. Duran, C. Santiago, and A. Lucia. 2020. The Genetics of Spondyloarthritis. *J Pers Med* 10:

Dincer, U., E. Cakar, M.Z. Kiralp, and H. Dursun. 2008. Diagnosis delay in patients with ankylosing spondylitis: possible reasons and proposals for new diagnostic criteria. *Clin Rheumatol* 27:457-462.

Dispinseri, S., M. Secchi, M.F. Pirillo, M. Tolazzi, M. Borghi, C. Brigatti, M.L. De Angelis, M. Baratella, E. Bazzigaluppi, G. Venturi, F. Sironi, A. Canitano, I. Marzinotto, C. Tresoldi, F. Ciceri, L. Piemonti, D. Negri, A. Cara, V. Lampasona, and G. Scarlatti. 2021. Neutralizing antibody responses to SARS-CoV-2 in symptomatic COVID-19 is persistent and critical for survival. *Nat Commun* 12:2670.

Donaldson, G.P., M.S. Ladinsky, K.B. Yu, J.G. Sanders, B.B. Yoo, W.C. Chou, M.E. Conner, A.M. Earl, R. Knight, P.J. Bjorkman, and S.K. Mazmanian. 2018. Gut microbiota utilize immunoglobulin A for mucosal colonization. *Science* 360:795-800.

Durack, J., and S.V. Lynch. 2019. The gut microbiome: Relationships with disease and opportunities for therapy. *J Exp Med* 216:20-40.

Fagarasan, S., K. Kinoshita, M. Muramatsu, K. Ikuta, and T. Honjo. 2001. In situ class switching and differentiation to IgA-producing cells in the gut lamina propria. *Nature* 413:639-643.

Fagarasan, S., M. Muramatsu, K. Suzuki, H. Nagaoka, H. Hiai, and T. Honjo. 2002. Critical roles of activation-induced cytidine deaminase in the homeostasis of gut flora. *Science* 298:1424-1427.

Falony, G., M. Joossens, S. Vieira-Silva, J. Wang, Y. Darzi, K. Faust, A. Kurilshikov, M.J. Bonder, M. Valles-Colomer, D. Vandeputte, R.Y. Tito, S. Chaffron, L. Rymenans, C. Verspecht, L. De Sutter, G. Lima-

Mendez, K. D'Hoe, K. Jonckheere, D. Homola, R. Garcia, E.F. Tigchelaar, L. Eeckhaudt, J. Fu, L. Henckaerts, A. Zhernakova, C. Wijmenga, and J. Raes. 2016. Population-level analysis of gut microbiome variation. *Science* 352:560-564.

Felfoldi, T., A. Vengring, Z. Keki, K. Marialigeti, P. Schumann, and E.M. Toth. 2014. Eoetvoesia caeni gen. nov., sp. nov., isolated from an activated sludge system treating coke plant effluent. *Int J Syst Evol Microbiol* 64:1920-1925.

Ferreira-Gomes, M., A. Kruglov, P. Durek, F. Heinrich, C. Tizian, G.A. Heinz, A. Pascual-Reguant, W. Du, R. Mothes, C. Fan, S. Frischbutter, K. Habenicht, L. Budzinski, J. Ninnemann, P.K. Jani, G.M. Guerra, K. Lehmann, M. Matz, L. Ostendorf, L. Heiberger, H.D. Chang, S. Bauherr, M. Maurer, G. Schonrich, M. Raftery, T. Kallinich, M.A. Mall, S. Angermair, S. Treskatsch, T. Dorner, V.M. Corman, A. Diefenbach, H.D. Volk, S. Elezkurtaj, T.H. Winkler, J. Dong, A.E. Hauser, H. Radbruch, M. Witkowski, F. Melchers, A. Radbruch, and M.F. Mashreghi. 2021. SARS-CoV-2 in severe COVID-19 induces a TGF-beta-dominated chronic immune response that does not target itself. *Nat Commun* 12:1961.

Forbes, S.J., M. Eschmann, and N.J. Mantis. 2008. Inhibition of Salmonella enterica serovar typhimurium motility and entry into epithelial cells by a protective antilipopolysaccharide monoclonal immunoglobulin A antibody. *Infect Immun* 76:4137-4144.

Friedman, E.S., K. Bittinger, T.V. Esipova, L. Hou, L. Chau, J. Jiang, C. Mesaros, P.J. Lund, X. Liang, G.A. FitzGerald, M. Goulian, D. Lee, B.A. Garcia, I.A. Blair, S.A. Vinogradov, and G.D. Wu. 2018. Microbes vs. chemistry in the origin of the anaerobic gut lumen. *Proc Natl Acad Sci U S A* 115:4170-4175.

Fritz, J.H., O.L. Rojas, N. Simard, D.D. McCarthy, S. Hapfelmeier, S. Rubino, S.J. Robertson, M. Larijani, J. Gosselin, Ivanov, II, A. Martin, R. Casellas, D.J. Philpott, S.E. Girardin, K.D. McCoy, A.J. Macpherson, C.J. Paige, and J.L. Gommerman. 2011. Acquisition of a multifunctional IgA+ plasma cell phenotype in the gut. *Nature* 481:199-203.

Fujinami, R.S., M.B. Oldstone, Z. Wroblewska, M.E. Frankel, and H. Koprowski. 1983. Molecular mimicry in virus infection: crossreaction of measles virus phosphoprotein or of herpes simplex virus protein with human intermediate filaments. *Proc Natl Acad Sci U S A* 80:2346-2350.

Furusawa, Y., Y. Obata, S. Fukuda, T.A. Endo, G. Nakato, D. Takahashi, Y. Nakanishi, C. Uetake, K. Kato, T. Kato, M. Takahashi, N.N. Fukuda, S. Murakami, E. Miyauchi, S. Hino, K. Atarashi, S. Onawa, Y.

Fujimura, T. Lockett, J.M. Clarke, D.L. Topping, M. Tomita, S. Hori, O. Ohara, T. Morita, H. Koseki, J. Kikuchi, K. Honda, K. Hase, and H. Ohno. 2013. Commensal microbe-derived butyrate induces the differentiation of colonic regulatory T cells. *Nature* 504:446-450.

Gaboriau-Routhiau, V., S. Rakotobe, E. Lecuyer, I. Mulder, A. Lan, C. Bridonneau, V. Rochet, A. Pisi, M. De Paepe, G. Brandi, G. Eberl, J. Snel, D. Kelly, and N. Cerf-Bensussan. 2009. The key role of segmented filamentous bacteria in the coordinated maturation of gut helper T cell responses. *Immunity* 31:677-689.

Geva-Zatorsky, N., E. Sefik, L. Kua, L. Pasman, T.G. Tan, A. Ortiz-Lopez, T.B. Yanortsang, L. Yang, R. Jupp, D. Mathis, C. Benoist, and D.L. Kasper. 2017. Mining the Human Gut Microbiota for Immunomodulatory Organisms. *Cell* 168:928-943 e911.

Gil-Cruz, C., C. Perez-Shibayama, A. De Martin, F. Ronchi, K. van der Borght, R. Niederer, L. Onder, M. Lutge, M. Novkovic, V. Nindl, G. Ramos, M. Arnoldini, E.M.C. Slack, V. Boivin-Jahns, R. Jahns, M. Wyss, C. Mooser, B.N. Lambrecht, M.T. Maeder, H. Rickli, L. Flatz, U. Eriksson, M.B. Geuking, K.D. McCoy, and B. Ludewig. 2019. Microbiota-derived peptide mimics drive lethal inflammatory cardiomyopathy. *Science* 366:881-886.

Goel, R.R., M.M. Painter, S.A. Apostolidis, D. Mathew, W. Meng, A.M. Rosenfeld, K.A. Lundgreen, A. Reynaldi, D.S. Khoury, A. Pattekar, S. Gouma, L. Kuri-Cervantes, P. Hicks, S. Dysinger, A. Hicks, H. Sharma, S. Herring, S. Korte, A.E. Baxter, D.A. Oldridge, J.R. Giles, M.E. Weirick, C.M. McAllister, M. Awofolaju, N. Tanenbaum, E.M. Drapeau, J. Dougherty, S. Long, K. D'Andrea, J.T. Hamilton, M. McLaughlin, J.C. Williams, S. Adamski, O. Kuthuru, U.P.C.P.U. dagger, I. Frank, M.R. Betts, L.A. Vella, A. Grifoni, D. Weiskopf, A. Sette, S.E. Hensley, M.P. Davenport, P. Bates, E.T. Luning Prak, A.R. Greenplate, and E.J. Wherry. 2021. mRNA vaccines induce durable immune memory to SARS-CoV-2 and variants of concern. *Science* 374:abm0829.

Goettel, J.A., R. Gandhi, J.E. Kenison, A. Yeste, G. Murugaiyan, S. Sambanthamoorthy, A.E. Griffith, B. Patel, D.S. Shouval, H.L. Weiner, S.B. Snapper, and F.J. Quintana. 2016. AHR Activation Is Protective against Colitis Driven by T Cells in Humanized Mice. *Cell Rep* 17:1318-1329.

Gohda, M., J. Kunisawa, F. Miura, Y. Kagiyama, Y. Kurashima, M. Higuchi, I. Ishikawa, I. Ogahara, and H. Kiyono. 2008. Sphingosine 1-phosphate regulates the egress of IgA plasmablasts from Peyer's patches for intestinal IgA responses. *J Immunol* 180:5335-5343.

Grasset, E.K., A. Chorny, S. Casas-Recasens, C. Gutzeit, G. Bongers, I. Thomsen, L. Chen, Z. He, D.B. Matthews, M.A. Oropallo, P.

Veeramreddy, M. Uzzan, A. Mortha, J. Carrillo, B.S. Reis, M. Ramanujam, J. Sintes, G. Magri, P.J. Maglione, C. Cunningham-Rundles, R.J. Bram, J. Faith, S. Mehandru, O. Pabst, and A. Cerutti. 2020. Gut T cell-independent IgA responses to commensal bacteria require engagement of the TACI receptor on B cells. *Sci Immunol* 5:

Gronlund, M.M., H. Arvilommi, P. Kero, O.P. Lehtonen, and E. Isolauri. 2000. Importance of intestinal colonisation in the maturation of humoral immunity in early infancy: a prospective follow up study of healthy infants aged 0-6 months. *Arch Dis Child Fetal Neonatal Ed* 83:F186-192.

Guzman, M., L.R. Lundborg, S. Yeasmin, C.J. Tyler, N.R. Zgajnar, V. Taupin, K. Dobaczewska, Z. Mikulski, G. Bamias, and J. Rivera-Nieves. 2021. An integrin alphaEbeta7-dependent mechanism of IgA transcytosis requires direct plasma cell contact with intestinal epithelium. *Mucosal Immunol* 14:1347-1357.

Hapfelmeier, S., M.A. Lawson, E. Slack, J.K. Kirundi, M. Stoel, M. Heikenwalder, J. Cahenzli, Y. Velykoredko, M.L. Balmer, K. Endt, M.B. Geuking, R. Curtiss, 3rd, K.D. McCoy, and A.J. Macpherson. 2010. Reversible microbial colonization of germ-free mice reveals the dynamics of IgA immune responses. *Science* 328:1705-1709.

He, G., R.A. Shankar, M. Chzhan, A. Samouilov, P. Kuppusamy, and J.L. Zweier. 1999. Noninvasive measurement of anatomic structure and intraluminal oxygenation in the gastrointestinal tract of living mice with spatial and spectral EPR imaging. *Proc Natl Acad Sci U S A* 96:4586-4591.

Hillman, E.T., H. Lu, T. Yao, and C.H. Nakatsu. 2017. Microbial Ecology along the Gastrointestinal Tract. *Microbes Environ* 32:300-313.

Hoces, D., M. Arnoldini, M. Diard, C. Loverdo, and E. Slack. 2020. Growing, evolving and sticking in a flowing environment: understanding IgA interactions with bacteria in the gut. *Immunology* 159:52-62.

Hoffmann, M., H. Kleine-Weber, S. Schroeder, N. Kruger, T. Herrler, S. Erichsen, T.S. Schiergens, G. Herrler, N.H. Wu, A. Nitsche, M.A. Muller, C. Drosten, and S. Pohlmann. 2020. SARS-CoV-2 Cell Entry Depends on ACE2 and TMPRSS2 and Is Blocked by a Clinically Proven Protease Inhibitor. *Cell* 181:271-280 e278.

Hold, G.L., S.E. Pryde, V.J. Russell, E. Furrie, and H.J. Flint. 2002. Assessment of microbial diversity in human colonic samples by 16S rDNA sequence analysis. *FEMS Microbiol Ecol* 39:33-39.

Human Microbiome Project, C. 2012. Structure, function and diversity of the healthy human microbiome. *Nature* 486:207-214.

Hung, Y.P., C.C. Lee, J.C. Lee, P.J. Tsai, and W.C. Ko. 2021. Gut Dysbiosis during COVID-19 and Potential Effect of Probiotics. *Microorganisms* 9:

Huus, K.E., C. Petersen, and B.B. Finlay. 2021. Diversity and dynamism of IgA-microbiota interactions. *Nat Rev Immunol* 21:514-525.

Ichinohe, T., I.K. Pang, Y. Kumamoto, D.R. Peaper, J.H. Ho, T.S. Murray, and A. Iwasaki. 2011. Microbiota regulates immune defense against respiratory tract influenza A virus infection. *Proc Natl Acad Sci U S A* 108:5354-5359.

Ivanov, II, K. Atarashi, N. Manel, E.L. Brodie, T. Shima, U. Karaoz, D. Wei, K.C. Goldfarb, C.A. Santee, S.V. Lynch, T. Tanoue, A. Imaoka, K. Itoh, K. Takeda, Y. Umesaki, K. Honda, and D.R. Littman. 2009. Induction of intestinal Th17 cells by segmented filamentous bacteria. *Cell* 139:485-498.

Jarvis, B., P. Van Berkum, W. Chen, S. Nour, M. Fernandez, J. Cleyet-Marel, and M. Gillis. 1997. Transfer of Rhizobium loti, Rhizobium huakuii, Rhizobium ciceri, Rhizobium mediterraneum, and Rhizobium tianshanense to Mesorhizobium gen. nov. *International Journal of Systematic and Evolutionary Microbiology* 47:895-898.

Jeffries, T.L., Jr., C.R. Sacha, J. Pollara, J. Himes, F.H. Jaeger, S.M. Dennison, E. McGuire, E. Kunz, J.A. Eudailey, A.M. Trama, C. LaBranche, G.G. Fouda, K. Wiehe, D.C. Montefiori, B.F. Haynes, H.X. Liao, G. Ferrari, S.M. Alam, M.A. Moody, and S.R. Permar. 2016. The function and affinity maturation of HIV-1 gp120-specific monoclonal antibodies derived from colostral B cells. *Mucosal Immunol* 9:414-427.

Johansen, F.E., R. Braathen, and P. Brandtzaeg. 2001. The J chain is essential for polymeric Ig receptor-mediated epithelial transport of IgA. *J Immunol* 167:5185-5192.

Johansson, M.E., and G.C. Hansson. 2016. Immunological aspects of intestinal mucus and mucins. *Nat Rev Immunol* 16:639-649.

Ju, B., Q. Zhang, J. Ge, R. Wang, J. Sun, X. Ge, J. Yu, S. Shan, B. Zhou, S. Song, X. Tang, J. Yu, J. Lan, J. Yuan, H. Wang, J. Zhao, S. Zhang, Y. Wang, X. Shi, L. Liu, J. Zhao, X. Wang, Z. Zhang, and L. Zhang. 2020. Human neutralizing antibodies elicited by SARS-CoV-2 infection. *Nature* 584:115-119.

Kabbert, J., J. Benckert, T. Rollenske, T.C.A. Hitch, T. Clavel, V. Cerovic, H. Wardemann, and O. Pabst. 2020. High microbiota reactivity of adult human intestinal IgA requires somatic mutations. *J Exp Med* 217:

Kallies, A., J. Hasbold, D.M. Tarlinton, W. Dietrich, L.M. Corcoran, P.D. Hodgkin, and S.L. Nutt. 2004. Plasma cell ontogeny defined by quantitative changes in blimp-1 expression. *J Exp Med* 200:967-977.

Kastl, A.J., Jr., N.A. Terry, G.D. Wu, and L.G. Albenberg. 2020. The Structure and Function of the Human Small Intestinal Microbiota: Current Understanding and Future Directions. *Cell Mol Gastroenterol Hepatol* 9:33-45.

Kiss, E.A., C. Vonarbourg, S. Kopfmann, E. Hobeika, D. Finke, C. Esser, and A. Diefenbach. 2011. Natural aryl hydrocarbon receptor ligands control organogenesis of intestinal lymphoid follicles. *Science* 334:1561-1565.

Klein, S., M. Cortese, S.L. Winter, M. Wachsmuth-Melm, C.J. Neufeldt, B. Cerikan, M.L. Stanifer, S. Boulant, R. Bartenschlager, and P. Chlanda. 2020. SARS-CoV-2 structure and replication characterized by in situ cryo-electron tomography. *Nat Commun* 11:5885.

Klingberg, E., M.K. Magnusson, H. Strid, A. Deminger, A. Stahl, J. Sundin, M. Simren, H. Carlsten, L. Ohman, and H. Forsblad-d'Elia. 2019. A distinct gut microbiota composition in patients with ankylosing spondylitis is associated with increased levels of fecal calprotectin. *Arthritis Res Ther* 21:248.

Kreye, J., S.M. Reincke, H.C. Kornau, E. Sanchez-Sendin, V.M. Corman, H. Liu, M. Yuan, N.C. Wu, X. Zhu, C.D. Lee, J. Trimpert, M. Holtje, K. Dietert, L. Stoffler, N. von Wardenburg, S. van Hoof, M.A. Homeyer, J. Hoffmann, A. Abdelgawad, A.D. Gruber, L.D. Bertzbach, D. Vladimirova, L.Y. Li, P.C. Barthel, K. Skriner, A.C. Hocke, S. Hippenstiel, M. Witzenrath, N. Suttorp, F. Kurth, C. Franke, M. Endres, D. Schmitz, L.M. Jeworowski, A. Richter, M.L. Schmidt, T. Schwarz, M.A. Muller, C. Drosten, D. Wendisch, L.E. Sander, N. Osterrieder, I.A. Wilson, and H. Pruss. 2020. A Therapeutic Non-self-reactive SARS-CoV-2 Antibody Protects from Lung Pathology in a COVID-19 Hamster Model. *Cell* 183:1058-1069 e1019.

Kroes, I., P.W. Lepp, and D.A. Relman. 1999. Bacterial diversity within the human subgingival crevice. *Proc Natl Acad Sci U S A* 96:14547-14552.

Kunisawa, J., M. Gohda, E. Hashimoto, I. Ishikawa, M. Higuchi, Y. Suzuki, Y. Goto, C. Panea, Ivanov, II, R. Sumiya, L. Aayam, T. Wake, S. Tajiri, Y. Kurashima, S. Shikata, S. Akira, K. Takeda, and H. Kiyono. 2013. Microbe-dependent CD11b+ IgA+ plasma cells mediate robust early-phase intestinal IgA responses in mice. *Nat Commun* 4:1772.

Kunkel, E.J., J.J. Campbell, G. Haraldsen, J. Pan, J. Boisvert, A.I. Roberts, E.C. Ebert, M.A. Vierra, S.B. Goodman, M.C. Genovese, A.J. Wardlaw, H.B. Greenberg, C.M. Parker, E.C. Butcher, D.P. Andrew, and W.W.

Agace. 2000. Lymphocyte CC chemokine receptor 9 and epithelial thymus-expressed chemokine (TECK) expression distinguish the small intestinal immune compartment: Epithelial expression of tissue-specific chemokines as an organizing principle in regional immunity. *J Exp Med* 192:761-768.

Kurdi, P., K. Kawanishi, K. Mizutani, and A. Yokota. 2006. Mechanism of growth inhibition by free bile acids in lactobacilli and bifidobacteria. *J Bacteriol* 188:1979-1986.

Lamers, M.M., J. Beumer, J. van der Vaart, K. Knoops, J. Puschhof, T.I. Breugem, R.B.G. Ravelli, J. Paul van Schayck, A.Z. Mykytyn, H.Q. Duimel, E. van Donselaar, S. Riesebosch, H.J.H. Kuijpers, D. Schipper, W.J. van de Wetering, M. de Graaf, M. Koopmans, E. Cuppen, P.J. Peters, B.L. Haagmans, and H. Clevers. 2020. SARS-CoV-2 productively infects human gut enterocytes. *Science* 369:50-54.

Lane, D.P., and W.K. Hoeffler. 1980. SV40 large T shares an antigenic determinant with a cellular protein of molecular weight 68,000. *Nature* 288:167-170.

Laranjo, M., A. Alexandre, and S. Oliveira. 2014. Legume growth-promoting rhizobia: an overview on the Mesorhizobium genus. *Microbiol Res* 169:2-17.

Lebman, D.A., D.Y. Nomura, R.L. Coffman, and F.D. Lee. 1990. Molecular characterization of germ-line immunoglobulin A transcripts produced during transforming growth factor type beta-induced isotype switching. *Proc Natl Acad Sci U S A* 87:3962-3966.

Lecuyer, E., S. Rakotobe, H. Lengline-Garnier, C. Lebreton, M. Picard, C. Juste, R. Fritzen, G. Eberl, K.D. McCoy, A.J. Macpherson, C.A. Reynaud, N. Cerf-Bensussan, and V. Gaboriau-Routhiau. 2014. Segmented filamentous bacterium uses secondary and tertiary lymphoid tissues to induce gut IgA and specific T helper 17 cell responses. *Immunity* 40:608-620.

Leeming, E.R., A.J. Johnson, T.D. Spector, and C.I. Le Roy. 2019. Effect of Diet on the Gut Microbiota: Rethinking Intervention Duration. *Nutrients* 11:

Leite, G.G.S., S. Weitsman, G. Parodi, S. Celly, R. Sedighi, M. Sanchez, W. Morales, M.J. Villanueva-Millan, G.M. Barlow, R. Mathur, S.K. Lo, L.H. Jamil, S. Paski, A. Rezaie, and M. Pimentel. 2020. Mapping the Segmental Microbiomes in the Human Small Bowel in Comparison with Stool: A REIMAGINE Study. *Dig Dis Sci* 65:2595-2604.

Li, H., J.P. Limenitakis, V. Greiff, B. Yilmaz, O. Scharen, C. Urbaniak, M. Zund, M.A.E. Lawson, I.D. Young, S. Rupp, M. Heikenwalder, K.D.

McCoy, S. Hapfelmeier, S.C. Ganal-Vonarburg, and A.J. Macpherson. 2020. Mucosal or systemic microbiota exposures shape the B cell repertoire. *Nature* 584:274-278.

Lin, R., H. Chen, W. Shu, M. Sun, L. Fang, Y. Shi, Z. Pang, W. Wu, and Z. Liu. 2018. Clinical significance of soluble immunoglobulins A and G and their coated bacteria in feces of patients with inflammatory bowel disease. *J Transl Med* 16:359.

Litvak, Y., M.X. Byndloss, and A.J. Baumler. 2018. Colonocyte metabolism shapes the gut microbiota. *Science* 362:

Liu, L., P. Wang, M.S. Nair, J. Yu, M. Rapp, Q. Wang, Y. Luo, J.F. Chan, V. Sahi, A. Figueroa, X.V. Guo, G. Cerutti, J. Bimela, J. Gorman, T. Zhou, Z. Chen, K.Y. Yuen, P.D. Kwong, J.G. Sodroski, M.T. Yin, Z. Sheng, Y. Huang, L. Shapiro, and D.D. Ho. 2020. Potent neutralizing antibodies against multiple epitopes on SARS-CoV-2 spike. *Nature* 584:450-456.

Llorens-Rico, V., A.C. Gregory, J. Van Weyenbergh, S. Jansen, T. Van Buyten, J. Qian, M. Braz, S.M. Menezes, P. Van Mol, L. Vanderbeke, C. Dooms, J. Gunst, G. Hermans, P. Meersseman, C. collaborators, E. Wauters, J. Neyts, D. Lambrechts, J. Wauters, and J. Raes. 2021. Clinical practices underlie COVID-19 patient respiratory microbiome composition and its interactions with the host. *Nat Commun* 12:6243.

Lu, Y., C. Fan, P. Li, Y. Lu, X. Chang, and K. Qi. 2016. Short Chain Fatty Acids Prevent High-fat-diet-induced Obesity in Mice by Regulating G Protein-coupled Receptors and Gut Microbiota. *Sci Rep* 6:37589.

Lycke, N.Y., and M. Bemark. 2017. The regulation of gut mucosal IgA B-cell responses: recent developments. *Mucosal Immunol* 10:1361-1374.

Macpherson, A.J., D. Gatto, E. Sainsbury, G.R. Harriman, H. Hengartner, and R.M. Zinkernagel. 2000. A primitive T cell-independent mechanism of intestinal mucosal IgA responses to commensal bacteria. *Science* 288:2222-2226.

Macpherson, A.J., K.D. McCoy, F.E. Johansen, and P. Brandtzaeg. 2008. The immune geography of IgA induction and function. *Mucosal Immunol* 1:11-22.

Macpherson, A.J., and T. Uhr. 2004. Induction of protective IgA by intestinal dendritic cells carrying commensal bacteria. *Science* 303:1662-1665.

Maeda, Y., and K. Takeda. 2017. Role of Gut Microbiota in Rheumatoid Arthritis. *J Clin Med* 6:

Majdoubi, A., C. Michalski, S.E. O'Connell, S. Dada, S. Narpala, J. Gelinas, D. Mehta, C. Cheung, D.F. Winkler, M. Basappa, A.C. Liu, M. Gorges, V.E. Barakauskas, M. Irvine, J. Mehalko, D. Esposito, I. Sekirov, A.N.

Jassem, D.M. Goldfarb, S. Pelech, D.C. Douek, A.B. McDermott, and P.M. Lavoie. 2021. A majority of uninfected adults show preexisting antibody reactivity against SARS-CoV-2. *JCI Insight* 6:

Malek, T.R., K.M. Danis, and E.K. Codias. 1989. Tumor necrosis factor synergistically acts with IFN-gamma to regulate Ly-6A/E expression in T lymphocytes, thymocytes and bone marrow cells. *J Immunol* 142:1929-1936.

Mantis, N.J., N. Rol, and B. Corthesy. 2011. Secretory IgA's complex roles in immunity and mucosal homeostasis in the gut. *Mucosal Immunol* 4:603-611.

Mao, T., B. Israelow, A. Suberi, L. Zhou, M. Reschke, M.A. Pena-Hernandez, H. Dong, R.J. Homer, W.M. Saltzman, and A. Iwasaki. 2022. Unadjuvanted intranasal spike vaccine booster elicits robust protective mucosal immunity against sarbecoviruses. *bioRxiv*

Masella, A.P., A.K. Bartram, J.M. Truszkowski, D.G. Brown, and J.D. Neufeld. 2012. PANDAseq: paired-end assembler for illumina sequences. *BMC Bioinformatics* 13:31.

Mauro, D., R. Thomas, G. Guggino, R. Lories, M.A. Brown, and F. Ciccia. 2021. Ankylosing spondylitis: an autoimmune or autoinflammatory disease? *Nat Rev Rheumatol* 17:387-404.

McCarville, J.L., G.Y. Chen, V.D. Cuevas, K. Troha, and J.S. Ayres. 2020. Microbiota Metabolites in Health and Disease. *Annu Rev Immunol* 38:147-170.

McLoughlin, K., J. Schluter, S. Rakoff-Nahoum, A.L. Smith, and K.R. Foster. 2016. Host Selection of Microbiota via Differential Adhesion. *Cell Host Microbe* 19:550-559.

McMurdie, P.J., and S. Holmes. 2013. phyloseq: an R package for reproducible interactive analysis and graphics of microbiome census data. *PLoS One* 8:e61217.

Monteleone, I., A. Rizzo, M. Sarra, G. Sica, P. Sileri, L. Biancone, T.T. MacDonald, F. Pallone, and G. Monteleone. 2011. Aryl hydrocarbon receptor-induced signals up-regulate IL-22 production and inhibit inflammation in the gastrointestinal tract. *Gastroenterology* 141:237-248, 248 e231.

Moor, K., M. Diard, M.E. Sellin, B. Felmy, S.Y. Wotzka, A. Toska, E. Bakkeren, M. Arnoldini, F. Bansept, A.D. Co, T. Voller, A. Minola, B. Fernandez-Rodriguez, G. Agatic, S. Barbieri, L. Piccoli, C. Casiraghi, D. Corti, A. Lanzavecchia, R.R. Regoes, C. Loverdo, R. Stocker, D.R. Brumley, W.D. Hardt, and E. Slack. 2017. High-avidity IgA protects the intestine by enchaining growing bacteria. *Nature* 544:498-502.

Mora, J.R., M. Iwata, B. Eksteen, S.Y. Song, T. Junt, B. Senman, K.L. Otipoby, A. Yokota, H. Takeuchi, P. Ricciardi-Castagnoli, K. Rajewsky, D.H. Adams, and U.H. von Andrian. 2006. Generation of gut-homing IgA-secreting B cells by intestinal dendritic cells. *Science* 314:1157-1160.

Moreau, M.C., R. Ducluzeau, D. Guy-Grand, and M.C. Muller. 1978. Increase in the population of duodenal immunoglobulin A plasmocytes in axenic mice associated with different living or dead bacterial strains of intestinal origin. *Infect Immun* 21:532-539.

Moro-Sibilot, L., P. Blanc, M. Taillardet, E. Bardel, C. Couillault, G. Boschetti, A. Traverse-Glehen, T. Defrance, D. Kaiserlian, and B. Dubois. 2016. Mouse and Human Liver Contain Immunoglobulin A-Secreting Cells Originating From Peyer's Patches and Directed Against Intestinal Antigens. *Gastroenterology* 151:311-323.

Mowat, A.M. 2003. Anatomical basis of tolerance and immunity to intestinal antigens. *Nat Rev Immunol* 3:331-341.

Mowat, A.M., and W.W. Agace. 2014. Regional specialization within the intestinal immune system. *Nat Rev Immunol* 14:667-685.

Muller, M., E.E. Canfora, and E.E. Blaak. 2018. Gastrointestinal Transit Time, Glucose Homeostasis and Metabolic Health: Modulation by Dietary Fibers. *Nutrients* 10:

Muramatsu, M., K. Kinoshita, S. Fagarasan, S. Yamada, Y. Shinkai, and T. Honjo. 2000. Class switch recombination and hypermutation require activation-induced cytidine deaminase (AID), a potential RNA editing enzyme. *Cell* 102:553-563.

Nakagawa, Y., T. Sakane, and A. Yokota. 1996. Transfer of "Pseudomonas riboflavina" (Foster 1944), a gram-negative, motile rod with long-chain 3-hydroxy fatty acids, to Devosia riboflavina gen. nov., sp. nov., nom. rev. *Int J Syst Bacteriol* 46:16-22.

Nakajima, A., A. Vogelzang, M. Maruya, M. Miyajima, M. Murata, A. Son, T. Kuwahara, T. Tsuruyama, S. Yamada, M. Matsuura, H. Nakase, D.A. Peterson, S. Fagarasan, and K. Suzuki. 2018. IgA regulates the composition and metabolic function of gut microbiota by promoting symbiosis between bacteria. *J Exp Med* 215:2019-2034.

Ng, K.W., N. Faulkner, G.H. Cornish, A. Rosa, R. Harvey, S. Hussain, R. Ulferts, C. Earl, A.G. Wrobel, D.J. Benton, C. Roustan, W. Bolland, R. Thompson, A. Agua-Doce, P. Hobson, J. Heaney, H. Rickman, S. Paraskevopoulou, C.F. Houlihan, K. Thomson, E. Sanchez, G.Y. Shin, M.J. Spyer, D. Joshi, N. O'Reilly, P.A. Walker, S. Kjaer, A. Riddell, C. Moore, B.R. Jebson, M. Wilkinson, L.R. Marshall, E.C. Rosser, A. Radziszewska, H. Peckham, C. Ciurtin, L.R. Wedderburn, R. Beale, C.

Swanton, S. Gandhi, B. Stockinger, J. McCauley, S.J. Gamblin, L.E. McCoy, P. Cherepanov, E. Nastouli, and G. Kassiotis. 2020. Preexisting and de novo humoral immunity to SARS-CoV-2 in humans. *Science* 370:1339-1343.

Nicholson, A.C., A.M. Whitney, B. Humrighouse, B. Emery, V. Loparev, and J.R. McQuiston. 2015. Complete Genome Sequence of Strain H5989 of a Novel Devosia Species. *Genome Announc* 3:

Nutt, S.L., K.A. Fairfax, and A. Kallies. 2007. BLIMP1 guides the fate of effector B and T cells. *Nat Rev Immunol* 7:923-927.

Okada, T., V.N. Ngo, E.H. Ekland, R. Forster, M. Lipp, D.R. Littman, and J.G. Cyster. 2002. Chemokine requirements for B cell entry to lymph nodes and Peyer's patches. *J Exp Med* 196:65-75.

Onderdonk, A.B., J.A. Richardson, R.E. Hammer, and J.D. Taurog. 1998. Correlation of cecal microflora of HLA-B27 transgenic rats with inflammatory bowel disease. *Infect Immun* 66:6022-6023.

Pabst, O. 2012. New concepts in the generation and functions of IgA. *Nat Rev Immunol* 12:821-832.

Pabst, O., H. Herbrand, M. Friedrichsen, S. Velaga, M. Dorsch, G. Berhardt, T. Worbs, A.J. Macpherson, and R. Forster. 2006. Adaptation of solitary intestinal lymphoid tissue in response to microbiota and chemokine receptor CCR7 signaling. *J Immunol* 177:6824-6832.

Pabst, O., and E. Slack. 2020. IgA and the intestinal microbiota: the importance of being specific. *Mucosal Immunol* 13:12-21.

Palm, N.W., M.R. de Zoete, T.W. Cullen, N.A. Barry, J. Stefanowski, L. Hao, P.H. Degnan, J. Hu, I. Peter, W. Zhang, E. Ruggiero, J.H. Cho, A.L. Goodman, and R.A. Flavell. 2014. Immunoglobulin A coating identifies colitogenic bacteria in inflammatory bowel disease. *Cell* 158:1000-1010.

Pan, J., E.J. Kunkel, U. Gosslar, N. Lazarus, P. Langdon, K. Broadwell, M.A. Vierra, M.C. Genovese, E.C. Butcher, and D. Soler. 2000. A novel chemokine ligand for CCR10 and CCR3 expressed by epithelial cells in mucosal tissues. *J Immunol* 165:2943-2949.

Patricia, J.J., and A.S. Dhamoon. 2022. Physiology, Digestion. In StatPearls. Treasure Island (FL).

Petersen, C., and J.L. Round. 2014. Defining dysbiosis and its influence on host immunity and disease. *Cell Microbiol* 16:1024-1033.

Peterson, D.A., N.P. McNulty, J.L. Guruge, and J.I. Gordon. 2007. IgA response to symbiotic bacteria as a mediator of gut homeostasis. *Cell Host Microbe* 2:328-339.

Pollard, M., and N. Sharon. 1970. Responses of the Peyer's Patches in Germ-Free Mice to Antigenic Stimulation. *Infect Immun* 2:96-100.

Project, N.H.M. 2007.

Ramasamy, M.N., A.M. Minassian, K.J. Ewer, A.L. Flaxman, P.M. Folegatti, D.R. Owens, M. Voysey, P.K. Aley, B. Angus, G. Babbage, S. Belij-Rammerstorfer, L. Berry, S. Bibi, M. Bittaye, K. Cathie, H. Chappell, S. Charlton, P. Cicconi, E.A. Clutterbuck, R. Colin-Jones, C. Dold, K.R.W. Emary, S. Fedosyuk, M. Fuskova, D. Gbesemete, C. Green, B. Hallis, M.M. Hou, D. Jenkin, C.C.D. Joe, E.J. Kelly, S. Kerridge, A.M. Lawrie, A. Lelliott, M.N. Lwin, R. Makinson, N.G. Marchevsky, Y. Mujadidi, A.P.S. Munro, M. Pacurar, E. Plested, J. Rand, T. Rawlinson, S. Rhead, H. Robinson, A.J. Ritchie, A.L. Ross-Russell, S. Saich, N. Singh, C.C. Smith, M.D. Snape, R. Song, R. Tarrant, Y. Themistocleous, K.M. Thomas, T.L. Villafana, S.C. Warren, M.E.E. Watson, A.D. Douglas, A.V.S. Hill, T. Lambe, S.C. Gilbert, S.N. Faust, A.J. Pollard, and C.V.T.G. Oxford. 2021. Safety and immunogenicity of ChAdOx1 nCoV-19 vaccine administered in a prime-boost regimen in young and old adults (COV002): a single-blind, randomised, controlled, phase 2/3 trial. *Lancet* 396:1979-1993.

Ramos, M., I. Alvarez, L. Sesma, A. Logean, D. Rognan, and J.A. Lopez de Castro. 2002. Molecular mimicry of an HLA-B27-derived ligand of arthritis-linked subtypes with chlamydial proteins. *J Biol Chem* 277:37573-37581.

Reboldi, A., T.I. Arnon, L.B. Rodda, A. Atakilit, D. Sheppard, and J.G. Cyster. 2016. IgA production requires B cell interaction with subepithelial dendritic cells in Peyer's patches. *Science* 352:aaf4822.

Reboldi, A., and J.G. Cyster. 2016. Peyer's patches: organizing B-cell responses at the intestinal frontier. *Immunol Rev* 271:230-245.

Reimold, A.M., N.N. Iwakoshi, J. Manis, P. Vallabhajosyula, E. Szomolanyi-Tsuda, E.M. Gravallese, D. Friend, M.J. Grusby, F. Alt, and L.H. Glimcher. 2001. Plasma cell differentiation requires the transcription factor XBP-1. *Nature* 412:300-307.

Ren, Z., Y. Wang, T. Duan, J. Patel, T. Liggett, E. Loda, S. Brahma, R. Goswami, C. Grouse, R. Byrne, D. Stefoski, A. Javed, S.D. Miller, and R. Balabanov. 2012. Cross-immunoreactivity between bacterial aquaporin-Z and human aquaporin-4: potential relevance to neuromyelitis optica. *J Immunol* 189:4602-4611.

Renegar, K.B., P.A. Small, Jr., L.G. Boykins, and P.F. Wright. 2004. Role of IgA versus IgG in the control of influenza viral infection in the murine respiratory tract. *J Immunol* 173:1978-1986.

Rigottier-Gois, L. 2013. Dysbiosis in inflammatory bowel diseases: the oxygen hypothesis. *ISME J* 7:1256-1261.

Robak, O.H., M.M. Heimesaat, A.A. Kruglov, S. Prepens, J. Ninnemann, B. Gutbier, K. Reppe, H. Hochrein, M. Suter, C.J. Kirschning, V. Marathe, J. Buer, M.W. Hornef, M. Schnare, P. Schneider, M. Witzenrath, S. Bereswill, U. Steinhoff, N. Suttorp, L.E. Sander, C. Chaput, and B. Opitz. 2018. Antibiotic treatment-induced secondary IgA deficiency enhances susceptibility to Pseudomonas aeruginosa pneumonia. *J Clin Invest* 128:3535-3545.

Rollenske, T., S. Burkhalter, L. Muerner, S. von Gunten, J. Lukasiewicz, H. Wardemann, and A.J. Macpherson. 2021. Parallelism of intestinal secretory IgA shapes functional microbial fitness. *Nature* 598:657-661.

Rollenske, T., V. Szijarto, J. Lukasiewicz, L.M. Guachalla, K. Stojkovic, K. Hartl, L. Stulik, S. Kocher, F. Lasitschka, M. Al-Saeedi, J. Schroder-Braunstein, M. von Frankenberg, G. Gaebelein, P. Hoffmann, S. Klein, K. Heeg, E. Nagy, G. Nagy, and H. Wardemann. 2018. Cross-specificity of protective human antibodies against Klebsiella pneumoniae LPS O-antigen. *Nat Immunol* 19:617-624.

Royle, L., A. Roos, D.J. Harvey, M.R. Wormald, D. van Gijlswijk-Janssen, R.M. Redwan el, I.A. Wilson, M.R. Daha, R.A. Dwek, and P.M. Rudd. 2003. Secretory IgA N- and O-glycans provide a link between the innate and adaptive immune systems. *J Biol Chem* 278:20140-20153.

Sahin, U., A. Muik, E. Derhovanessian, I. Vogler, L.M. Kranz, M. Vormehr, A. Baum, K. Pascal, J. Quandt, D. Maurus, S. Brachtendorf, V. Lorks, J. Sikorski, R. Hilker, D. Becker, A.K. Eller, J. Grutzner, C. Boesler, C. Rosenbaum, M.C. Kuhnle, U. Luxemburger, A. Kemmer-Bruck, D. Langer, M. Bexon, S. Bolte, K. Kariko, T. Palanche, B. Fischer, A. Schultz, P.Y. Shi, C. Fontes-Garfias, J.L. Perez, K.A. Swanson, J. Loschko, I.L. Scully, M. Cutler, W. Kalina, C.A. Kyratsous, D. Cooper, P.R. Dormitzer, K.U. Jansen, and O. Tureci. 2020. COVID-19 vaccine BNT162b1 elicits human antibody and TH1 T cell responses. *Nature* 586:594-599.

Salzman, N.H., M.A. Underwood, and C.L. Bevins. 2007. Paneth cells, defensins, and the commensal microbiota: a hypothesis on intimate interplay at the intestinal mucosa. *Semin Immunol* 19:70-83.

Savage, D.C. 1977. Microbial ecology of the gastrointestinal tract. *Annu Rev Microbiol* 31:107-133.

Schaedler, R.W., R. Dubos, and R. Costello. 1965. The Development of the Bacterial Flora in the Gastrointestinal Tract of Mice. *J Exp Med* 122:59-66.

Schepici, G., S. Silvestro, P. Bramanti, and E. Mazzon. 2019. The Gut Microbiota in Multiple Sclerosis: An Overview of Clinical Trials. *Cell Transplant* 28:1507-1527.

Schirmer, M., E.A. Franzosa, J. Lloyd-Price, L.J. McIver, R. Schwager, T.W. Poon, A.N. Ananthakrishnan, E. Andrews, G. Barron, K. Lake, M. Prasad, J. Sauk, B. Stevens, R.G. Wilson, J. Braun, L.A. Denson, S. Kugathasan, D.P.B. McGovern, H. Vlamakis, R.J. Xavier, and C. Huttenhower. 2018. Dynamics of metatranscription in the inflammatory bowel disease gut microbiome. *Nat Microbiol* 3:337-346.

Schwimmbeck, P.L., T. Dyrberg, D.B. Drachman, and M.B. Oldstone. 1989. Molecular mimicry and myasthenia gravis. An autoantigenic site of the acetylcholine receptor alpha-subunit that has biologic activity and reacts immunochemically with herpes simplex virus. *J Clin Invest* 84:1174-1180.

Schwimmbeck, P.L., and M.B. Oldstone. 1988. Molecular mimicry between human leukocyte antigen B27 and Klebsiella. Consequences for spondyloarthropathies. *Am J Med* 85:51-53.

Selva, K.J., C.E. van de Sandt, M.M. Lemke, C.Y. Lee, S.K. Shoffner, B.Y. Chua, S.K. Davis, T.H.O. Nguyen, L.C. Rowntree, L. Hensen, M. Koutsakos, C.Y. Wong, F. Mordant, D.C. Jackson, K.L. Flanagan, J. Crowe, S. Tosif, M.R. Neeland, P. Sutton, P.V. Licciardi, N.W. Crawford, A.C. Cheng, D.L. Doolan, F. Amanat, F. Krammer, K. Chappell, N. Modhiran, D. Watterson, P. Young, W.S. Lee, B.D. Wines, P. Mark Hogarth, R. Esterbauer, H.G. Kelly, H.X. Tan, J.A. Juno, A.K. Wheatley, S.J. Kent, K.B. Arnold, K. Kedzierska, and A.W. Chung. 2021. Systems serology detects functionally distinct coronavirus antibody features in children and elderly. *Nat Commun* 12:2037.

Sender, R., S. Fuchs, and R. Milo. 2016. Revised Estimates for the Number of Human and Bacteria Cells in the Body. *PLoS Biol* 14:e1002533.

Shaffer, A.L., M. Shapiro-Shelef, N.N. Iwakoshi, A.H. Lee, S.B. Qian, H. Zhao, X. Yu, L. Yang, B.K. Tan, A. Rosenwald, E.M. Hurt, E. Petroulakis, N. Sonenberg, J.W. Yewdell, K. Calame, L.H. Glimcher, and L.M. Staudt. 2004. XBP1, downstream of Blimp-1, expands the secretory apparatus and other organelles, and increases protein synthesis in plasma cell differentiation. *Immunity* 21:81-93.

Suzuki, K., S. Kawamoto, M. Maruya, and S. Fagarasan. 2010. GALT: organization and dynamics leading to IgA synthesis. *Adv Immunol* 107:153-185.

Suzuki, K., B. Meek, Y. Doi, M. Muramatsu, T. Chiba, T. Honjo, and S. Fagarasan. 2004. Aberrant expansion of segmented filamentous bacteria in IgA-deficient gut. *Proc Natl Acad Sci U S A* 101:1981-1986.

Talham, G.L., H.Q. Jiang, N.A. Bos, and J.J. Cebra. 1999. Segmented filamentous bacteria are potent stimuli of a physiologically normal state of the murine gut mucosal immune system. *Infect Immun* 67:1992-2000.

Talwar, C., S. Nagar, R. Kumar, J. Scaria, R. Lal, and R.K. Negi. 2020. Defining the Environmental Adaptations of Genus Devosia: Insights into its Expansive Short Peptide Transport System and Positively Selected Genes. *Sci Rep* 10:1151.

Tang, W.H., Z. Wang, B.S. Levison, R.A. Koeth, E.B. Britt, X. Fu, Y. Wu, and S.L. Hazen. 2013. Intestinal microbial metabolism of phosphatidylcholine and cardiovascular risk. *N Engl J Med* 368:1575-1584.

Taurog, J.D., J.A. Richardson, J.T. Croft, W.A. Simmons, M. Zhou, J.L. Fernandez-Sueiro, E. Balish, and R.E. Hammer. 1994. The germfree state prevents development of gut and joint inflammatory disease in HLA-B27 transgenic rats. *J Exp Med* 180:2359-2364.

Tezuka, H., Y. Abe, M. Iwata, H. Takeuchi, H. Ishikawa, M. Matsushita, T. Shiohara, S. Akira, and T. Ohteki. 2007. Regulation of IgA production by naturally occurring TNF/iNOS-producing dendritic cells. *Nature* 448:929-933.

Tierney, B.T., Z. Yang, J.M. Luber, M. Beaudin, M.C. Wibowo, C. Baek, E. Mehlenbacher, C.J. Patel, and A.D. Kostic. 2019. The Landscape of Genetic Content in the Gut and Oral Human Microbiome. *Cell Host Microbe* 26:283-295 e288.

Trama, A.M., M.A. Moody, S.M. Alam, F.H. Jaeger, B. Lockwood, R. Parks, K.E. Lloyd, C. Stolarchuk, R. Scearce, A. Foulger, D.J. Marshall, J.F. Whitesides, T.L. Jeffries, Jr., K. Wiehe, L. Morris, B. Lambson, K. Soderberg, K.K. Hwang, G.D. Tomaras, N. Vandergrift, K.J.L. Jackson, K.M. Roskin, S.D. Boyd, T.B. Kepler, H.X. Liao, and B.F. Haynes. 2014. HIV-1 envelope gp41 antibodies can originate from terminal ileum B cells that share cross-reactivity with commensal bacteria. *Cell Host Microbe* 16:215-226.

Turner, C.A., Jr., D.H. Mack, and M.M. Davis. 1994. Blimp-1, a novel zinc finger-containing protein that can drive the maturation of B lymphocytes into immunoglobulin-secreting cells. *Cell* 77:297-306.

Valdes, A.M., J. Walter, E. Segal, and T.D. Spector. 2018. Role of the gut microbiota in nutrition and health. *BMJ* 361:k2179.

Vandeputte, D., G. Kathagen, K. D'Hoe, S. Vieira-Silva, M. Valles-Colomer, J. Sabino, J. Wang, R.Y. Tito, L. De Commer, Y. Darzi, S. Vermeire, G. Falony, and J. Raes. 2017. Quantitative microbiome profiling links gut community variation to microbial load. *Nature* 551:507-511.

Wang, J., L.B. Thingholm, J. Skieceviciene, P. Rausch, M. Kummen, J.R. Hov, F. Degenhardt, F.A. Heinsen, M.C. Ruhlemann, S. Szymczak, K. Holm, T. Esko, J. Sun, M. Pricop-Jeckstadt, S. Al-Dury, P. Bohov, J. Bethune, F. Sommer, D. Ellinghaus, R.K. Berge, M. Hubenthal, M. Koch, K. Schwarz, G. Rimbach, P. Hubbe, W.H. Pan, R. Sheibani-Tezerji, R. Hasler, P. Rosenstiel, M. D'Amato, K. Cloppenborg-Schmidt, S. Kunzel, M. Laudes, H.U. Marschall, W. Lieb, U. Nothlings, T.H. Karlsen, J.F. Baines, and A. Franke. 2016. Genome-wide association analysis identifies variation in vitamin D receptor and other host factors influencing the gut microbiota. *Nat Genet* 48:1396-1406.

Wang, Q., G.M. Garrity, J.M. Tiedje, and J.R. Cole. 2007. Naive Bayesian classifier for rapid assignment of rRNA sequences into the new bacterial taxonomy. *Appl Environ Microbiol* 73:5261-5267.

Weigmann, B., I. Tubbe, D. Seidel, A. Nicolaev, C. Becker, and M.F. Neurath. 2007. Isolation and subsequent analysis of murine lamina propria mononuclear cells from colonic tissue. *Nat Protoc* 2:2307-2311.

Wen, C., Z. Zheng, T. Shao, L. Liu, Z. Xie, E. Le Chatelier, Z. He, W. Zhong, Y. Fan, L. Zhang, H. Li, C. Wu, C. Hu, Q. Xu, J. Zhou, S. Cai, D. Wang, Y. Huang, M. Breban, N. Qin, and S.D. Ehrlich. 2017. Quantitative metagenomics reveals unique gut microbiome biomarkers in ankylosing spondylitis. *Genome Biol* 18:142.

Williams, W.B., H.X. Liao, M.A. Moody, T.B. Kepler, S.M. Alam, F. Gao, K. Wiehe, A.M. Trama, K. Jones, R. Zhang, H. Song, D.J. Marshall, J.F. Whitesides, K. Sawatzki, A. Hua, P. Liu, M.Z. Tay, K.E. Seaton, X. Shen, A. Foulger, K.E. Lloyd, R. Parks, J. Pollara, G. Ferrari, J.S. Yu, N. Vandergrift, D.C. Montefiori, M.E. Sobieszczyk, S. Hammer, S. Karuna, P. Gilbert, D. Grove, N. Grunenberg, M.J. McElrath, J.R. Mascola, R.A. Koup, L. Corey, G.J. Nabel, C. Morgan, G. Churchyard, J. Maenza, M. Keefer, B.S. Graham, L.R. Baden, G.D. Tomaras, and B.F. Haynes. 2015. HIV-1 VACCINES. Diversion of HIV-1 vaccine-induced immunity by gp41-microbiota cross-reactive antibodies. *Science* 349:aab1253.

Wilmore, J.R., D.D. Jones, and D. Allman. 2017. Protocol for improved resolution of plasma cell subpopulations by flow cytometry. *Eur J Immunol* 47:1386-1388.

Winsauer, C., S. Prepens, D. Schlienz, S. Nedospasov, and A.A. Kruglov. 2015. Novel mouse model to study T cell-dependent IgA induction in vivo. *J Immunol Methods* 421:54-60.

Wold, A.E., J. Mestecky, M. Tomana, A. Kobata, H. Ohbayashi, T. Endo, and C.S. Eden. 1990. Secretory immunoglobulin A carries oligosaccharide receptors for Escherichia coli type 1 fimbrial lectin. *Infect Immun* 58:3073-3077.

Wong, J.M., R. de Souza, C.W. Kendall, A. Emam, and D.J. Jenkins. 2006. Colonic health: fermentation and short chain fatty acids. *J Clin Gastroenterol* 40:235-243.

Woo, P.C., P.K. Leung, K.W. Leung, and K.Y. Yuen. 2000. Identification by 16S ribosomal RNA gene sequencing of an Enterobacteriaceae species from a bone marrow transplant recipient. *Mol Pathol* 53:211-215.

Woof, J.M., and M.W. Russell. 2011. Structure and function relationships in IgA. *Mucosal Immunol* 4:590-597.

Wrammert, J., E. Kallberg, W.W. Agace, and T. Leanderson. 2002. Ly6C expression differentiates plasma cells from other B cell subsets in mice. *Eur J Immunol* 32:97-103.

Xiao, F., M. Tang, X. Zheng, Y. Liu, X. Li, and H. Shan. 2020. Evidence for Gastrointestinal Infection of SARS-CoV-2. *Gastroenterology* 158:1831-1833 e1833.

Yamanaka, T., L. Helgeland, I.N. Farstad, H. Fukushima, T. Midtvedt, and P. Brandtzaeg. 2003. Microbial colonization drives lymphocyte accumulation and differentiation in the follicle-associated epithelium of Peyer's patches. *J Immunol* 170:816-822.

Yang, C., I. Mogno, E.J. Contijoch, J.N. Borgerding, V. Aggarwala, Z. Li, S. Siu, E.K. Grasset, D.S. Helmus, M.C. Dubinsky, S. Mehandru, A. Cerutti, and J.J. Faith. 2020. Fecal IgA Levels Are Determined by Strain-Level Differences in Bacteroides ovatus and Are Modifiable by Gut Microbiota Manipulation. *Cell Host Microbe* 27:467-475 e466.

Yang, X., L. Xie, Y. Li, and C. Wei. 2009. More than 9,000,000 unique genes in human gut bacterial community: estimating gene numbers inside a human body. *PLoS One* 4:e6074.

Yeoh, Y.K., T. Zuo, G.C. Lui, F. Zhang, Q. Liu, A.Y. Li, A.C. Chung, C.P. Cheung, E.Y. Tso, K.S. Fung, V. Chan, L. Ling, G. Joynt, D.S. Hui, K.M. Chow, S.S.S. Ng, T.C. Li, R.W. Ng, T.C. Yip, G.L. Wong, F.K.

Chan, C.K. Wong, P.K. Chan, and S.C. Ng. 2021. Gut microbiota composition reflects disease severity and dysfunctional immune responses in patients with COVID-19. *Gut* 70:698-706.

Yin, J., P.R. Sternes, M. Wang, J. Song, M. Morrison, T. Li, L. Zhou, X. Wu, F. He, J. Zhu, M.A. Brown, and H. Xu. 2020. Shotgun metagenomics reveals an enrichment of potentially cross-reactive bacterial epitopes in ankylosing spondylitis patients, as well as the effects of TNFi therapy upon microbiome composition. *Ann Rheum Dis* 79:132-140.

Zenewicz, L.A., A. Antov, and R.A. Flavell. 2009. CD4 T-cell differentiation and inflammatory bowel disease. *Trends Mol Med* 15:199-207.

Zhang, L., R. Han, X. Zhang, G. Fang, J. Chen, J. Li, S. Xu, L. Qian, W. Chen, and F. Pan. 2019a. Fecal microbiota in patients with ankylosing spondylitis: Correlation with dietary factors and disease activity. *Clin Chim Acta* 497:189-196.

Zhang, L., Y. Hu, Y. Xu, P. Li, H. Ma, X. Li, and M. Li. 2019b. The correlation between intestinal dysbiosis and the development of ankylosing spondylitis. *Microb Pathog* 132:188-192.

Zhao, L., F. Zhang, X. Ding, G. Wu, Y.Y. Lam, X. Wang, H. Fu, X. Xue, C. Lu, J. Ma, L. Yu, C. Xu, Z. Ren, Y. Xu, S. Xu, H. Shen, X. Zhu, Y. Shi, Q. Shen, W. Dong, R. Liu, Y. Ling, Y. Zeng, X. Wang, Q. Zhang, J. Wang, L. Wang, Y. Wu, B. Zeng, H. Wei, M. Zhang, Y. Peng, and C. Zhang. 2018. Gut bacteria selectively promoted by dietary fibers alleviate type 2 diabetes. *Science* 359:1151-1156.

Zheng, L., C.J. Kelly, K.D. Battista, R. Schaefer, J.M. Lanis, E.E. Alexeev, R.X. Wang, J.C. Onyiah, D.J. Kominsky, and S.P. Colgan. 2017. Microbial-Derived Butyrate Promotes Epithelial Barrier Function through IL-10 Receptor-Dependent Repression of Claudin-2. *J Immunol* 199:2976-2984.

Zhou, C., H. Zhao, X.Y. Xiao, B.D. Chen, R.J. Guo, Q. Wang, H. Chen, L.D. Zhao, C.C. Zhang, Y.H. Jiao, Y.M. Ju, H.X. Yang, Y.Y. Fei, L. Wang, M. Shen, H. Li, X.H. Wang, X. Lu, B. Yang, J.J. Liu, J. Li, L.Y. Peng, W.J. Zheng, C.Y. Zhang, J.X. Zhou, Q.J. Wu, Y.J. Yang, J.M. Su, Q. Shi, D. Wu, W. Zhang, F.C. Zhang, H.J. Jia, D.P. Liu, Z.Y. Jie, and X. Zhang. 2020a. Metagenomic profiling of the pro-inflammatory gut microbiota in ankylosing spondylitis. *J Autoimmun* 107:102360.

Zhou, F., T. Yu, R. Du, G. Fan, Y. Liu, Z. Liu, J. Xiang, Y. Wang, B. Song, X. Gu, L. Guan, Y. Wei, H. Li, X. Wu, J. Xu, S. Tu, Y. Zhang, H. Chen, and B. Cao. 2020b. Clinical course and risk factors for mortality of adult inpatients with COVID-19 in Wuhan, China: a retrospective cohort study. *Lancet* 395:1054-1062.

Zou, X., K. Chen, J. Zou, P. Han, J. Hao, and Z. Han. 2020. Single-cell RNA-seq data analysis on the receptor ACE2 expression reveals the potential risk of different human organs vulnerable to 2019-nCoV infection. *Front Med* 14:185-192.

Zuo, T., F. Zhang, G.C.Y. Lui, Y.K. Yeoh, A.Y.L. Li, H. Zhan, Y. Wan, A.C.K. Chung, C.P. Cheung, N. Chen, C.K.C. Lai, Z. Chen, E.Y.K. Tso, K.S.C. Fung, V. Chan, L. Ling, G. Joynt, D.S.C. Hui, F.K.L. Chan, P.K.S. Chan, and S.C. Ng. 2020. Alterations in Gut Microbiota of Patients With COVID-19 During Time of Hospitalization. *Gastroenterology* 159:944-955 e948.

7 Abbreviations

ACE2	angiotensin-converting enzyme 2
AChR	acetylcholine receptor
AhR	aryl hydrocarbon receptor
AID	activation induced cytidine deaminase
AMP	antimicrobial peptide
APRIL	a proliferation inducing ligand
AS	ankylosing spondylitis
AUC	area under the curve
BAFF	B cell-activating factor
Bcl-6	B-cell lymphoma 6
BCR	B cell receptor
BLAST	Basic Local Alignment Search Tool
BLIMP-1	B lymphocyte-induced maturation protein-1
CCF	commensal colonization factor
CCR	C-C chemokine receptor
CD	Crohn's disease
Cdc6	cell division control protein 6 homolog
CDR	complementarity-determining region
CFU	colony forming units
COVID-19	Coronavirus Disease 2019
CPS	capsular polysaccharide synthesis
CSF	cerebrospinal fluid
CSR	class switch recombination
CT	cholera toxin
CXCL	C-X-C chemokine ligand
CXCR	C-X-C chemokine receptor
Cα	constant region α
EC	epithelial cell
ER	endoplasmic reticulum
Fab	fragment antigen binding
FACS	fluorescence activated cell sorting
FAE	follicle associated epithelium
Fc	fragment crystallizable
FDC	follicular dendritic cell
GABA	gamma-amino butyric acid
GALT	gut associated lymphatic tissue
GC	germinal center
GI	gastrointestinal

HC	healthy control
HEV	high endothelial venule
HIV	human immunodeficiency virus
HLA	human leukocyte antigen
HSV	herpes simplex virus
IBD	inflammatory bowel disease
ICU	intensive care unit
IgA	immunoglobulin A
ILC	innate lymphoid cell
ILF	isolated lymphoid follicle
iNOS	inducible nitric oxide synthase
IRF4	interferon-regulatory factor 4
J chain	joining chain
LefSE	linear discriminant combined with effect size
LI	large intestine
LP	lamina propria
LPS	lipopolysaccharide
Ly6C	lymphocyte antigen 6C
M cell	microfold cells
MAFF	Mucus-associated Functional Factor
MCM	DNA replication licensing factor Minichromosome maintenance protein complex
MDA	mean decrease accuracy
MFI	mean fluorescence intensity
MG	myasthenia gravis
MHCI	major histocompatibility complex class I
mLN	mesenteric lymph node
MS	multiple sclerosis
mTOR	Mammalian Target of Rapamycin
MYH	myosin heavy chain
NGS	Next generation sequencing
NMDS	Non-metric Multidimensional Scaling
NMO	neuromyelitis optica
NO	nitric oxide
NTD	N-terminal domain
OD	optical density
Pax5	paired box protein 5
PC	plasma cell
PCoA	principal coordinate analysis

pIgR	polymeric Ig receptor
PP	Peyer's patch
PUL	polysaccharide utilization loci
RA	rheumatoid arthritis
RBD	receptor binding domain
REGIIIα	regenerating islet-derived protein IIIα
REGIIIγ	regenerating islet-derived protein IIIγ
rRNA	ribosomal ribonucleic acid
S protein	Spike protein
SARS-Cov-2	Severe acute respiratory syndrome coronavirus 2
SC	secretory component
Sca-1	stem cell antigen 1
SCFA	short chain fatty acid
SED	subepithelial dome
SFB	segmented filamentous bacteria
SHM	somatic hypermutation
SI	small intestine
SIgA	secretory IgA
SiPR1	sphingosine-1-phosphate receptor 1
SpA	spondyloarthritis
SV40	simian virus 40
TACI	transmembrane activator and calcium-modulating cyclophilin-ligand interactor
TFH	T follicular helper cell
TGF-β	transforming growth factor β
TLR	toll-like receptor
TMA	trimethylamine
TNFα	tumor necrosis factor α
Treg	regulatory T cell
UC	Ulcerative colitis
XBPI	X-box binding protein 1
β-gal	β-galactosidase

8 List of figures and tables

All illustrations were created with BioRender.com.

9 Eidesstattliche Erklärung

Hiermit erkläre ich an Eides statt, die vorliegende Dissertation selbstständig gemäß guter wissenschaftlicher Praxis angefertigt und keine anderen als die angegebenen Hilfsmittel verwendet zu haben.

Des Weiteren erkläre ich hiermit, dass die Dissertation oder Teile davon nicht bereits bei einer anderen wissenschaftlichen Einrichtung eingereicht, angenommen oder abgelehnt wurden und auch kein anderwärtiger Doktorgrad erworben wurde.

Berlin, den

Teile der vorliegenden Dissertation wurden bereits vorveröffentlich und sind seit dem 08.08.2021 auf bioRxiv einsehbar unter dem Titel:

„Induction of cross-reactive antibody responses against the RBD domain of the spike protein of SARS-CoV-2 by commensal microbiota”

doi: https://doi.org/10.1101/2021.08.08.455272

Die in Kooperation erzeugten Daten sind im Abbildungsverzeichnis aufgeführt.